
Electric potential and ion drag force in highly collisional complex plasma

Manis Chaudhuri



München 2008

Electric potential and ion drag force in highly collisional complex plasma

Manis Chaudhuri

Dissertation
der Fakultät für Physik
der Ludwig–Maximilians–Universität
München

vorgelegt von
Manis Chaudhuri
aus Indien

München, den 20. August 2008

Erstgutachter: Prof. Dr. Gregor E. Morfill

Zweitgutachter: Prof. Dr. Hartmut Zohm

Tag der mündlichen Prüfung: 16.10.2008

Contents

Abstract	ix
Abstract in German	xi
1 Introduction	1
1.1 History of complex plasma	1
1.1.1 Dust in space	1
1.1.2 Dust in laboratory	4
1.2 Basics of Complex plasma	7
1.2.1 Dust particle charging	7
1.2.2 Dust charge screening	9
1.2.3 Characteristic frequencies	10
1.2.4 Coupling parameter	10
1.3 Phase space diagram	12
1.4 Electrostatic potential	15
1.5 Ion drag force	16
2 Cumulative thesis	21
2.1 Electrostatic potential behind a macroparticle in a drifting collisional plasma: Effect of plasma absorption	22
2.1.1 Objectives	22
2.1.2 Model	22
2.1.3 Results	23
2.1.4 Discussion	24

2.2	Effective charge of a small absorbing body in highly collisional plasma subject to an external electric field	25
2.2.1	Objectives	25
2.2.2	Model	25
2.2.3	Results	26
2.2.4	Discussion	26
2.3	Ion drag force on a small grain in highly collisional weakly anisotropic plasma: Effect of plasma production and loss mechanisms	27
2.3.1	Objectives	27
2.3.2	Model	27
2.3.3	Results	28
2.3.4	Discussion	29
3	Conclusion	31
3.1	Outlook	31
3.2	Future works	32
	Bibliography	33
	Acknowledgements	43
	Curriculum Vitae	45
	Publication list	47
3.3	Publication in refereed journals:	47
3.4	Publication in conference proceedings:	47
	Enclosed papers	49

List of Figures

1.1	Dust in space	3
1.2	Dust in laboratory	6
1.3	Phase diagram of plasma	12
1.4	Phase diagram of complex plasma	14
1.5	Ion drag force in collisional plasma	18
2.1	Spatial electric field distribution behind a dust particle	24
2.2	Parameter regime for the positive and negative ion drag force	29

Abstract

This PhD thesis is a cumulative dissertation that consists of three papers.

The first paper describes the qualitative as well as quantitative nature of the electrostatic potential behind a macroparticle in a drifting collisional plasma and also the ion drag force taking into account plasma absorption on the grain surface. Plasma absorption on the grain surface is one of the fundamental properties of complex (dusty) plasmas which results in the “openness” of these systems. It is shown that in the considered regime plasma absorption determines completely the long-range potential. Physically, absorption of the drifting ions on the grain surface generates ion rarefaction behind the grain which opposes the ion focussing effect. In certain parameter regime ion rarefaction effect dominates over focussing effect which makes ion drag force to act in the opposite direction of ion flow *i.e* we obtain *negative ion drag force*.

In the second paper both the ion drag and electron drag forces acting on an absorbing grain have been calculated in the limit of highly collisional weakly ionized plasmas. The plasma is exposed to an external weak electric field so that both ions and electrons drift with subthermal velocities. The effect of plasma absorption reduces the absolute magnitude of the ion drag force and even can change its sign in certain parameter regimes whereas this effect increases the magnitude of the electron drag force. The total force which is the sum of electric, ion drag and electron drag forces is proportional to the electric field. The proportionality constant represents the effective charge. The calculated value of the effective charge turns out to be of the order of the actual charge. This fact implies that in this parameter regime the drag forces are of minor importance compared to the electric force.

The third paper deals with the isotropic potential distribution and the ion drag force acting on an isolated dust particle in highly collisional weakly anisotropic plasma. But unlike the previous two cases where plasma absorption and loss processes were neglected in the vicinity of the grain, in this work we consider these processes. The plasma production is assumed to be due to electron impact ionization whereas for the loss processes two different mechanisms are considered: in high pressure plasmas the loss is mainly due to electron-ion volume recombination and in low/moderate pressure gas discharges the plasma loss is due to ambipolar diffusion towards the chamber walls or electrodes. In the first case the potential consists of two exponential terms and the long range potential is of Yukawa type. In the second case the long range potential is Coulomb-like. It is found that the purely Debye-Hückel potential is obtained only in absence of ionization-recombination processes. The ion drag force is negative when the ionization rate is low, but becomes positive for sufficiently high ionization rate in both cases. The parameter regimes for the positive and negative ion drag forces have been identified.

Zusammenfassung

Diese kumulative Dissertation besteht aus drei Veröffentlichungen.

Die erste Publikation beschreibt die qualitative und quantitative Natur des elektrostatischen Potentials hinter einem Makroteilchen in einem stoßdominierten Plasma, sowie der Ionenreibungskraft durch Plasmaabsorption auf der Teilchenoberfläche. Plasmaabsorption auf der Teilchenoberfläche ist eine der grundlegenden Eigenschaften der komplexen (staubigen) Plasmen, welche die “Offenheit” dieser Systeme zur Folge hat. Es wird gezeigt, dass im analysierten Bereich Plasmaabsorption das Fernfeld dominiert. Absorption der treibenden Ionen auf der Teilchenoberfläche erzeugt Ionenausdünnung hinter dem Teilchen, das dem Ionenfokussierungseffekt entgegengesetzt wirkt. In einem bestimmten Parameterbereich dominiert der Ionenausdünnungseffekt über den Fokussierungseffekt, welcher die Ionenreibungskraft in die dem Ionenfluss entgegengesetzte Richtung wirken lässt. Wir erhalten *negative Ionenreibungskraft*.

In der zweiten Veröffentlichung wurden sowohl die Ionenreibungskraft, als auch die Elektronenreibungskraft, welche auf ein absorbierendes Teilchen wirken, für den Grenzfall stark stoßdominierter, schwach ionisierter Plasmen berechnet. Das Plasma wurde einem schwachen, externen elektrischen Feld ausgesetzt, so dass Ionen und Elektronen mit sub-thermischer Geschwindigkeit driften. Der Effekt der Plasmaabsorption verringert die Stärke der Ionenreibungskraft und kann in einem bestimmten Parameterbereich, in dem dieser Effekt die Stärke der Elektronenreibungskraft erhöht, sogar ihr Vorzeichen umkehren. Die Gesamtkraft, welche sich aus der elektrischen Kraft, der Ionenreibungskraft und der Elektronenreibungskraft zusammensetzt ist proportional zu dem elektrischen Feld. Die Proportionalitätskonstante wird als effektive Ladung bezeichnet. Es stellt sich heraus, dass ihr berechneter Wert von der gleichen Größenordnung wie die wirkliche Ladung ist. Dieses impliziert, dass in diesem Parameterbereich die Reibungskraft von geringerer Bedeutung als die elektrische Kraft ist.

Die dritte Publikation beschäftigt sich mit der isotropen Potenzialverteilung und der Ionenreibungskraft, welche auf ein isoliertes Staubteilchen in einem stark stoßdominierten, schwach anisotropen Plasma, wirkt. Im Gegensatz zu den anderen beiden Fällen, in denen Plasmaabsorption und Verlustprozesse in der Nähe des Teilchens vernachlässigt wurden, werden sie in dieser Arbeit berücksichtigt. Es wird angenommen, daß das Plasma durch Elektronstoßionisation erzeugt wird, wohingegen für die Verlustprozesse mehrere Mechanismen in Frage kommen: in Hochdruckplasmen entsteht der Verlust im Wesentlichen durch Elektronen-Ionen Volumenrekombination und in Nieder/Mitteldruckplasmen durch ambipolar Diffusion gegen die Kammerwände und Elektroden. Im ersten Fall besteht das Potenzial aus zwei exponentiellen Termen und einem langreichweitigen Yukawa-Potenzial. Im zweiten Fall ist das Fernfeld Coulomb-artig. Es wurde herausgefunden, dass das Debye-Hückel-Potenzial nur unter Abwesenheit von Ionenrekombinationsprozessen erreicht wird. Die Ionenreibungskraft ist negativ wenn die Ionisierungsrate niedrig ist, wird aber in beiden Fällen positiv, wenn die Ionisierungsrate ausreichend groß ist. Der Parameterbereich wurde sowohl für positive, wie auch für negative Ionenreibungskraft bestimmt.

Chapter 1

Introduction

1.1 History of complex plasma

1.1.1 Dust in space

The important role of dust in space physics was realized a century ago [1]. There is a number of well known systems in space where dusty plasmas occur, *e.g.* Earth's atmosphere [2, 3, 4], planetary rings, comets [5], interplanetary medium [6], interstellar clouds [7], dynamics of stellar wind, nova-supernova explosions, formation of stars, planets etc. [8].

Dust in Earth's atmosphere: The closest example of naturally occurring dusty plasma in Earth's environment have been observed in the lower part of the ionosphere (polar mesosphere at altitudes of 80 to 90 km) where summer temperature is much smaller than winter temperature. Several phenomena occur in this region, such as formation of noctilucent cloud (NLC) [9], polar mesospheric summer echoes (PMSE) [4] and strong radar backscattering at frequencies from 50MHz to 1.3GHz. Also dust particles having cosmic origin are found in the magnetosphere. The magnetosphere acts as a shield with an efficiency that depends on the size and velocity of the incoming dust particles. Simulations for dust particles of cometary, interplanetary and lunar origin indicate that magnetospheric effects reduce the flux of interplanetary and lunar dust with sizes below $0.1\mu m$. However, the shielding is much less effective for cometary grains because of their much higher approach velocities [10].

Dust in Planetary rings: Most of the rings of the outer giant planets (Jupiter, Saturn, Uranus and Neptune) are made of micron-to submicron sized dust particles and a wealth of information was recovered [11]. Jupiter’s ring system was discovered in a single image from the Voyager 1 fly by in 1979 and subsequently imaged in greater detail by Voyager 2. The ring system of Jupiter is composed of three distinct components: the main ring, the halo and the gossamer ring. The main ring scatters more light into large phase angles than into smaller ones which indicates the presence of considerable dust concentration. The main ring encompasses the orbits of two small moons, Adrastea and Metis, which may act as the source for the dust that makes up most of the ring. The puzzles regarding the Saturn’s ring system was significantly increased since Voyagers 1 and 2 imaged the ring system extensively in 1980 and 1981. The main rings are known as C, B and A (from the outward direction). The Cassini division named after the discoverer Giovanni Cassini is the largest gap in the rings and separates the rings B and A. Subsequently a faint ring D was discovered which lies closest to the planet. The F ring is narrow and just outside the A ring. There are two other far fainter rings named G and E. The particles in Saturn’s rings are composed primarily of ice and range from micron to meters in size. One of the most interesting features observed in the Saturn’s ring system were the nearly-radial, wedge shaped features in the B ring, the Spokes [12, 13, 14, 15, 16]. The wedge becomes wider towards the planet. The spokes are confined with an inner boundary at $\sim 1.72R_s$ (R_s is the radius of the Saturn) and an outer boundary at approximately the outer edge of the B ring. The formation and evolution of spokes are explained in Ref. [14, 15]. The next planetary ring system is of Uranus which consists of nine major rings: δ , ϵ , ζ , η , θ , ι , κ , λ and μ (from outward direction). These rings have high optical depths and hence very little dust. A narrow λ ring was discovered in the backscattered Voyager images. Between the δ and λ ring a region is encountered which is mostly forward scattering, called the dust belt [17]. The characteristic of the constituents of Uranian rings was studied using photometric analysis which shows that the brightness distribution is dominated by backscattering and indicates the presence of macroscopic dust grains [18]. Neptune also has an external ring system which consists of a large proportion of microscopic dust particles [19]. The most prominent ring is the narrow outer *Adams ring*. It includes several longitudinal “arcs” along their length which are much brighter and much more opaque than the remainder of the ring. The other rings are: the innermost *Galle ring*, the narrow *LeVerrier ring* and the broad *Lassell ring*. Observations revealed a power law distribution (with an index 4)

for the dust grains.

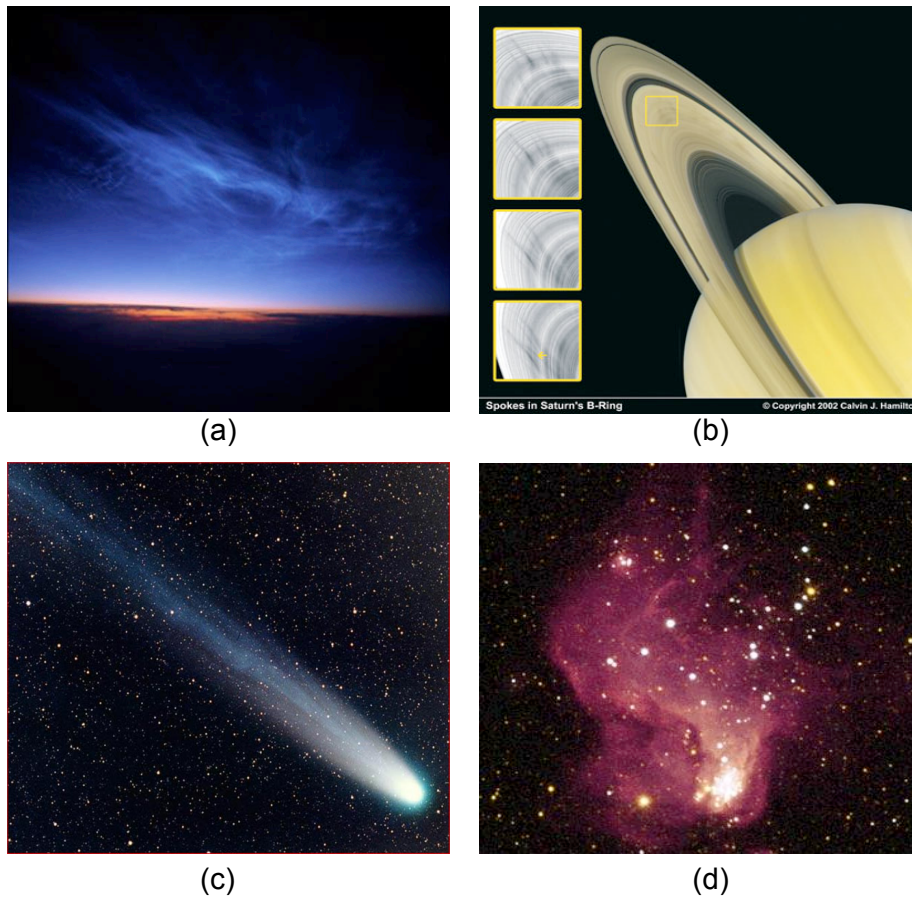


Figure 1.1: (a) Noctilucent cloud in Earth's atmosphere (b) Spokes in the Saturn's ring (c) dust in cometary tail (d) Interstellar dust

Dust in Interplanetary space and comets: The origin of interplanetary dust is mainly from comets (due to collisional fragmentation of debris) and asteroids. These dust particles have very fragile and fluffy appearance and are mainly composed of carbon, submicrometer mineral grains. The existence of interplanetary dust particles was known from zodiacal light. An outstanding example of dust environment in the solar system are the “comets” which consist of a cloud of diffuse material, called coma and a small, bright nucleus in the middle of the coma. The coma and the nucleus together constitute the head of the comet. As comets approach the Sun, they develop one of the optically largest dust structures by solar radiation and wind pressure: cometary dust tails. The physics of cometary tails is now quite well understood and can reveal lots of important scientific

information on dust properties.

Dust in Interstellar medium: In Interstellar medium dust particles are extremely small (fraction of μm), irregularly shaped and are composed of silicates, carbon, ice, and/or iron compounds. When light from other stars passes through the dust, several things can happen. If the dust cloud is thick enough, the light will be completely blocked, leading to dark areas. These dark clouds are known as dark nebulae. Light passing through a dust cloud may not be completely blocked, although all wavelengths of light passing through will be dimmed somewhat. This phenomenon is known as extinction. The amount that the light is dimmed depends upon the thickness and density of the dust cloud (= the optical depth), as well as the wavelength (color) of the light. Because of the tiny size of the dust particles, scattering of blue light is favored which implies that the light that reaches us is more red than it would have been without the interstellar dust. This effect is known as interstellar reddening. In turn, a dust cloud that is illuminated by star light, when viewed from the side appears blue (similar to the blue sky we see, due to the scattered sunlight by the Earth's atmosphere). Light may also be reflected from the clouds of Interstellar dust which is seen as a reflection nebula. A reflection nebula is a region of dusty gas surrounding a star where the dust reflects the starlight, making it visible to us.

1.1.2 Dust in laboratory

Dusty plasmas in laboratories differ significantly from those in space and astrophysical dusty plasmas due to mainly two reasons: (1) laboratory discharges are usually confined by geometric boundaries which influence the formation and transport of the dust grains and (2) the external circuit, which maintains the dusty plasma, imposes spatiotemporal varying boundary conditions on the discharge. In the early 1990s, etching, surface-processing and computer chips manufacturing were faced with serious problems due to the presence of levitating grain clouds which contaminated substrates [20, 21, 22]. The grains either start to grow by chemical processes or are emitted directly from the walls as a result of etching process. The physics of grain formation and grain growth in the first stage of etching is an actively investigated topic [23, 24]. To control these processes, it is necessary to understand the basic mechanisms of transport of dust particles, influence of dust on plasma parameters, etc.

The investigation in complex plasmas was triggered in the mid 1990's by the labora-

tory discovery of plasma crystals. The possibility of dust subsystem crystallization in a nonequilibrium gas discharge plasma due to strong electrostatic coupling between the dust particles was predicted by Ikezi in 1986 [25]. The first experimental observations of ordered particle structures were reported in 1994 in rf discharge [26, 27, 28, 29]. Transitions from a disordered gaseous-like phase to a liquid-like phase and the formation of ordered structures of dust particles, the plasma crystals were observed [30]. Later on, plasma crystals were also found in dc discharges [31], thermal plasmas at atmospheric pressure [32], and even in nuclear-induced dusty plasmas [33].

In ground based laboratory investigations of complex plasmas the effect of gravity is unavoidable. To support particles against gravity strong electric fields are required leading to a high degree of plasma anisotropy and suprathermal ion flows. The plasma conditions yield forces on the particles, which are comparable to the inter-particle forces. Hence most complex plasmas investigated on Earth are strongly compressed, inhomogeneous (in the vertical direction), and anisotropic. Under microgravity conditions the particles move into the bulk of the plasma and can form large three dimensional (3D) weakly compressed “quasi-isotropic” complex plasmas as shown in Fig. 1.2 (c). A research program on complex plasmas under microgravity conditions was initiated in 1994, shortly after the discovery of plasma crystals in the laboratory. The microgravity has a profound influence on the properties, structure, dynamics, and physical state of complex plasmas, making possible experimental investigations that cannot be conducted on Earth. The plasma crystal experiment “PKE-Nefedov”, a joint German/Russian scientific project for the long-term investigations of complex plasmas under microgravity conditions was installed on the International Space Station (ISS) in February 2001 [34]. In December 2005 the next-generation complex plasma experiment facility “PK-3 Plus” was installed onboard the International Space Station and first experiments were performed in January 2006 [35]. The “PK-3 Plus” laboratory provides new possibilities for microgravity investigations due to its design improvements relative to the first long-term experiment “PKE-Nefedov”. Both the above mentioned projects are based on rf discharge. The next generation “PK-4” project is a continuation of the successful “PKE-Nefedov” and its successor, “PK-3 Plus” projects and combines both dc and rf discharges.

The presence of dust particles in fusion devices (tokamaks, stellarators, etc.) has been known for a long time. However, their possible consequences for plasma operations and performances become a topic of interest in late 1990s [36, 37, 38]. The dust particles are

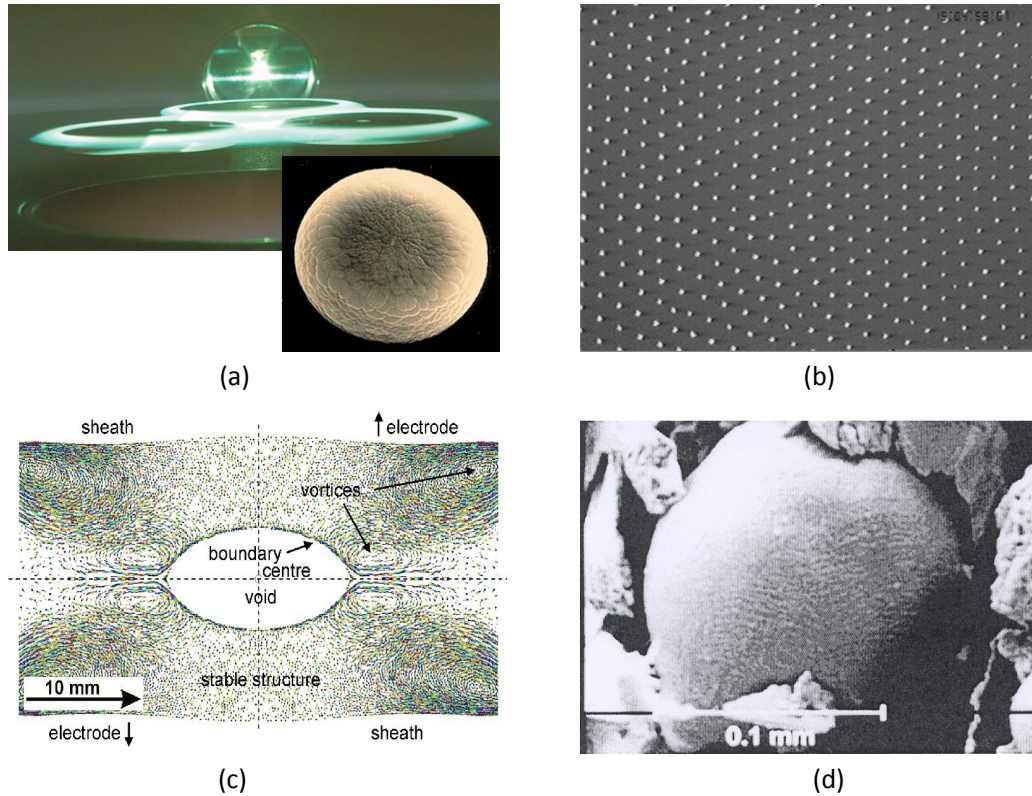


Figure 1.2: (a) Rings of dust particles encircling silicon wafers in a plasma processing device. (Inset) An electron-microscope image of a $20\mu\text{m}$ diameter particle from such a dust cloud [21]. (b) A CCD image of a horizontal lattice plane of a plasma crystal [26] (c) Complex plasma experiment in microgravity onboard the International Space Station (PKE-Nefedov experiments) [34] (d) Example of large dust particles collected after many discharges in a fusion devices [36].

generated by a number of processes, such as desorption, arcing, sputtering, evaporation and sublimation of thermally overloaded wall material [39, 40, 41, 42, 43, 44]. The sizes may vary from a few nanometers to few tenths of a millimeter. Dust can affect the plasma performance and stability, as well as the operation of fusion devices. In the framework of the development of the International Thermonuclear Experimental Reactor (ITER) project it became obvious that dust represents a serious safety hazard. Thus, the problem of dust removal from thermonuclear devices represents one of the most important scientific and technical problem.

1.2 Basics of Complex plasma

Complex (dusty) plasma is an overall charge neutral assembly of ions, electrons, highly charged microparticles and neutral gas. The micro-particles are large enough to be visualized individually which allows experimental investigations with high temporal and spatial resolution (in terms of the appropriate plasma frequency and particle separation). Hence, complex plasma is used as a valuable model system to investigate various phenomena (e.g, phase transitions, self-organizations, waves, transport, etc.) at the most fundamental kinetic level [45, 46, 47, 48, 49]. Below some characteristic properties of complex plasmas are briefly mentioned.

1.2.1 Dust particle charging

In complex (dusty) plasmas most of the dust particle charging theories are based on the theories of the electrostatic probes in plasmas [50, 51]. Due to the higher mobility of electrons the non-emitting particles become negatively charged and the concentration of free electrons in plasmas is reduced. This effect often leads to considerable changes in plasma charge composition. Conversely, in case of emitting particles (*e.g.*, thermionic emission, photo emission, secondary electron emission) the dust grains emit electrons and may become positively charged which may increase the electron concentrations in plasmas. In equilibrium condition, the “quasineutrality” condition in complex plasmas can be written as

$$Z_{d0}n_{d0} + n_{i0} = n_{e0}$$

where n_{s0} is the equilibrium number density of the plasma species s ($s = e, i, d$ for electrons, ions and dust particles) and Z_{d0} is the particle charge number on dust particles. For negatively charged particle $Z_{d0} < 0$ and $Z_{d0} > 0$ for positively charged particle. The above condition can be used to estimate when the influence of dust component on the charge composition in complex plasmas is considerable using the inequality $|Z_{d0}n_{d0}/n_{e0}| = P \geq 1$. In the absence of emission processes, electrons and ions recombine on the dust particles *i.e.* the particles act as a plasma sink. The dust grain charge $Q_d (= Z_d e)$ is related to the grain’s floating potential ϕ_f by the “vacuum” relation, $Q_d = C\phi_f$, where $C = a$ is the grain’s capacitance, provided the grain is small. Here, a is the dust grain radius. However, there may be some deviations from this approximation due to strongly nonlinear screening

and/or non-equilibrium distribution of the electrons and ions around the dust grain. The electron and ion currents collected by an isolated dust particle from the plasma strongly depends on its floating potential ϕ_f . The charge evolution is then determined by

$$\frac{dQ_d}{dt} = J_i(\phi_f) + J_e(\phi_f).$$

Setting the sum in the right-hand-side to zero yields the steady-state floating potential ϕ_f and grain charge Q_d .

In the limiting case of collisionless complex plasmas the following inequality usually holds: $a \ll \lambda_D \ll \ell_{i(e)}$, where λ_D is the Debye length and $\ell_{i(e)}$ is the collisional mean free path of ions (electrons). In this regime the floating potential can be calculated using orbital motion (OM) theory. In its simplest form, the orbital motion limited theory (OML), the floating potential depends upon electron-to-ion mass and temperature ratios and is insensitive to the body radius [52]. The OML theory is strictly valid when there is no potential barrier for the ion motion. In the presence of a potential barrier some low energy ions will be reflected and can't reach the grain surface. This effect leads to a decrease in the ion current compared to the OML theory. Although some questions have been raised regarding the validity of the OML theory [53], it is shown that in the limit of vanishingly small grains which is a common situation in complex plasmas, it is still an excellent approximation for the quantitative calculations [54]. The full orbital motion theory is much more complicated as it requires the solution of the nonlinear Poisson equation as well as the particle trajectories. Some research has been done for monoenergetic [55, 56] and Maxwellian ions [57, 58], while electrons have always been considered Maxwellian. It is to be noted that these theories do not take into account the effect of trapped ions [59, 60], and are applicable only in the absence of relative drift velocity between plasma and dust grains. The last assumption assumes spherical symmetry of the problem and uses conservation laws for angular momentum and energy. Another effect important for dust particle charging is *ion-neutral collisions*, which is neglected in these theories on the basis that the ion mean free paths are large compared to the plasma screening length. However, theory has shown that ion-neutral charge-exchange collisions in the vicinity of the dust grain substantially increase the ion current to the dust surface even when ℓ_i is larger than λ_D [60, 61, 62]. An increase in the ion current considerably suppresses the grain charge [63, 64].

In the limiting case of high pressure plasmas, $\ell_i \ll \lambda_D$, ion motion is mobility controlled due to high collisionality [65, 66, 67, 68]. Mobility decreases with pressure and

so does the ion flow and hence the surface potential (floating potential) increases in the absolute magnitude. However, when the electron transport becomes collisional too, the grain surface potential does not depend on neutral gas pressure, and its absolute magnitude is approximately given by the logarithm of the ratio of the electron and ion diffusion coefficients.

In the above discussion, the charge of dust particles is treated as a continuous regular variable. However, in real situation the charging process is random in nature due to discreteness of electron and ion absorption on the grain surface. As a result, the particle charge can fluctuate around its average value. The importance of charge fluctuations was recognized in the early 1980's by Morfill *et. al.* in explaining dust transport in astrophysical plasmas [69, 70] and studied later extensively [71, 72, 73, 74, 75]. It has been recognized that charge fluctuation can generate dust grain "heating" in external electric fields [76, 77, 78], affect grain coagulation process [71, 72], cause instabilities of grain oscillations [79, 80], is responsible for dust particle transport across a magnetic field in astrophysical plasma [81] etc. Another major consequence of the fact that depending on the surrounding plasma parameter variations the electrostatic field force acting on grains $-Z_d e \mathbf{E}$ is not potential since $\nabla Z_d \nabla \phi \neq 0$ in general case. Thus complex plasmas can be considered as non-Hamiltonian system [82, 83].

1.2.2 Dust charge screening

It is well known that a fundamental characteristic of plasma is its ability to shield any externally applied electric potential by the formation of a shielding charged cloud with a typical length scale defined as the Debye length, λ_D [84]. In complex plasmas it is often assumed that the massive dust particles ($m_d \gg m_i \gg m_e$) form a stationary uniform background while electrons and ions obey the Boltzmann distribution. Then solving the Poisson equation within linear approximations for electron and ion perturbations ($|e\phi_f/T_i| \ll 1$) one can obtain an expression for the Debye radius as [85],

$$\lambda_D = \frac{\lambda_{De} \lambda_{Di}}{\sqrt{\lambda_{De}^2 + \lambda_{Di}^2}}$$

where $\lambda_{De(i)} = (T_{e(i)}/4\pi n_{e0(i0)} e^2)^{1/2}$. Here, $T_{e(i)}$ is the electron (ion) temperature, $n_{e0(i0)}$ is the equilibrium densities of electrons (ions) and e is the electronic charge. Under typical conditions $T_e \gg T_i$ *i.e.* $\lambda_{De} \gg \lambda_{Di}$. In this case $\lambda_D \simeq \lambda_{Di}$ which means that the shielding

distance is mainly determined by the ions. Non-linear screening effects can play an important role near highly charged dust grain surface [86, 87]. One of the most important parameters determining the non-linearity in screening is the so-called *scattering parameter*, $\beta = R_c/\lambda_D$, where $R_c(= |Q_d|e/m_i v^2)$ is the Coulomb radius at which the ion-grain electrostatic interaction energy is of the order of ion kinetic energy. Here, m_i and v are the ion mass and velocity respectively. The effect of non-linearity is small when $\beta \ll 1$ while for $\beta \gg 1$ it can be dominant.

1.2.3 Characteristic frequencies

As mentioned before, the presence of charged dust particles modifies the macroscopic space charge neutrality condition. When a plasma is instantaneously disturbed from its equilibrium, the resulting internal electric field gives rise to collective particle motions which tends to restore the charge neutrality. These collective motions are characterized by a natural frequency of oscillations known as the plasma frequency, $\omega_{ps} = (4\pi n_{s0} Q_s^2 / m_s)^{1/2}$ associated with the plasma species s . These frequencies are not same for electrons, ions and dust grains, but depend on the mass and charge of the plasma species ($\omega_{pe} \gg \omega_{pi} \gg \omega_{pd}$).

In weakly ionized plasmas the (charged) plasma particles collide mostly with neutral atoms. These collisions are characterized by electron-neutral collision frequency ν_{en} , the ion-neutral collision frequency ν_{in} and the dust-neutral collision frequency ν_{dn} . The collision frequencies are defined as $\nu_{sn} = n_n \sigma_s^n v_{Ts}$, where n_n is the neutral number density, σ_s^n is the effective collision cross-section and v_{Ts} is the thermal speed of the s 'th species. Collisions of the plasma particles with neutrals tend to damp their collective oscillations.

1.2.4 Coupling parameter

In many particle interacting system one of the fundamental characteristic is the coupling parameter Γ which is defined as the ratio of the potential energy of interaction between neighboring particles to their kinetic energy *i.e.* $\Gamma = Q^2 n^{1/3} / T$ where Q , n and T are the charge, density and the temperature of the particles respectively. For the Coulomb interaction between charged dust particles,

$$\Gamma_C = \frac{Q_d^2}{\Delta T_d}$$

where $\Delta = n_d^{-1/3}$ characterizes the average interparticle spacing and T_d characterizes dust component kinetic energy. For a one component plasma with uniform and stationary neutralizing background it is shown by numerical computation that the transition to crystalline state occurs at $\Gamma_C \sim 106$ (or $\Gamma_C \sim 171$ if the interparticle spacing Δ is defined through the Wigner-Seitz radius, $(\frac{4\pi}{3}n_d)^{-1/3}$) [88]. However, in dusty plasma the interaction between charged dust particles can be often approximated by the isotropic Debye-Hückel (Yukawa) type repulsive potential, with the screening determined by the plasma electrons and ions. In this case the coupling ratio is characterized by the electrostatic “screened” coupling parameter $\Gamma_{ES} = \Gamma_C \exp(-\kappa)$, where $\kappa = \Delta/\lambda$ is the structure (lattice) parameter - the interparticle spacing normalized by the effective screening length. A dusty plasma is said to be weakly coupled when $\Gamma_{ES} < 1$, while it is strongly coupled when $\Gamma_{ES} \geq 1$. In laboratory dusty plasma systems, massive dust grains are strongly coupled because of their huge electric charge, low temperature and small intergrain distance. This model gives a rather simplified picture of dusty plasmas and does not account for plasma anisotropy, charge variations, collective interactions, exact form of confining potential, etc.

1.3 Phase space diagram

The phase space diagram for plasmas (in absence of dust) are characterized by two parameters: density (n) and temperature (T) as shown in Fig. 1.3(a). It is assumed that the temperatures of different plasma components (*i.e.* electrons, ions and neutrals) are same. Plasma densities vary from less than one particle per cubic meter (tenuous intergalactic/interstellar region) to 10^{26} cm^{-3} (center of the sun) and even upto 10^{30} cm^{-3} (white dwarfs). Temperature varies from less than 10^{-6} K (laser cooled OCP) to tens of millions Kelvin (Center of the Sun) and even upto billions of degree (Compact stellar object). The

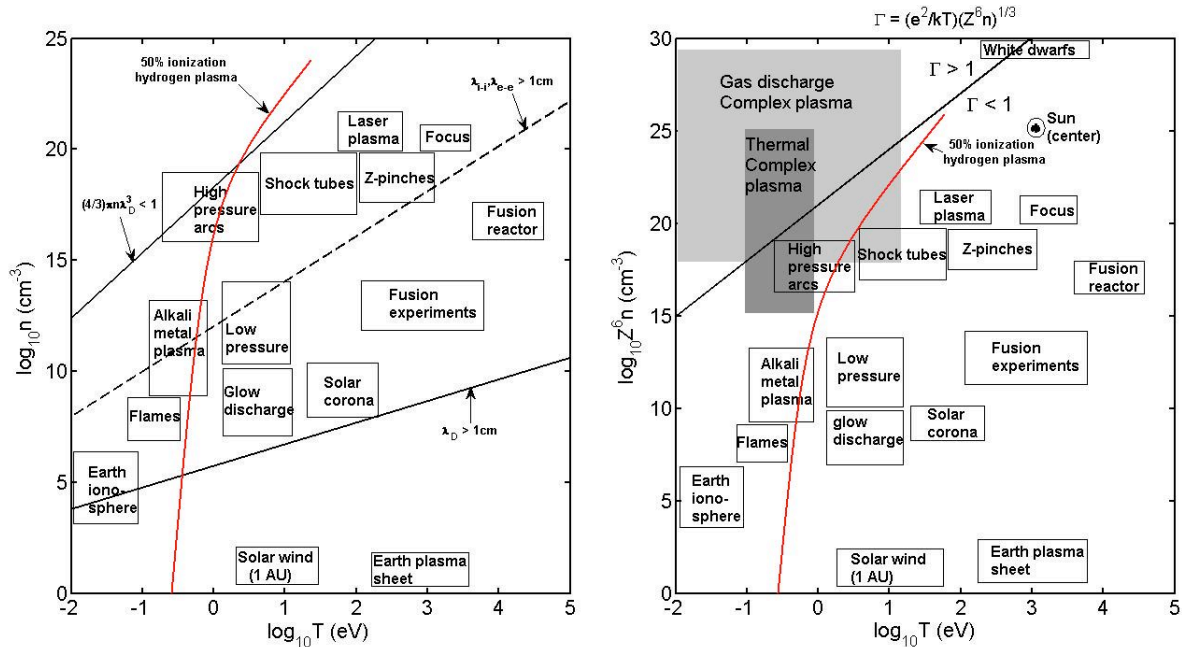


Figure 1.3: (a) Phase diagram showing different plasmas existing in space and laboratory. Here, n is the number of particles in cm^{-3} , λ_D is the Debye length and T is the temperature [89] (b) Same phase space diagram with the parameter regime applicable for complex plasma (grey shaded). Note that the “complex plasmas” allow the experimental investigations of the strong coupling regime, including liquid and crystalline plasma states. The solid line shows the $\Gamma = 1$ line, which marks the transition from strongly to weakly coupled plasmas [90].

red line indicates the (n, T) values at which a hydrogen plasma at local thermal equilibrium would be 50% ionized. To the left of this line the ionization fraction is smaller and to the right of it ideal fully ionized plasma state is obtained. The upper continuous black line represents the boundary between ‘strongly coupled’ and ‘weakly coupled’ plasmas. The

strong coupling is defined here by setting the thermal energy T equal to the mean Coulomb energy between neighboring particles, $Q^2 n^{1/3}$. In this case the strong coupling is in between plasma particles (in absence of dust particles). In Fig. 1.3(a) it is assumed that the atoms are singly ionized and the solid line gives $\Gamma = 1$. Above this line plasma is strongly coupled and can form ordered structures. Below this line the system behaves like a hot gas where frequent collisions between electrons and ions thermalize the system. The parameter Γ increases with density and decreases with temperature. It should be noted that earlier it was quite difficult to explore the strongly coupled phase space region experimentally, since one must achieve extremely high density at very low temperature.

The breakthrough for the problem of strongly coupled plasmas came from the discovery of complex plasmas where highly charged dust grains appear as an additional charged component in addition to electrons and ions. Since the coupling parameter has quadratic dependence on the charge $Q(= Ze)$, the dust grains can be strongly coupled while the other plasma particles interact weakly. To show the accessible range of complex plasma in phase space the Fig. 1.3(a) has been redrawn in slightly different way in Fig. 1.3(b). The vertical axis is now $Z^6 n$, which is proportional to $\Gamma^3 T^3$. The shaded region corresponds to the accessible region in phase space using complex plasma. The lower limit is due to the electrostatic levitation against gravity, and the upper limit is due to the electron depletion caused by plasma absorption on the dust particles. From Fig. 1.3(b) it is clear that all stages of plasma condensation can in principle be examined experimentally in a wide region of parameter space.

Now, the detailed features of the phase diagram for complex plasmas as functions of coupling parameter, Γ_{ES} , finiteness parameter, $\alpha = \Delta/a$ and lattice parameter, $\kappa = \Delta/\lambda$ are shown in Fig. 1.4 where Δ is the mean grain separation and a is the grain size. In this calculation it is assumed that the dust grains interact via isotropic Debye-Hückel (Yukawa) potential. The typical parameter range of complex plasmas studied so far is, $\lambda/a \sim \alpha/\kappa = 100$. The vertical line $\kappa = 1$ divides the diagram into weakly screened (Coulomb) and strongly screened (Yukawa) parts. The upper solid line represents the “melting line” which indicates the liquid-solid phase transition and the lower solid line indicates the transition between “ideal” and “nonideal” plasmas. Above the lower solid line the interaction is essentially collective, whereas below this line only pair interactions are important. From the thermodynamical point of view, this line determines the limit of employing expansions of the thermodynamical functions over the small coupling parameters. The regions where

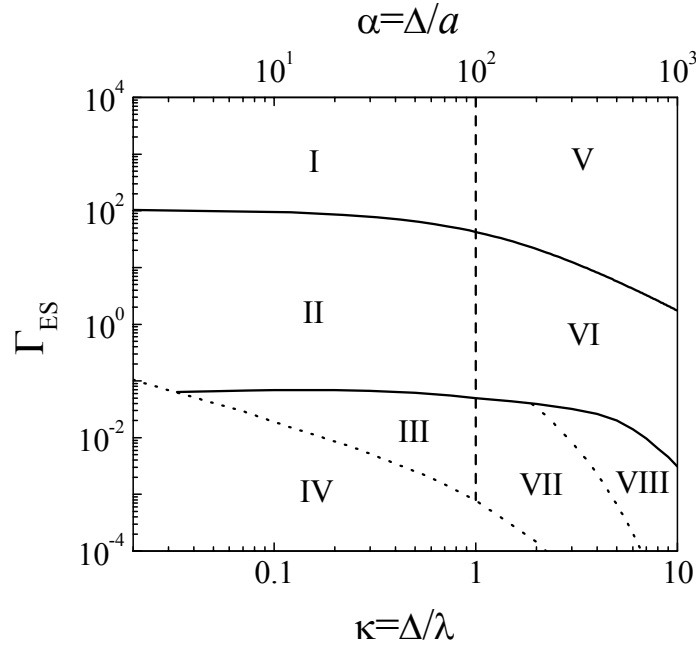


Figure 1.4: Phase diagram of complex plasmas. Regions I (V) represent Coulomb (Yukawa) crystals. Regions II (VI) are for Coulomb (Yukawa) non-ideal plasmas. Regions III (VII and VIII) correspond to Coulomb (Yukawa) ideal gases. In the region VIII, the pair Yukawa interaction asymptotically reduces to the hard sphere limit, forming a “Yukawa granular medium”. In region IV, the electrostatic interaction is unimportant and the system is like a usual granular medium.

the system is similar to a granular medium are also shown. The region below the lower dotted curve is identified as usual granular medium where the electrostatic interaction is too weak and the momentum exchange occurs due to direct grain collisions *i.e.* the charges do not play any significant role. The upper dotted curve represents the transition boundary for “Yukawa granular medium” where strongly screened electrostatic interaction reduces asymptotically to the hard sphere limit.

1.4 Electrostatic potential

A dust particle in a plasma acquires a high electric charge and interacts with other dust particles. The character of the intergrain interaction is one of the most fundamental questions for understanding the physics of complex plasma in laboratory as well as in space. The point is that the interaction potential is not fixed but depends considerably on complex plasma conditions. Diverse mechanisms of attractive and repulsive interactions have been discussed in the literature [46, 48, 91].

One of the main interaction mechanisms is the electrostatic repulsion between like charged particles. In isotropic collisionless plasmas the potential is often assumed to be of Debye-Hückel (Yukawa) form at relatively short distances (up to a few plasma screening lengths) [56, 92]. At larger distances the effect of continuous plasma absorption on the grain leads to much more slow decay of the potential [53, 91, 93, 94, 95], and it scales with distance as $\propto r^{-2}$. In isotropic collisional plasmas the electrostatic potential around an absorbing body in the absence of ionization/recombination processes in its vicinity has even more slowly decaying $\propto r^{-1}$ long-range asymptote [65, 68, 96, 97, 98].

In anisotropic plasma, the potential distribution can be calculated using the linear dielectric response formalism [99]. This approach is applicable when the nonlinear region around the dust grain is small compared to the plasma screening length *i.e.* when the ions are weakly coupled to the particle. The electric potential of a test particle (with fixed charge Q) moving with a constant velocity \mathbf{u} is [100]

$$\phi(\mathbf{r}) = \frac{Q}{2\pi^2} \int \frac{e^{i\mathbf{k}\mathbf{r}} d\mathbf{k}}{k^2 \epsilon(\mathbf{k}, -\mathbf{k}\mathbf{u})}$$

where $\epsilon(\mathbf{k}, -\mathbf{k}\mathbf{u})$ is the plasma permittivity. Using this approach Montgomery *et al.* [101] calculated the far field potential of a moving test charge in a uniform electron-ion plasma and showed that it decreases as the inverse cube of the distance from the test charge ($\phi \propto r^{-3}$). On the other hand, in a collisional electron-ion plasma it may decay as r^{-2} [102]. In presence of large electric fields (in rf sheaths or dc striations) ions start to drift relative to the particle and this creates a non-monotonic potential distribution (with well pronounced extremum) within a certain solid angle downstream from the flow - a wake [103, 104, 105, 106, 107, 108]. The shape of the wake potential is sensitive to the value of the ion Mach number [106], electron-to-ion temperature ratio [109] and ion-neutral collisions [110].

1.5 Ion drag force

The interaction and momentum transfer between different plasma components and charged grains play an exceptionally important role in complex plasmas [111]. In this section we focus on the ion drag force which is caused by the momentum transfer from flowing ions to a negatively charged grain. This force appears to be quite important in describing a number of interesting phenomena in complex plasma like void formation in the central region of an rf discharge under microgravity condition [112, 113, 114, 115, 116], rotation of the dust structures in the presence of the magnetic field [117, 118], location and configuration of the dust structures in laboratory experiments [119, 120], properties of low-frequency waves [121, 122, 123], *etc.* Not surprisingly, the ion drag force has been the subject of extensive investigation over the last few years. This includes analytical theories [120, 124, 125, 126, 127, 128, 129, 130], numerical simulations [131, 132, 133, 134], and experiments [135, 136, 137, 138, 139, 140].

It should be noted that despite its high importance in complex plasmas, a complete self-consistent model of the ion drag force, describing all cases of interest, has not yet been developed. Rather there exist several approaches, which are formulated under certain well defined conditions [46, 48, 127, 141]. Let us briefly outline these approaches. The traditional way to derive ion-drag force is the “binary collision (BC) formalism”, which is based on the solution of the mechanical problem of the ion motion in the field of the charged particle. Analyzing ion trajectories one can obtain the velocity-dependent momentum-transfer cross section $\sigma(v)$ integration of which with appropriate velocity distribution function of the ions gives the ion-drag force. In deriving $\sigma(v)$ an isotropic attractive Debye-Hückel(Yukawa) interaction potential between the ions and the grain is typically assumed. An important quantity characterizing momentum transfer in the Yukawa potential is the so-called *scattering parameter*, β . For a small (point-like) grain the normalized momentum transfer cross section, $\sigma(v)/\lambda^2$, depends only on β [126]. Thus, β is a unique parameter which describes scattering for Debye-Hückel (Yukawa)central potential. The value of β which measures the strength of the ion-grain coupling determines how the momentum transfer occurs. Different approaches can be employed in different regimes. For weak coupling ($\beta \ll 1$), the length scale of non-linear interaction and scattering at large angles ($\sim R_c$) is much shorter than the screening length, λ . In this regime the conventional Coulomb scattering theory (small-angle scattering approximation) is applicable. An

extension of the Coulomb scattering theory to the regime of moderate coupling ($\beta \sim 1$) has been developed in Ref. [125]. In this case the interaction range can be comparable or even exceed the screening length which requires a proper choice of the upper cutoff impact parameter and basically leads to a modification of the Coulomb logarithm. This model has been shown to agree reasonably well with experimental results at low and moderate neutral gas pressures [139], as well as with PIC simulation [134]. In the case of strong ion-grain coupling ($\beta \gg 1$) the interaction range considerably exceeds the screening length and most of the contribution to the momentum transfer is from scattering with large angles. In this regime traditional Coulomb scattering theory is not applicable and hence a corresponding new approach has been developed for subthermal ion drift in Refs. [126, 127]. This approach is further extended taking into account both subthermal and suprathreshold ion drift velocities and is compared with experiments in Ref. [140]. In this regime the experimental results agree reasonably well with analytical theories. Thus, within the BC formalism one can describe the momentum transfer for any given degree of ion-grain coupling. Overall, there is a reasonable quantitative agreement between theory and experiments in collisionless and weakly collisional plasma. However, since this approach considers only the ballistic ion trajectories, the effect of ion-neutral collisions, which is often important in complex plasmas cannot be consistently accounted for.

An alternative way to calculate the ion drag force is based on the so-called “linear dielectric response (LR) formalism”. Unlike the BC approach, instead of calculating single ion trajectories and then the momentum transfer cross section, one can solve the Poisson equation coupled to the kinetic (or hydrodynamic) equations for the ions and electrons and obtain the self-consistent electrostatic potential distribution around the grain. Then the product of the polarization component of the electric field induced by the ion flow at the position of the grain and grain charge gives the ion drag force on the grain [128, 129, 141, 98]. As far as LR formalism is concerned, the whole problem is basically reduced to the calculation of the proper plasma response function (permittivity). This approach consistently accounts for ion-neutral collisions, potential anisotropy caused by the ion flow and allows to calculate the ion velocity distribution function self-consistently, but is applicable only for weak ion-grain coupling, $\beta \leq 1$, since linearization is used.

In highly collisional plasma the ion drag force acting on a non-absorbing grain increases due to ion focussing effect behind the grain. This effect is related with the local increase in the ion density downstream from the grain which induces an additional electric field

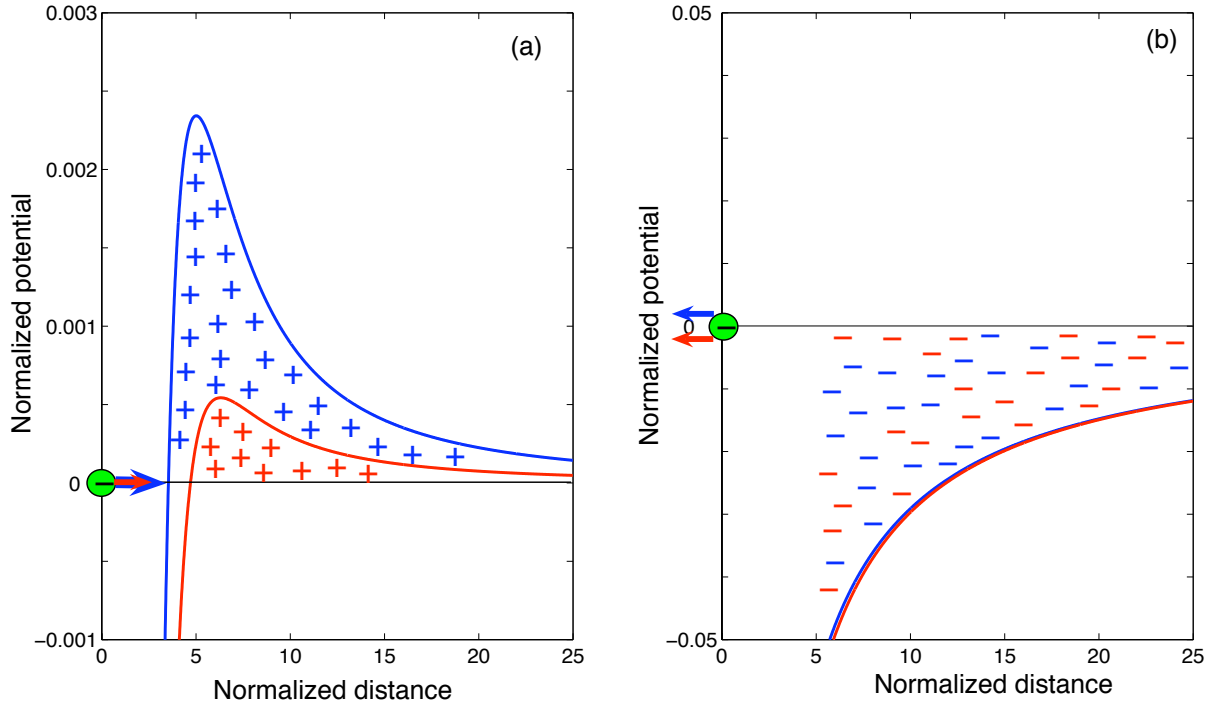


Figure 1.5: Spatial distribution of normalized electric potential behind a small negatively charged moving grain in highly collisional plasma. (a) corresponds to a nonabsorbing grain, while (b) corresponds to an absorbing grain. The grain is moving to the left. The direction of the force associated with (a) ion focusing and (b) ion depletion behind the grain is shown by arrows. Positive and negative sign corresponds to the positive and negative space charge regions, respectively. The plasma parameters are, $T_e = T_i$, $Qe/aT = 3$, $a/\lambda_D = 0.2$, $u/v_T = 0.003$ and $\ell_i/\lambda_D = 0.03(0.01)$ for red (blue) curves. For details see Ref. [142]

which creates a drag force in the direction of the ion drift for a negatively charged particle. With increasing ion-neutral collisionality the magnitude of the ion space charge density increases and the focussing point shifts towards the grain which implies further increase of the ion drag force [Fig 1.5(a)]. Ion absorption on the grain surface causes a rarefaction of the ion density downstream from the grain and hence reduces the ion drag force. These two effects oppose each other and in certain parameter regime rarefaction effect due to plasma absorption can dominate over the focussing effect which leads to the negative ion drag force [Fig 1.5(b)]. The interesting possibility for the ion drag force to reverse sign was predicted recently in Refs. [98, 131, 132, 143, 144].

Chapter 2

Cumulative thesis

This cumulative thesis consists of the following papers which were published during the PhD work:

1. M. Chaudhuri, S. A. Khrapak and G. E. Morfill, Electrostatic potential behind a macroparticle in a drifting collisional plasma: Effect of plasma absorption, *Phys. Plasmas* **14**, 022102 (2007).
2. M. Chaudhuri, S. A. Khrapak and G. E. Morfill, Effective charge of a small absorbing body in highly collisional plasma subject to an external electric field, *Phys. Plasmas* **14**, 054503 (2007).
3. M. Chaudhuri, S. A. Khrapak and G. E. Morfill, Ion drag force on a small absorbing grain in highly collisional weakly anisotropic plasma: Effect of plasma production and loss mechanisms, *Phys. Plasmas* **15**, 053703 (2008).

The main ideas and results of these papers (1) to (3) are summarized in sections 2.1 to 2.3, respectively.

2.1 Electrostatic potential behind a macroparticle in a drifting collisional plasma: Effect of plasma absorption

2.1.1 Objectives

The intergrain interaction potential is one of the most fundamental problems in complex plasma. In isotropic collisionless plasmas the potential is often assumed to be of Debye-Hückel (Yukawa) form at relatively short distances (up to a few plasma screening lengths) [48, 56, 92]. At larger distances the effect of plasma absorption on the grain surface determines the long-range asymptote of the potential which decays much more slowly with distance ($\propto r^{-2}$) [91, 145, 93, 94, 95]. In isotropic collisional plasmas the electrostatic potential around an absorbing body in the absence of ionization/recombination processes in its vicinity has even more slowly decaying long-range asymptote ($\propto r^{-1}$) [65, 68, 96, 97, 98]. However in the presence of large scale electric fields the plasma flows relative to the grain component, and complex plasma becomes anisotropic. In case of anisotropic collisionless plasma the long-range electric potential behind a test charge has $\propto r^{-3}$ asymptote [101, 146, 147], whereas for anisotropic collisional plasma it scales as $\propto r^{-2}$ [102]. The theory of wakes behind an object in flowing plasmas has been developed in both collisionless and collisional regimes [103, 104, 105, 106, 107, 108], but the plasma absorption on the grain was usually neglected.

In this work, an analytical expression for the electric field behind a stationary spherical grain has been derived in the limit of highly collisional plasma using linear approximation and taking into account plasma absorption on the grain surface. An analytical expression for the ion drag force has also been calculated.

2.1.2 Model

In this model a stationary, negatively charged spherical particle is considered which is immersed in a highly collisional, weakly ionized quasineutral plasma with a constant weak ambipolar electric field. The electric field is sufficiently weak so that ions drift with subthermal velocity while electrons form a stationary background. There are no plasma sources and sinks in the vicinity of the grain except on the grain surface which is fully absorbing.

The collisional ion component is described by the continuity and momentum equations in the hydrodynamic approximation while the electron component is described by a Boltzmann distribution. An analytical expression for the self-consistent electric potential behind a stationary grain has been derived in the linear approximation by solving Poisson equation.

2.1.3 Results

The analytical expression for the electric field behind a stationary grain consists of four terms [Eqn.(10)]. The first and second terms represent respectively the isotropic Debye-Hückel potential and anisotropic electric field behind a non-absorbing grain. The third and fourth terms represent respectively the isotropic and anisotropic parts of the electric field associated with the plasma absorption on the grain surface. The effect of absorption reduces the amplitude of the anisotropic electric field and can even change its sign. However, at large distances, the dominant contribution comes from the isotropic part associated with absorption *i.e.* absorption completely determines the long range asymptote of the potential. The behavior of the normalized electric field downstream from the grain is determined by three dimensionless parameters: electron-to-ion temperature ratio (τ), ion drift velocity normalized to the ion thermal velocity (M_T), and the ratio of the ion mean free path to the plasma screening length (ξ). The analysis shows that depending on these parameters the electric field is either negative for all distances or can assume positive values at intermediate distances as shown in Fig. (2.1). In the first case two negatively charged particles would repel each other, while in the second case they would attract each other.

The ion drag force associated with the plasma anisotropy induced by the ion flow has been calculated for an absorbing grain [Eqn.(11)]. This expression is identical to that obtained by Khrapak *et. al.* [98] and it consists of two terms. The first term of this expression represents the ion drag force acting on the non-absorbing grain in highly collisional plasmas. It coincides with the expression obtained earlier by Ivlev *et. al.* [128] using more general kinetic approach. The second term is associated with the plasma absorption on the grain surface. The absorption effect gives a negative contribution to the force (for a negatively charged grain) so that in the highly collisional regime the magnitude of the total ion drag force decreases considerably and in certain parameter regimes it can change sign. The sign reversal indicates the existence of *negative ion drag force* in highly collisional plasma.

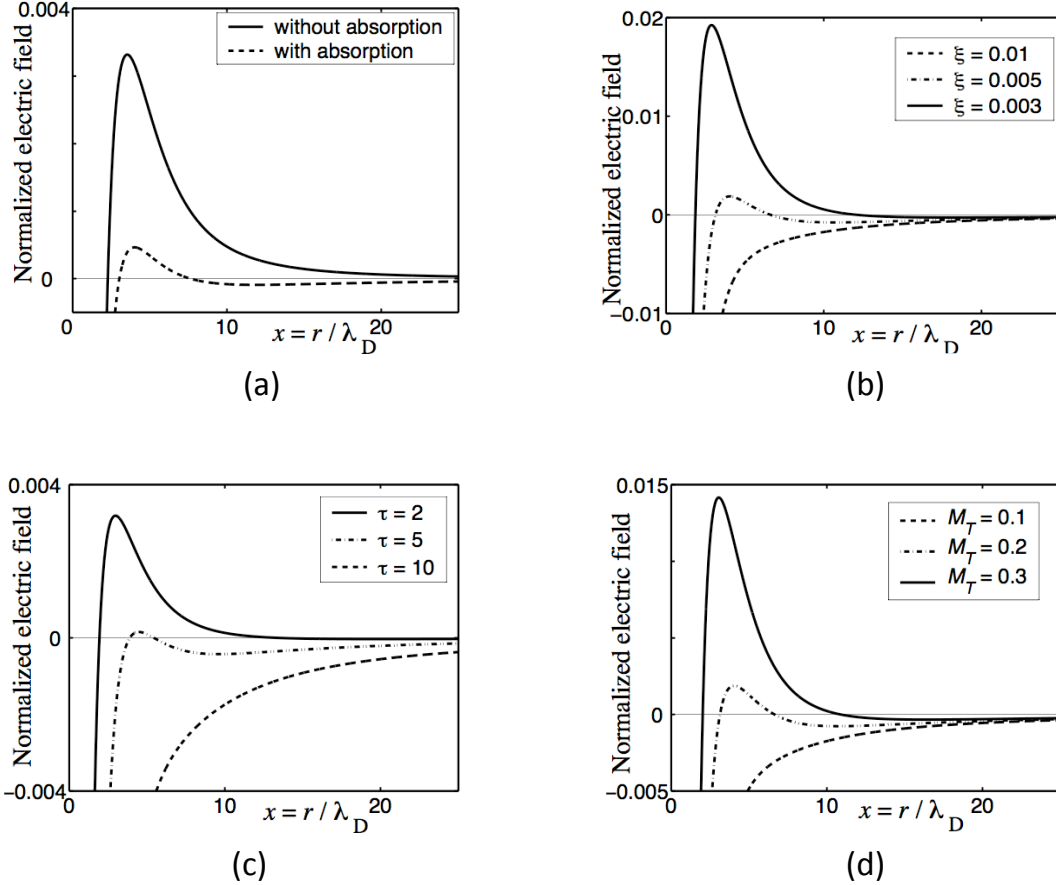


Figure 2.1: (a) Spatial variation of the normalized electric field behind a non-absorbing and absorbing spherical grain in highly collisional plasma (b)(c)(d) Spatial variation of the normalized electric field behind an absorbing spherical grain in highly collisional plasma for three different values of the normalized ion mean-free paths, $\xi = \ell_i/\lambda_D$, electron-to-ion temperature ratio, $\tau = T_e/T_i$ and the thermal Mach number, M_T . For detailed values of the parameters look at Ref. [144].

2.1.4 Discussion

The importance of plasma absorption in the limiting case of highly collisional flowing plasma has been discussed. At large distances absorption completely determines the behavior of the electric field, and it decays as $\propto r^{-2}$. It is shown that both short- and long-range asymptotes are repulsive for a pair of negatively charged grains aligned along the ion flow, but at moderate distances attraction can take place in certain parameter regimes. It was shown that a negative ion drag force is possible in certain parameter regimes and the main physical process responsible for this effect is identified as *ion absorption* on the grain surface.

2.2 Effective charge of a small absorbing body in highly collisional plasma subject to an external electric field

2.2.1 Objectives

Often large-scale electric fields exist in complex plasmas. The direct effect of the electric field is to exert an electric force on the highly charged dust particles. On the other hand, the indirect effect is to produce ion and electron drag forces on the grains which are nothing but the momentum transfer rates from drifting ions and electrons to the grains. The competition between these forces is responsible for different types of static and dynamic properties of the grain component, affect wave phenomena, etc. [45, 46, 47, 48]. Often the ion drag force dominates over the electron drag force because of the large ion-to-electron mass ratio. However, this situation may change when the electrons drift much faster than the ions because of their much higher mobility. It was shown in an earlier work by Khrapak and Morfill [148] that in the collisionless regime the electron drag force can indeed dominate over the electric and ion drag forces provided the electron-to-ion temperature ratio is not too high.

In this work we analyze the electric force, ion and electron drag forces in a highly collisional plasma subject to a weak electric field taking into account plasma absorption on the grain surface. The characteristic of the total force which is the sum of electric, ion drag and electron drag forces is analyzed. The “effective charge” which is the ratio of total force to the electric field is calculated.

2.2.2 Model

A small spherical negatively charged stationary grain is placed in highly collisional, weakly ionized plasma with a constant weak external electric field. The ions drift in the direction of the electric field, whereas electrons drift in the opposite direction. The electric field is sufficiently weak so that both electron and ion drifts are subthermal. There are no plasma sources or sinks except at the grain surface, which is fully absorbing. Both the ion and electron components are suitably described by the corresponding continuity and momentum equations. The self-consistent electrostatic potential around the absorbing point-like grain

is obtained by solving Poisson equation using linear dielectric response formalism. From this the polarization part of the total force is calculated.

2.2.3 Results

The total drag force acting on a floating absorbing test grain has been calculated [Eqn.(8)]. The first term in this expression represents the sum of ion and electron drag forces acting on a non-absorbing grain. These two forces are directed along the drift velocities of the corresponding species, *i.e.* they act in the opposite directions and the ratio of their absolute magnitude is $(T_e/T_i)^2$. This implies that in one temperature plasma ($T_e = T_i$) they exactly cancel each other. In highly non-thermal plasma ($T_e \gg T_i$) the ion drag force always dominates, in contrast to the collisionless regime. The ratio of the ion drag force to electric one is $(1/6)\beta$ where β is the scattering parameter. The second sum in Eq.(8) represents the contributions to the drag forces associated with ion and electron absorptions on the grain. Under typical conditions the ratio of the ion and electron drag forces due to absorption is $|F_i/F_e|_{abs} \approx (T_e/T_i)^2$. The ion absorption on the grain surface changes the direction of the ion drag force in highly collisional plasma, whilst electron absorption increases the magnitude of the electron drag force. The absolute ratio of total ion-to-electron drag force is, $|F_i/F_e| \approx (T_e/T_i)$. The total force which is the sum of electric, ion drag and electron drag forces is proportional to the electric field and the proportionality constant represents the “effective” charge such as $\mathbf{F} = Q_{eff}\mathbf{E}$. In the considered regime the grain effective charge can be written as, $Q_{eff}/Q = 1 + (1/6)\beta(T_i/T_e)$.

2.2.4 Discussion

The effect of ion absorption reduces the absolute magnitude of the ion drag force for negatively charged grains whereas the effect of electron absorption increases the magnitude of the electron drag force. In the continuum regime and for infinitesimal small grain it is shown that both ion and electron drag forces are directed in the same direction (opposite to the electric field). The electric force acts in the same direction. The applicability of linear theory requires $\beta < 1$ while usually $T_i \ll T_e$. Thus, we have $Q_{eff} \approx Q$ which implies that both the ion and electron drag forces acting on the absorbing grain are small compared to the electric force in the considered case of highly collisional plasma.

2.3 Ion drag force on a small grain in highly collisional weakly anisotropic plasma: Effect of plasma production and loss mechanisms

2.3.1 Objectives

In the two previous studies of this cumulative thesis it is assumed that plasma sources and sinks are absent in the vicinity of the grain. However, even when plasma losses on the grain component due to absorption are unimportant (*e.g.* individual grain) other loss mechanisms such as three body volume recombination and/or ambipolar diffusion towards discharge walls and electrodes are still present. Hence, in a realistic plasma environment, some plasma production and loss processes are always present in the vicinity of a grain.

The motivation of this work is to investigate the effect of these processes on the (isotropic) potential distribution around the dust grain and also on the ion drag force acting on them.

2.3.2 Model

A small stationary negatively charged spherical grain is immersed in a weakly ionized quasineutral, highly collisional plasma. Plasma sources and sinks are present in the vicinity of the grain which itself also acts as a sink due to plasma absorption on its surface. The plasma production is only due to electron impact ionization ($Q_I = \nu_I n_e$). For the plasma loss processes two mechanisms are considered: in high pressure plasma the loss is mainly due to electron-ion volume recombination ($Q_L = \nu_R n_i$) and in low/moderate pressure gas discharge the plasma loss is due to ambipolar diffusion towards the discharge chamber walls or electrodes ($Q_L = \nu_L n_i$). Here, ν_I , ν_R and ν_L are ionization frequency, electron-ion volume recombination frequency and loss frequency due to ambipolar diffusion loss. The collisional ion component is described by the continuity and momentum equations in the hydrodynamic approximation. For electrons the Boltzmann distribution is used. The self-consistent potential distribution around the grain is obtained by solving the Poisson equation using linear response technique.

2.3.3 Results

Considering both types of loss mechanisms, analytical expressions for the isotropic potential distribution around the grain and ion drag force have been obtained. When the plasma loss is due to electron-ion volume recombination, the potential is described by the superposition of the two exponentials with different inverse screening lengths and with different effective charges. Both these screening lengths and effective charges depend on the strength of plasma production. Depending on the strength of plasma production two limiting cases have been considered: low and high ionization rate. In the limit of low ionization rate ($\nu_I/D_i \ll k_D^2$), the characteristic screening length is $\lambda_{De}(\ell_i k_D) \sqrt{\nu/\nu_I}$ which is much larger than the electron Debye radius since $(\ell_i k_D) \gg \sqrt{\nu/\nu_I}$ in the considered regime. Here D_i is the ion diffusion coefficient. For distances $\lambda_D \ll r \ll \lambda_{De}(\ell_i k_D) \sqrt{\nu/\nu_I}$ the potential is Coulomb-like. This is a familiar expression for the potential in the absence of ionization-recombination process in the vicinity of the grain. Thus the distance $\lambda_{De}(\ell_i k_D) \sqrt{\nu/\nu_I}$ determines the length scale below which plasma production is not important and sets up the upper limit of applicability of the results obtained within the assumption of no ionization/recombination processes in the vicinity of the grain [98, 149]. In the opposite case of high ionization rate ($\nu_I/D_i \gg k_D^2$), the potential is again screened completely with the screening length equal to the electron Debye radius λ_{De} and is independent of the ionization rate ν_I . The expression for the ion drag force is derived [Eq. (17)]. Three dimensionless parameters enter into this expression: $\vartheta = \nu_I/\nu$, the ratio of ionization and ion-neutral collision frequencies, $\tau = T_e/T_i$, the electron-to-ion temperature ratio and $\xi_i = \lambda_{Di}/\ell_i$, the inverse normalized ion mean free path. In the absence of ionization and recombination the ion drag force is negative *i.e.* it is directed oppositely to the ion drift. The same is true for low ionization rate. When the ionization rate increases the ion drag force reverses its direction. The value of ϑ for which this reversal occurs is plotted as a function of ξ_i in Fig.(2.2) for three different values of τ . Note that for large ξ_i the transition from negative to positive values of the ion drag force can be well described by $\vartheta \approx 1/\xi_i \sqrt{\tau}$. Thus, in a plasma with sufficiently developed ionization the ion drag force is always directed along the ion motion.

When the plasma loss is due to ambipolar diffusion the potential is not completely screened, but has a Coulomb-like long-range asymptote. It is shown that in the limit of low ionization rate the plasma production/loss processes are of minor importance. However, in

the opposite limit of high ionization rate, the screening length is completely determined by ionization and ambipolar loss processes. The *effective charge* that governs the long-range asymptote of the potential is of the order of the *actual charge* which implies that even partial plasma screening is of minor importance. The ion drag force is again expressed in terms of the three dimensionless parameters (τ, ξ_i, ϑ) mentioned above. In the absence of ionization and ambipolar loss ($\vartheta = 0$) as well as for sufficiently low ionization strength the ion drag force remains negative. The transition from negative-to-positive ion drag forces occurs when $\vartheta \simeq 1/\tau$, as can be seen from Fig.(2.2). Unlike in the previous case when the transitional value of θ depends on both ξ_i and τ , now it depends only on τ . Thus, for both considered mechanisms of plasma loss the ion drag force becomes positive, *i.e.* directed along the ion drift provided the ionization strength is high enough.

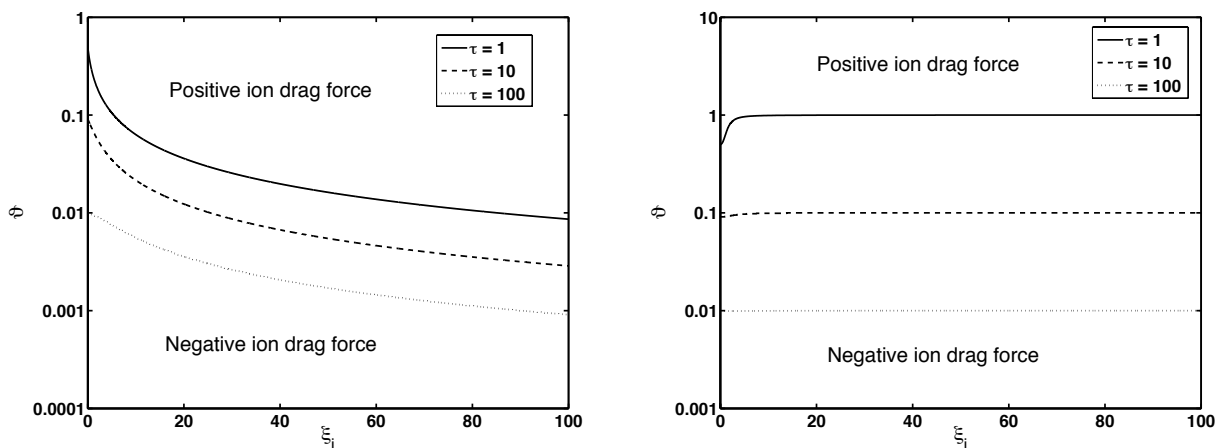


Figure 2.2: Variation of transitional normalized ionization frequency, ϑ with normalized inverse ion mean free path, ξ_i for three different electron-to-ion temperature ratios, $\tau = 1, 10$ and 100 . Curves correspond to transition between positive and negative values of the ion drag force. In the *left figure* the plasma production is due to electron impact ionization and plasma loss is due to electron-ion volume recombination. With a reasonable accuracy the transition occurs for $\vartheta \approx 1/\xi_i \sqrt{\tau}$. In the *right figure* the plasma production is due to electron impact ionization and plasma loss is due to ambipolar diffusion to discharge walls and electrodes. In this case the transition occurs when $\vartheta \approx 1/\tau$.

2.3.4 Discussion

We have analyzed the electric potential distribution in isotropic plasmas and the ion drag force acting on an absorbing grain in weakly anisotropic plasmas taking into account ionization and loss processes in the vicinity of the grain. It is shown that the conventional

Debye-Hückel (Yukawa) potential distribution around the grain operates only in the absence of ionization and absorption processes. For volume recombination mechanism the potential consists of two exponential terms and the long-range potential is of Debye-Hückel type. On the other hand, for ambipolar diffusion loss mechanism the long-range potential is Coulomb-like with effective charge of the order of the actual one. The ion drag force acting on the absorbing grain is negative when the ionization rate is low. However, when the ionization rate increases the force eventually reverses its direction. For sufficiently high ionization rate the ion drag force is positive independent of the plasma loss mechanisms. The parameter regimes for the positive and negative ion drag forces have been identified for both plasma loss mechanisms considered.

Chapter 3

Conclusion

3.1 Outlook

The motivation to write this section is to mention briefly the applicability of this thesis work in different research areas in plasma physics. This work is concerned with some properties of charged dust particles in highly collisional complex plasma. Though there are many examples of highly collisional complex plasmas in nature as well as in industrial and medical applications, we mention here some of them briefly.

Experimental investigations of thermal complex plasmas were performed in a quasilaminar, weakly ionized plasma flow at temperatures of $1700 - 2200K$ and atmospheric pressure where dust particles form ordered structures [150, 151, 152]. Thermal plasma is defined as a low-temperature plasma characterized by equal temperatures of the electron, ion and neutral gas particles. The dust particles were charged by background electron and ion fluxes and also by thermionic emission. In this case the thermionic emission plays a dominant role due to which the dust particles become positively charged and contain thousands of elementary charges. The possible application of these plasmas are associated with the studies of the properties of rocket-fuel combustion products, synthesis of fine powders, plasma sintering of ceramic materials, plasma spraying, plasma in hydrocarbon flames etc. [153, 154, 155, 156].

Another important fact is to be noted that plasmas at low pressure are used with very high performance in many systems, such as, etching, plasma processing, deposition of complex nano structured layers, surface cleaning, bacterial sterilisation, biocompatible

coating, surface functionalisation for cell adhesion etc. [23, 157, 158, 159, 160]. However, the major drawback of low-pressure processing is the use of vacuum reactors which causes high cost, contamination, need of specific materials etc. Recently, new trends in plasma technology are associated with the construction of new non-thermal atmospheric plasma sources for the material processing and surface treatments [161, 162]. Plasma can be used for the treatment of living animal and human tissues. Non-thermal plasma at atmospheric pressure is an exceptional system which operate at the human body temperature, emit little or harmful radiation, secrete controllable amounts of active species and address only the target area without spreading over the whole treated object. Some of the medically applicable atmospheric plasma sources are high frequency plasma jets, torches, needles, microwave sources etc. [163, 164, 165, 166, 167].

3.2 Future works

- The effect of many dust particles (collective effects) on the potential distribution around an absorbing test grain in highly collisional plasmas.
- Stability of dust acoustic waves taking into account plasma absorption on the grain surface in highly collisional plasma. Effect of plasma production and loss as well as dust charge variations can also be taken into account. This would include investigation of instabilities (*e.g.* Rayleigh-Taylor) down to the discrete (single particle) level.
- The dust acoustic solitary (DAS) waves have been investigated using gas dynamical approach [168]. It would be interesting to investigate the effect of plasma production and loss as well as dust charge variations on DAS waves in highly collisional plasma.

Bibliography

- [1] L. Spitzer, *Physical Processes in the Interstellar Medium*, John Wiley and Sons, New York, 1978.
- [2] M. Horányi, H. Houpis, and D. A. Mendis, *Astrophys. Space Sci.* **144**, 212 (1988).
- [3] J. Cho and M. Kelley, *Rev. Geophys.* **31**, 243 (1993).
- [4] O. Havnes et al., *J. Geophys. Res.* **101**, 10839 (1996).
- [5] D. A. Mendis, *Annu. Rev. Astron. Astrophys.* **26**, 11 (1988).
- [6] N. Divine, *J. Geophys. Res.* **98**, 17029 (1993).
- [7] S. Kaplan, *Interstellar Gas Dynamics*, Pergamon Press, 1966.
- [8] G. Morfill and M. Scholer, *Physical Processes in Intrstellar Clouds*, Reidel Publ. Comp., 1992.
- [9] T. W. Backhouse, *Meteorol. Mag.* **20**, 133 (1985).
- [10] A. Juhász and M. Horányi, *J. Geophys. Res.* **104**, 12577 (1999).
- [11] R. Greenberg, A. Brahic, and eds., *Planetary Rings*, The University of Arizona Press, Arizona, 1984.
- [12] B. A. Smith et al., *Science* **212**, 163 (1981).
- [13] B. A. Smith et al., *Science* **215**, 504 (1982).
- [14] C. K. Goertz and G. E. Morfill, *Icarus* **53**, 219 (1983).

-
- [15] E. Grün, G. E. Morfill, R. J. Terrile, T. V. Johnson, and G. Schwehm, *Icarus* **54**, 227 (1983).
- [16] G. E. Morfill and H. M. Thomas, *Icarus* **179**, 539 (2005).
- [17] J. T. Bergstrahl, E. D. Miner, and M. S. Matthews, *Uranus*, The University of Arizona Press, Tuscon, 1991.
- [18] M. E. Ockert, J. N. Cuzzi, C. C. Porco, and T. V. Johnson, *J. Geophys. Res.* **92**, 14696 (1987).
- [19] D. P. Cruikshank, *Neptune and Triton*, The University of Arizona Press, Tuscon, 1996.
- [20] G. S. Selwyn, J. Singh, and R. S. Bennett, *J. Vac. Sci. Technol. A* **7**, 2758 (1989).
- [21] G. S. Selwyn, *Plasma Sources Sci. Technol.* **3**, 340 (1994).
- [22] H. Kersten et al., *Contrib. Plasma Phys.* **41**, 598 (2001).
- [23] A. Bouchoule, *Technological impacts of dusty plasmas*, in: *A. Bouchoule (Ed.), Dusty Plasmas: Physics, Chemistry and Technological Impacts in Plasma Processing*, Wiley, Chichester, 1999.
- [24] S. V. Vladimirov, K. Ostrikov, and A. A. Samarian, *Physics and applications of Complex Plasmas*, Imperial College, Lonon, 2005.
- [25] H. Ikezi, *Phys. Fluids* **29**, 1764 (1986).
- [26] H. Thomas et al., *Phys. Rev. Lett.* **73**, 652 (1994).
- [27] J. Chu and L. I, *Phys. Rev. Lett.* **72**, 4009 (1994).
- [28] Y. Hayashi and S. Tachibana, *Jpn. J. Appl. Phys.* **33**, L804 (1994).
- [29] A. Melzer, T. Trottenberg, and A. Piel, *Phys. Lett. A* **191**, 301 (1994).
- [30] H. M. Thomas and G. E. Morfill, *Nature (London)* **379**, 806 (1996).
- [31] V. E. Fortov et al., *JETP Lett.* **64**, 92 (1996).

-
- [32] V. E. Fortov et al., JETP Lett. **63**, 187 (1996).
- [33] V. E. Fortov et al., Dokl. Phys. **44**, 279 (1999).
- [34] A. Nefedov et al., New J. Phys. **5**, 33 (2003).
- [35] H. Thomas et al., New J. Phys. **10**, 033036 (2008).
- [36] J. Winter, Plasma Phys. Control. Fusion **40**, 1201 (1998).
- [37] V. Tsytovich and J. Winter, Phys. Usp. **41**, 815 (1998).
- [38] J. Winter and G. Gebauer, J. Nucl. Mater **266**, 228 (1999).
- [39] J. Winter, Phys. Plasmas **7**, 3862 (2000).
- [40] S. I. Krasheninnikov, Y. Tomita, R. Smirnov, and R. Janev, Phys. Plasmas **11**, 3141 (2004).
- [41] J. Winter, V. Fortov, and A. Nefedov, J. Nucl. Mater **290-293**, 509 (2001).
- [42] J. D. Martin, M. Coppins, and G. Counsell, J. Nucl. Mater **337-339**, 114 (2005).
- [43] C. Castaldo et al., Nucl. Fusion **47**, L5 (2007).
- [44] S. Ratynskaia et al., Nucl. Fusion **48**, 015006 (2008).
- [45] P. K. Shukla and A. A. Mamun, *Introduction to Dusty Plasma Physics*, IoP Publishing Ltd, London, 2002.
- [46] V. E. Fortov, A. G. Khrapak, S. A. Khrapak, V. I. Molotkov, and O. F. Petrov, Phys. Usp. **47**, 447 (2004).
- [47] S. V. Vladimirov and K. Ostrikov, Phys. Reports **393**, 175 (2004).
- [48] V. E. Fortov, A. V. Ivlev, S. A. Khrapak, A. G. Khrapak, and G. E. Morfill, Phys. Reports **421**, 1 (2005).
- [49] V. N. Tsytovich, G. E. Morfill, S. V. Vladimirov, and H. M. Thomas, *Elementary Physics of Complex Plasmas*, Springer, Berlin Heidelberg, 2008.

-
- [50] J. D. Swift and M. J. R. Schwar, *Electric Probes for Plasma Diagnostics*, Iliffe Books, London, 1971.
- [51] P. M. Chung, L. Talbot, and K. J. Touryan, *Electric Probes in Stationary and Flowing Plasmas: Theory and Application*, Springer, New York, 1975.
- [52] H. M. Mott-Smith and I. Langmuir, *Phys. Rev.* **28**, 727 (1926).
- [53] J. E. Allen, B. M. Annaratone, and U. de Angelis, *J. Plasma Phys.* **63**, 299 (2000).
- [54] M. Lampe, *J. Plasma Phys.* **65**, 171 (2001).
- [55] I. B. Bernstein and I. M. Rabinowitz, *Phys. Fluids* **2**, 112 (1959).
- [56] J. E. Dougherty, M. D. Kilgore, R. K. Porteous, and D. B. Graves, *J. Appl. Phys.* **72**, 3934 (1992).
- [57] J. G. Laframboise, *The Theory of Spherical and Cylindrical Probes in a Collisionless, Maxwellian Plasma at Rest*, Institute for Aerospace Studies, University of Toronto, Toronto, 1966.
- [58] R. V. Kennedy and J. E. Allen, *J. Plasma Phys.* **69**, 485 (2003).
- [59] J. Goree, *Phys. Rev. Lett.* **69**, 277 (1992).
- [60] M. Lampe, V. Gavrishchaka, G. Ganguli, and G. Joyce, *Phys. Rev. Lett.* **86**, 5278 (2001).
- [61] A. V. Zobnin, A. P. Nefedov, V. A. Sinel'shchikov, and V. E. Fortov, *JETP* **91**, 483 (2000).
- [62] M. Lampe et al., *Phys. Plasmas* **10**, 1500 (2003).
- [63] S. Ratynskaia et al., *Phys. Rev. Lett.* **93**, 085001 (2004).
- [64] S. A. Khrapak et al., *Phys. Rev. E* **72**, 016406 (2005).
- [65] C. H. Su and S. H. Lam, *Phys. Fluids* **6**, 1479 (1963).
- [66] E. Baum and R. L. Chapkis, *AIAA J.* **8**, 1073 (1970).

-
- [67] J.-S. Chang and J. G. Laframboise, *Phys. Fluids* **19**, 25 (1976).
- [68] S. Khrapak, G. Morfill, A. G. Khrapak, and L. G. D'yachkov, *Phys. Plasmas* **13**, 052114 (2006).
- [69] G. E. Morfill and E. Grün, *Planet. Space. Sci.* **27**, 1269 (1979).
- [70] G. E. Morfill, E. Grün, and T. V. Johnson, *Planet. Space. Sci.* **28**, 1087 (1980).
- [71] C. Cui and J. Goree, *IEEE Trans. Plasma Sci.* **22**, 151 (1994).
- [72] T. Matsoukas and M. Russell, *J. Appl. Phys.* **77**, 4285 (1995).
- [73] T. Matsoukas, M. Russell, and M. Smith, *J. Vac. Sci. Technol. A* **14**, 624 (1996).
- [74] T. Matsoukas and M. Russell, *Phys. Rev. E* **55**, 991 (1997).
- [75] O. Bystrenko, T. Bystrenko, and A. Zagorodny, *Phys. Lett. A* **329**, 83 (2004).
- [76] O. S. Vaulina, S. A. Khrapak, A. P. Nefedov, and O. F. Petrov, *Phys. Rev. E* **60**, 5959 (1999).
- [77] O. S. Vaulina, A. P. Nefedov, O. F. Petrov, and S. A. Khrapak, *JETP* **88**, 1130 (1999).
- [78] R. A. Quinn and J. Goree, *Phys. Rev. E* **61**, 3033 (2000).
- [79] G. E. Morfill, A. V. Ivlev, and J. R. Jokipii, *Phys. Rev. Lett.* **83**, 971 (1999).
- [80] A. V. Ivlev, U. Konopka, and G. E. Morfill, *Phys. Rev. E* **62**, 2739 (2000).
- [81] S. A. Khrapak and G. E. Morfill, *Phys. Plasmas* **9**, 619 (2002).
- [82] V. V. Zhakhovskii et al., *JETP Lett.* **66**, 419 (1997).
- [83] S. K. Zhdanov, A. V. Ivlev, and G. E. Morfill, *Phys. Plasmas* **12**, 072312 (2005).
- [84] F. F. Chen, *Introduction to Plasma Physics*, Plenum, New York, 1974.
- [85] P. K. Shukla, *Phys. Plasmas* **8**, 1791 (2001).

-
- [86] V. N. Tsytovich, G. E. Morfill, and H. Thomas, *Plasma Physics Reports* **28**, 623 (2002).
- [87] G. E. Morfill, V. N. Tsytovich, and H. Thomas, *Plasma Physics Reports* **29**, 1 (2003).
- [88] S. Ichimaru, *Rev. Mod. Phys.* **54**, 1017 (1982).
- [89] *NRL Plasma Formulary*, Naval Research Laboratory, Washington DC, 1990.
- [90] G. Morfill et al., *Phys. Plasmas* **6**, 1769 (1999).
- [91] V. N. Tsytovich, *Phys. Usp.* **40(1)**, 53 (1997).
- [92] U. Konopka, G. E. Morfill, and L. Ratke, *Phys. Rev. Lett.* **84**, 891 (2000).
- [93] Y. L. A'lpert, A. V. Gurevich, and L. P. Pitaevsky, *Plasma Physics with Artificial Satellites*, Consultants Bureau, New York, 1965.
- [94] S. Khrapak, A. Ivlev, and G. Morfill, *Phys. Rev. E* **64**, 046403 (2001).
- [95] S. Khrapak et al., *Phys. Rev. Lett.* **96**, 015001 (2006).
- [96] I. M. Cohen, *Phys. Fluids* **6**, 1492 (1963).
- [97] O. Bystrenko and A. Zagorodny, *Phys. Rev. E* **67**, 066403 (2003).
- [98] S. Khrapak, S. Zhdanov, A. Ivlev, and G. Morfill, *J. Appl. Phys.* **101**, 033307 (2007).
- [99] A. F. Aleksandrov, L. S. Bogdankevich, and A. A. Rukhadze, *Principles of Plasma Electrodynamics*, Springer, New York, 1984.
- [100] N. A. Krall and A. W. Trivelpiece, *Principles of Plasma Physics*, McGraw-Hill, New York, 1973.
- [101] D. Montgomery, G. Joyce, and R. Sugihara, *Plasma Phys.* **10**, 681 (1968).
- [102] L. Stenflo, M. Y. Yu, and P. K. Shukla, *Phys. Fluids* **16**, 450 (1973).
- [103] S. V. Vladimirov and M. Nambu, *Phys. Rev. E* **52**, R2172 (1995).
- [104] O. Ishihara and S. V. Vladimirov, *Phys. Plasmas* **4**, 69 (1997).

-
- [105] G. Lapenta, Phys. Rev. E **62**, 1175 (2000).
- [106] M. Lampe, G. Joyce, G. Ganguli, and V. Gavrishchaka, Phys. Plasmas **7**, 3851 (2000).
- [107] S. A. Maierov, S. V. Vladimirov, and N. F. Cramer, Phys. Rev. E **63**, 017401 (2001).
- [108] D. Winske, IEEE Trans. Plasma Sci. **29**, 191 (2001).
- [109] M. Lampe, G. Joyce, and G. Ganguli, Phys. Scripta **T89**, 106 (2001).
- [110] L.-J.Hou, Y.-N.Wang, and Z. L. Miškovič, Phys. Rev. E **68**, 016410 (2003).
- [111] S. A. Khrapak, A. V. Ivlev, and G. E. Morfill, Phys. Rev. E **70**, 056405 (2004).
- [112] G. E. Morfill et al., Phys. Rev. Lett. **83**, 1598 (1999).
- [113] J. Goree, G. E. Morfill, V. N. Tsytovich, and S. V. Vladimirov, Phys. Rev. E **59**, 7055 (1999).
- [114] M. Kretschmer et al., Phys. Rev. E **71**, 056401 (2005).
- [115] A. M. Lipaev et al., Phys. Rev. Lett. **98**, 265006 (2007).
- [116] M. Wolter, A. Melzer, O. Arp, M. Klindworth, and A. Piel, Phys. Plasmas **14**, 123707 (2007).
- [117] U. Konopka et al., Phys. Rev. E **61**, 1890 (2000).
- [118] P. K. Kaw, K. Nishikawa, and N. Sato, Phys. Plasmas **9**, 387 (2002).
- [119] D. Samsonov and J. Goree, Phys. Rev. E **59**, 1047 (1999).
- [120] M. Barnes, J. Keller, J. Forster, J. O'Neill, and D. Coultas, Phys. Rev. Lett. **68**, 313 (1992).
- [121] N. D'Angelo, Phys. Plasmas **5**, 3155 (1998).
- [122] A. Ivlev, D. Samsonov, J. Goree, G. Morfill, and V. Fortov, Phys. Plasmas **6**, 741 (1999).
- [123] S. A. Khrapak and V. V. Yaroshenko, Phys. Plasmas **10**, 4616 (2003).

-
- [124] A. Uglov and A. Gnedovets, *Plasma Chem. Plasma Proc.* **11**, 251 (1991).
- [125] S. Khrapak, A. Ivlev, G. Morfill, and H. Thomas, *Phys. Rev. E* **66**, 046414 (2002).
- [126] S. Khrapak, A. Ivlev, G. Morfill, and S. Zhdanov, *Phys. Rev. Lett.* **90**, 225002 (2003).
- [127] S. Khrapak, A. Ivlev, G. Morfill, S. Zhdanov, and H. M. Thomas, *IEEE Trans. Plasma Sci.* **32**, 555 (2004).
- [128] A. Ivlev, S. Khrapak, S. Zhdanov, G. Morfill, and G. Joyce, *Phys. Rev. Lett.* **92**, 205007 (2004).
- [129] A. Ivlev, S. Zhdanov, S. Khrapak, and G. Morfill, *Phys. Rev. E* **71**, 016405 (2005).
- [130] S. Khrapak, A. Ivlev, S. Zhdanov, and G. Morfill, *Phys. Plasmas* **12**, 042308 (2005).
- [131] I. V. Schweigert, A. L. Alexandrov, and F. M. Peeters, *IEEE Trans. Plasma Sci.* **32**, 623 (2004).
- [132] D. Winske, *IEEE Trans. Plasma Sci.* **32**, 623 (2004).
- [133] I. H. Hutchinson, *Plasma Phys. Controlled Fusion* **47**, 71 (2005).
- [134] I. H. Hutchinson, *Plasma Phys. Controlled Fusion* **48**, 185 (2006).
- [135] C. Zafiu, A. Melzer, and A. Piel, *Phys. Plasmas* **9**, 4794 (2002).
- [136] C. Zafiu, A. Melzer, and A. Piel, *Phys. Plasmas* **10**, 1278 (2003).
- [137] M. Hirt, D. Block, and A. Piel, *Phys. Plasmas* **11**, 5690 (2004).
- [138] K. Matyash et al., *J. Phys. D* **37**, 2703 (2004).
- [139] V. Yaroshenko et al., *Phys. Plasmas* **12**, 093503 (2005).
- [140] V. Nosenko et al., *Phys. Plasmas* **14**, 103702 (2007).
- [141] A. Ivlev, S. Zhdanov, S. Khrapak, and G. Morfill, *Plasma Phys. Control. Fusion* **46**, B267 (2004).

-
- [142] S. V. Vladimirov, S. A. Khrapak, M. Chaudhuri, and G. E. Morfill, *Phys. Rev. Lett.* **100**, 055002 (2008).
- [143] S. A. Maiorov, *Plasma Phys. Reports* **31**, 690 (2005).
- [144] M. Chaudhuri, S. Khrapak, and G. Morfill, *Phys. Plasmas* **14**, 022102 (2007).
- [145] J. E. Allen, B. M. Annaratone, and U. de Angelis, *J. Plasma Phys.* **63**, 299 (2000).
- [146] G. Cooper, *Phys. Fluids* **12**, 2707 (1969).
- [147] E. W. Laing, A. Lamont, and P. J. Fielding, *J. Plasma Phys.* **5**, 441 (1971).
- [148] S. A. Khrapak and G. E. Morfill, *Phys. Rev. E* **69**, 066411 (2004).
- [149] S. Khrapak et al., *Phys. Rev. Lett.* **99**, 055003 (2007).
- [150] V. E. Fortov et al., *JETP Lett.* **63**, 187 (1996).
- [151] V. E. Fortov, A. P. Nefedov, O. F. Petrov, A. A. Samarian, and A. V. Chernyshev, *Phys. Rev. E* **54**, R2236 (1996).
- [152] V. E. Fortov, A. P. Nefedov, O. F. Petrov, A. A. Samarian, and A. V. Chernyshev, *JETP* **84**, 256 (1997).
- [153] T. M. Sugden and B. A. Thrush, *Nature* **168**, 703 (1951).
- [154] K. E. Shuler and J. Weber, *J. Chem. Phys.* **22**, 491 (1954).
- [155] M. S. Sodha and S. Guha, *Adv. Plasma Phys.* **4**, 219 (1971).
- [156] I. T. Iakubov and A. G. Khrapak, *Therm Phys. Rev.* **2**, 269 (1989).
- [157] M. A. Libermann and A. J. Lichtenberg, *Principles of Plasma Discharges and Materials Processing*, John Wiley & Sons, Inc., Hoboken, New Jersey, 2005.
- [158] M. Moisan, J. Barbeau, M. C. Crevier, J. Pelletier, and B. S. N. Philip, *Pure and Applied Chemistry* **74**, 349 (2002).
- [159] S. F. Cogan, D. J. Edell, A. A. Guzelian, Y. P. Liu, and R. Edell, *Journal of Biomedical Materials Research A* **67**, 856 (2003).

- [160] M. Mattioli-Belmonte et al., *Journal of Bioactive and Compatible Polymers* **20**, 343 (2005).
- [161] K. H. Becker, U. Kogelschatz, K. H. Schoenbach, and R. J. Barker, *Non-equilibrium air plasmas at atmospheric pressure*, IoP Publishing, London, 2005.
- [162] G. S. Selwyn, H. W. Herrmann, J. Park, and I. Henins, *Contrib. Plasma Phys.* **6**, 610 (2001).
- [163] J. Park, I. Henins, H. W. Herrmann, and G. S. Selwyn, *Journal of Applied Physics* **89**, 20 (2001).
- [164] E. Stoffels, A. J. Flikweert, W. W. Stoffels, and G. M. W. Kroesen, *Plasma Sources Science & Technology* **11**, 383 (2002).
- [165] V. L evell e and S. Coulombe, *Plasma Sources Science & Technology* **14**, 467 (2005).
- [166] E. Stoffels, *Contrib. Plasma Phys.* **47**, 40 (2007).
- [167] T. Shimizu et al., *Plasma Process and Polymers* , in press (2008).
- [168] S. Maitra and R. Roychoudhury, *Phys. Plasmas* **12**, 064502 (2005).

Acknowledgements

The work leading up to this thesis was done during my years as a PhD student at the theory group for Complex plasma in Max-Planck-Institut für extraterrestrische Physik. These years have been very stimulating and instructive, and the cordial atmosphere in the group has given rise to several interesting discussions and ideas, on topics related to my research.

At first I would like to thank Prof. Dr. Gregor Morfill, my supervisor and at the same time the group leader as well as one of the director of MPE, not only for his support and encouragement during this work, but also for allowing me to join his research group in the first place.

I want to give special thanks to Dr. Sergei Khrapak for his guidance, help and sharing with me some of his profound knowledge on theoretical complex plasma physics.

The pleasant research atmosphere at the group is of course also a product of all the other members and the guest researchers of the group: Dr. Hubertus Thomas, Dr. Alexei Ivlev, Dr. Markus Thoma, Dr. Milenko Zuzic, Dr. Uwe Konopka, Prof. Vadim Tsytovich, Dr. Beatrice Annaratone, Dr. Sergei Zhdanov, Dr. Boris Klumov, Dr. Sergei Vladimirov, Dr. Yangfang Li, Dr. Michael Kretschmer, Herwig Höfner, Robert Sutterlin, Dr. Victoria Yaroshenko, Dr. Vladimir Nosenko, Dr. Mikhael Pustynnik, Dr. Tetsuji Shimizu, Dr. Satoshi Shimizu, Dr. Pintu Bandopadhyay, Dr. Roman Kompaneets, Dr. Tatiana Antonova, Martin Fink, Peter Huber, Christina Knapek, Mierk Schwabe, Ralf Heidemann, Slobodan Mitic, Philip Brandt, and Ke Jiang.

Of these I want to give special thanks to Beatrice and Hubertus for guiding me with some experimental knowledge in this field. I am thankful to Robert, Ralf, and Peter for helping me a lot concerning computers. Also I want to thank Dr. Sergei Zhdanov and Ralf for sharing the same office room with me and making some stimulative discussion on various interesting topics in the world.

I am thankful to our secretaries Angelika Langer and Elsbeth Collmar for their cordial support to solve any administrative problems I have faced in these days.

I also want to take the opportunity to thank Prof. Robindranath Pal, Prof. Sita Janaki and Dr. Nikhil Chakraborti for giving me the first lesson on Plasma physics at the post-MSc course work at Saha Institute of Nuclear Physics in India.

Finally I want to thank my parents Sitansu Chaudhuri and Santa Chaudhuri, along with my two beloved elder sisters, Sukrishna and Sulagna and their families for their constant support at every moment in my life. At the end, I am thankful to all my friends and well wishers (in particular, Anasuya, Piu and Mainak da) for their love and blessings without which it was not possible to cross this milestone.

Curriculum Vitae

Manis Chaudhuri

Date of birth January 20, 1978
Place of birth Serampore, India
Nationality Indian

Educational qualifications

1988 – 1994 Secondary education
 M. L. Boys' Academy, Serampore, India
1994 – 1996 Higher secondary education
 Chatra Nandalal Institution, Serampore, India
1996 – 1999 Bachelor of Science
 Serampore College, Calcutta University, India
1999 – 2001 Masters of Science
 Rajabazar Science College, Calcutta University, India
2003 – 2004 Post MSc
 Diploma thesis: Q-machine - A brief introduction
 Saha Institute of Nuclear Physics, Kolkata, India
2004 – 2005 PhD student at Saha Institute of Nuclear Physics, Kolkata, India
 working on Experimental and Theoretical Plasma Physics
 Thesis supervisor: Prof. Rabindranath Pal
2005 – 2008 PhD student
 Thesis topic: Electric potential and ion drag force in highly collisional
 complex plasma
 Thesis supervisor: Prof. Dr. Gregor Morfill
 Place: Max-Planck-Institut für extraterrestrische Physik, Garching and
 Ludwig-Maximilians-Universität, München, Germany

Awards

2003 Graduate Aptitude Test in Engineering (GATE), India
2003 Research Fellowship Award at Saha Institute of Nuclear Physics, India
2004 National Eligibility Test (NET) for CSIR-UGC Research Fellowship award

Working experience

2001 – 2003 Post Graduate Teacher

Publication list

3.3 Publication in refereed journals:

1. M. Chaudhuri, S. A. Khrapak and G. E. Morfill, Ion drag force on a small grain in highly collisional weakly anisotropic plasma: Effect of plasma production and loss mechanisms, *Phys. Plasmas* **15**, 053703 (2008).
2. S. V. Vladimirov, S. A. Khrapak, M. Chaudhuri and G. E. Morfill, Superfluid-like motion of an absorbing body in a collisional plasma, *Phys. Rev. Lett.* **93**, 085001 (2008)
3. M. Chaudhuri, S. A. Khrapak and G. E. Morfill, Effective charge of a small absorbing body in highly collisional plasma subject to an external electric field, *Phys. Plasmas* **14**, 054503 (2007).
4. M. Chaudhuri, S. A. Khrapak and G. E. Morfill, Electrostatic potential behind a macroparticle in a drifting collisional plasma: Effect of plasma absorption, *Phys. Plasmas* **14**, 022102 (2007).
5. B. M. Annaratone, P. Bandopadhyay, M. Chaudhuri and G. E. Morfill, A new diagnostic to characterize a plasma crystal, *New Journal of Physics*, **8**, 306 (2006).
6. M. Chaudhuri, N. Chakrabarti and R. Pal, Nonlinear hydromagnetic waves in two-ion-species plasmas, *Phys. Plasmas*, **12**, 112101 (2005).

3.4 Publication in conference proceedings:

1. M. Chaudhuri, S. A. Khrapak and G. E. Morfill, Ion drag force on an absorbing grain in highly collisional plasma in the presence of plasma production and loss processes, Fifth International Conference on Physics of Dusty Plasmas, 2008.
2. M. Chaudhuri, A. V. Ivlev, H. M. Thomas, G. E. Morfill, A. M. Lipaev, V. I. Molotkov, O. F. Petrov and V. E. Fortov, Complex Plasma Research under Microgravity, 58th International Astronautical Congress, 2007. Copyright IAF/IAA.
3. M. Chaudhuri, S. A. Khrapak and G. E. Morfill, Importance of plasma absorption to characterize the total force acting on a dust particle in highly collisional drifting plasma, 2nd International Conference on Dusty plasmas in applications, Odessa, Ukraine, 2007.

4. M. Chaudhuri, S. A. Khrapak and G. E. Morfill, Characterization of the electrostatic potential behind an absorbing dust particle in highly collisional drifting plasma, 34th European Physical Society Conference on Plasma Physics, Warsaw, ECA Vol.31F, 2007.
5. M. Chaudhuri, S. A. Khrapak and G. E. Morfill, Effect of plasma absorption on the total force acting on a dust grain in highly collisional drifting plasma, 34th European Physical Society Conference on Plasma Physics, Warsaw, ECA Vol.31F, 2007.
6. M. Chaudhuri, B. M. Annaratone and G. E. Morfill, Electrostatic forces on particles in plasma in presence of an electric field, 33rd European Physical Society Conference on Plasma Physics, Rome, ECA Vol.30I, 2006.
7. B. M. Annaratone, P. Bandopadhyay, M. Chaudhuri and G. E. Morfill, Measurement of the free electrons in a plasma crystal, 33rd European Physical Society Conference on Plasma Physics, Rome, ECA Vol.30I, 2006.

Enclosed papers

This cumulative thesis consists of following papers which are attached afterwords.

Copyright notice

Reprinted with permission from

- M. Chaudhuri, S. A. Khrapak and G. E. Morfill, Electrostatic potential behind a macroparticle in a drifting collisional plasma: Effect of plasma absorption, *Physics of Plasmas*, **14**, 022102 (2007).
- M. Chaudhuri, S. A. Khrapak and G. E. Morfill, Effective charge of a small absorbing body in highly collisional plasma subject to an external electric field, *Physics of Plasmas*, **14**, 054503 (2007).
- M. Chaudhuri, S. A. Khrapak and G. E. Morfill, Ion drag force on a small grain in highly collisional weakly anisotropic plasma: Effect of plasma production and loss mechanisms, *Phys. Plasmas* **15**, 053703 (2008).
- S. V. Vladimirov, S. A. Khrapak, M. Chaudhuri and G. E. Morfill, Superfluidlike Motion of an Absorbing Body in a Collisional Plasma, *Phys. Rev. Lett.*, **100**, 055003 (2008).

Copyright 2007, 2008, American Institute of Physics and American Physical Society.

Electrostatic potential behind a macroparticle in a drifting collisional plasma: Effect of plasma absorption

M. Chaudhuri, S. A. Khrapak, and G. E. Morfill

Max-Planck Institut für extraterrestrische Physik, D-85741 Garching, Germany

(Received 13 December 2006; accepted 28 December 2006; published online 2 February 2007)

The electric field and potential behind a small absorbing body (dust grain) at floating potential has been calculated analytically in a highly collisional drifting plasma. Linear plasma response formalism has been used and main attention has been focused on the effect of plasma absorption on the grain. It is shown that the long-range asymptote of the electric field is dominated by the effect of absorption and is always negative. Depending on plasma parameters, the electric field at intermediate distances can either increase monotonically or exhibit one maximum and one minimum. It can achieve positive values in certain parameter regimes, which indicates the possibility of electrostatic attraction between the grains aligned parallel to the flow. The obtained results can be important for understanding of the binary grain interactions in complex plasmas at elevated pressures. © 2007 American Institute of Physics. [DOI: 10.1063/1.2435707]

I. INTRODUCTION

“Dusty plasmas” (or “complex plasmas”) are plasmas containing micrometer-sized charged particles of solid matter (dust grains). The charged grains interact with each other, as well as with surrounding plasma, forming various self-organized structures. Since the grain component can be visualized and analyzed at the most fundamental kinetic level, complex plasmas are recognized as valuable model systems to investigate various phenomena (e.g., phase transitions, waves, transport, etc.).^{1–5}

The character of the intergrain interaction appears as one of the most fundamental questions for understanding the physics behind the observed phenomena in laboratory complex plasmas as well as in astrophysical plasmas,⁶ fusion devices,^{7–9} plasma processing,³ etc. The point is that the interaction potential is not fixed but depends considerably on complex plasma conditions. Diverse mechanisms of attractive and repulsive interactions have been discussed in the literature.^{2,5,10} One of the main interaction mechanisms is the electrostatic repulsion between like-charged particles. In isotropic collisionless plasmas the potential is often assumed to be of Debye-Hückel (Yukawa) form at relatively short distances (up to a few plasma screening lengths).^{2,11,12} At larger distances, the effect of continuous plasma absorption on the grain leads to much more slow decay of the potential,^{10,13–16} and it scales with distance as $\propto r^{-2}$. In isotropic collisional plasmas, the electrostatic potential around an absorbing body in the absence of ionization/recombination processes in its vicinity has an even more slowly decaying $\propto r^{-1}$ long-range asymptote.^{17–21}

However, complex plasmas are very often subject to self-consistent large-scale electric fields that induce plasma fluxes relative to the (often stationary) grain component. These flows, in addition to a direct dragging influence, are also responsible for the generation of collective plasma processes such as wake formation downstream from the grains, which strongly modify the electrostatic interaction compared to the isotropic case. From the collisionless kinetic theory of

conventional plasmas it is known that in anisotropic regime the long-range electric potential behind a test charge has an $\propto r^{-3}$ asymptote.^{22–24} Stenflo *et al.*²⁵ considered the effect of collisions and found out that the long-range potential around slowly moving test charge scales as $\propto r^{-2}$ if the collision frequency ν is larger than the plasma frequency, ω_p , and if $u/v_T \ll \omega_p/\nu$, where u is the test charge velocity and v_T is the thermal velocity of plasma particles. Recently, a theory of wakes behind an object in flowing plasmas has been developed in connection to complex plasmas.^{26–32} Both collisionless and collisional situations were studied, but the plasma absorption on the grain was usually neglected. To our knowledge, only Melandsø and Goree³³ took into account plasma absorption on a diffuse object in a supersonic flow of cold collisionless ions.

In the present paper, detailed analysis of highly collisional plasma limit where the plasma absorption by the grain can be easily accounted for has been performed. Using hydrodynamic description of slowly drifting ions and Boltzmann electrons, an analytical expression for the electric field behind a stationary grain has been derived in the linear approximation. It is shown that absorption has a considerable or even dominant effect on the electric field. The behavior of the electric field downstream from the grain is determined by three dimensionless parameters: electron-to-ion temperature ratio, ion drift velocity normalized to the ion thermal velocity, and the ratio of the ion mean-free path to the plasma screening length. The analysis shows that depending on these parameters the electric field is either negative for all distances or can assume positive values at intermediate distances. In the first case, two particles aligned in the ion flow would repel each other, while in the second case they would attract each other. This conclusion may be of interest for high-pressure collisional complex plasmas.

II. FORMULATION

We consider a stationary, negatively charged spherical particle that is immersed in a quasineutral, highly collisional

plasma. The ions are drifting with subthermal velocity while electrons form stationary background. Plasma absorption occurs on the grain surface; i.e., it acts as a plasma sink. Ionization/recombination processes are absent in the vicinity of the grain. The collisional ion component is described by the continuity and momentum equations in the hydrodynamic approximation:

$$\nabla(n_i \mathbf{v}_i) = -J_i \delta(\mathbf{r}), \quad (1)$$

$$(\mathbf{v}_i \nabla) \mathbf{v}_i = (e/m_i) \mathbf{E} - (\nabla n_i / n_i) v_{Ti}^2 - \nu \mathbf{v}_i. \quad (2)$$

The electron density satisfies Boltzmann relation

$$n_e \approx n_0 \exp(e\phi/T_e). \quad (3)$$

Here, $n_{i(e)}$ is the ion (electron) density, \mathbf{v}_i and m_i are the ion velocity and mass, respectively, J_i is the ion flux to the grain surface, $v_{Ti} = \sqrt{T_i/m_i}$ is the ion thermal velocity, ν is the (constant) momentum transfer frequency in ion-neutral collisions, n_0 is the unperturbed plasma density (far from the grain), $T_{i(e)}$ is the ion (electron) temperature, and \mathbf{E} is the total electric field. The above set of equations is closed with the Poisson equation

$$\Delta\phi = -4\pi e(n_i - n_e) - 4\pi Q\delta(\mathbf{r}). \quad (4)$$

The second term on the right-hand side of Eq. (4) represents the charge density distribution of a point-like grain located at the position \mathbf{r} . The point charge model gives reliable results when the plasma Debye length is much larger than the grain radius.

The system (1)–(4) constitutes in general a set of self-consistent nonlinear equations, which can only be solved numerically. However, for our purpose, which is to examine the effect of plasma absorption on the electric potential behind the grain in the ion flow, it is convenient to linearize the problem assuming $\mathbf{E} = \mathbf{E}_0 + \mathbf{E}_1$, $\mathbf{v}_i = \mathbf{u} + \mathbf{v}_1$, and $n_{i(e)} = n_0 + n_{i1(e1)}$, where \mathbf{E}_0 is the ambipolar electric field responsible for the ion drift (in the unperturbed state, $\mathbf{u} = e\mathbf{E}_0/m_i\nu$), \mathbf{E}_1 is the electric field perturbation, \mathbf{v}_1 is the ion velocity perturbation, and $n_{i1(e1)}$ is the perturbation of the ion (electron) density.

III. RESULTS

Assuming that the plasma perturbations are proportional to $\propto \exp(i\mathbf{k}\mathbf{r})$ and using linear response technique we get for the electric potential²¹

$$\phi_1(\mathbf{r}) = \frac{4\pi Q}{(2\pi)^3} \int \frac{\exp(i\mathbf{k}\mathbf{r}) d\mathbf{k}}{\chi_1(\mathbf{k}\mathbf{u}, k)} + \frac{4\pi e}{(2\pi)^3} \int \frac{\exp(i\mathbf{k}\mathbf{r}) d\mathbf{k}}{\chi_2(\mathbf{k}\mathbf{u}, k)}, \quad (5)$$

where

$$\chi_1(\mathbf{k}\mathbf{u}, k) = k^2 + k_{De}^2 + k_{Di}^2 \left[1 - \frac{\mathbf{k}\mathbf{u}(\mathbf{k}\mathbf{u} - i\nu)}{k^2 v_{Ti}^2} \right]^{-1}, \quad (6)$$

$$\chi_2(\mathbf{k}\mathbf{u}, k) = i \frac{k^2 v_{Ti}^2 (k^2 + k_{De}^2) - \mathbf{k}\mathbf{u}(\mathbf{k}\mathbf{u} - i\nu)(k^2 + k_{De}^2)}{J_i(\mathbf{k}\mathbf{u} - i\nu)}. \quad (7)$$

Here, $k_{Di(e)}$ is the inverse ion (electron) Debye radius and $k_D = \sqrt{k_{De}^2 + k_{Di}^2}$ is the inverse linearized Debye radius. The first term in Eq. (5) corresponds to the potential behind the point-like nonabsorbing grain in the limit of high collisionality.³⁴ The second term arises due to the ion absorption on the grain.

Inserting expressions (6) and (7) into Eq. (5) the potential can be in principle calculated. In order to proceed with analytical calculations let us consider the limit of very slow drift $k \gg u/\ell_i v_{Ti}$. The applicability of the hydrodynamic approximation requires $k \ll 1/\ell_i$. In this regime, the expressions for χ_1 and χ_2 can be simplified:

$$\chi_1^{-1} \approx \frac{1}{k^2 + k_D^2} + i \frac{k_{Di}^2}{(k^2 + k_D^2)^2} \frac{\mathbf{k}\mathbf{u}\nu}{k^2 v_{Ti}^2}, \quad (8)$$

$$\chi_2^{-1} = -\frac{J_i \nu}{k^2 v_{Ti}^2 (k^2 + k_D^2)} + i \frac{k^2 + k_{De}^2}{(k^2 + k_D^2)^2} \frac{J_i \mathbf{k}\mathbf{u} \nu^2}{k^4 v_{Ti}^4}. \quad (9)$$

From the point of view of integration over \mathbf{k} in Eq. (5), it is convenient to calculate the electric field $\mathbf{E}_1 = -\nabla\phi_1$, rather than the potential itself. After cumbersome but straightforward integrations, we get for the electric field downstream from the grain the following expression:

$$\begin{aligned} E_1 = & (Qk_D^2) \frac{(1+x)\exp(-x)}{x^2} \\ & - \left(\frac{Q\nu u k_{Di}^2}{2k_D v_{Ti}^2} \right) \frac{4 - (x^3 + 2x^2 + 4x + 4)\exp(-x)}{x^3} \\ & - \left(\frac{eJ_i \nu}{v_{Ti}^2} \right) \frac{1 - (1+x)\exp(-x)}{x^2} - \left(\frac{eJ_i u \nu^2}{2v_{Ti}^4 k_D} \right) \left(1 - \frac{2k_{De}^2}{k_D^2} \right) \\ & \times \frac{4 - [(1 - k_{De}^2/k_{Di}^2)^{-1} x^3 + 2x^2 + 4x + 4]\exp(-x)}{x^3}, \quad (10) \end{aligned}$$

where $x = rk_D$ is the normalized distance from the grain. The integration over k has been formally performed from zero to infinity. In fact, the used approximate expressions for χ_1 and χ_2 [Eqs. (8) and (9)] are valid only between $k_{\min} = u/v_{Ti}\ell_i$ and $k_{\max} = 1/\ell_i$. However, if $k_{\min} \ll k_D$ and $k_{\max} \gg k_D$, this does not affect the result considerably since it can be shown that the contribution to the integral from small and large ranges of k are of minor importance.²¹

Let us briefly analyze the structure of the obtained Eq. (10). The first term corresponds to the usual isotropic Debye-Hückel potential, the second term represents the anisotropic part of the electric field behind nonabsorbing grain, and the third and fourth terms represent, respectively, the isotropic and anisotropic part of the electric field associated with the effect of absorption. The isotropic terms are of the same (negative) sign (recall that $Q < 0$). The first anisotropic term changes sign from negative to positive at $x \approx 1.5$. The second anisotropic term (associated with plasm absorption) also change the sign, but from positive to negative, and at some x ,

which is a function of the electron-to-ion temperature ratio. Thus, absorption makes the electric field at large distances more negative.

Let us consider some limiting cases and compare our results with those known previously. From Eq. (10), we get for the long-range asymptote of the electric potential in the absence of absorption $\phi_1 \approx -(Q\nu/\omega_{pi}^2 r^2)(k_{Di}/k_D)^4$. Except for the factor $(k_{Di}/k_D)^4$, this expression is identical to that obtained by Stenflo *et al.*²⁵ for the potential behind a slowly moving nonabsorbing test charge in collisional plasma. The difference appears because Stenflo *et al.* considered only electron screening. In the presence of absorption, the long-range asymptote of the anisotropic part of the potential becomes $\phi_1 \approx -(Q\nu/\omega_{pi}^2 r^2)(k_{Di}/k_D)^4 [1 + (e/Q)(J_i/\omega_{pi}^2)(1 - 2k_{De}^2/k_D^2)]$. Thus, the effect of absorption decreases the amplitude of the anisotropic part of potential and, in principle, can even change its sign. At large distances, however, the dominant contribution comes from the isotropic part associated with absorption, $\phi_1 \approx -(eJ_i/\omega_{pi}^2 r)(k_{Di}/k_D)^2$, i.e., absorption completely determines the long-range asymptote of the potential.

From Eq. (10) we can also evaluate the ion-drag force, i.e., $F_i = QE_1|_{x=0}$, associated with the plasma anisotropy induced by the ion flow. Calculating the anisotropic part of the electric field at $x \rightarrow 0$, we get

$$F_{id} = (1/6)Q^2 k_{Di}^2 (\ell_i k_D)^{-1} M_T [1 + (e/Q)(J_i/k_{Di} v_{Ti}) \times (\ell_i k_{Di})^{-1} (1 + k_{De}^2/k_D^2)]. \quad (11)$$

This expression is identical to that obtained recently by Khrapak *et al.*²¹ The first term of the above expression represents the ion-drag force acting on the nonabsorbing grain and coincides with the expression obtained by Ivlev *et al.*³⁴ using more general kinetic approach in the limit of highly collisional ions ($\ell_i \ll \lambda_D$). The second term corresponds to the effect of plasma absorption on the grain surface and it gives negative contribution to the force since $Q < 0$. Thus, in the highly collisional regime, the ion-drag force decreases due to the plasma absorption on the grain surface.²¹

For further analysis, it is convenient to introduce the following normalized units: the dimensionless grain charge $z = |Q|e/aT_e$, the electron-to-ion temperature ratio $\tau = T_e/T_i$, the thermal Mach number for drifting ions $M_T = u/v_{Ti}$, normalized ion mean-free path $\xi = \ell_i/\lambda_D$, and the so-called scattering parameter^{35,36} $\beta = z\tau(a/\lambda_D)$. Furthermore, let us use a well-known asymptotic expression for the ion flux on a infinitesimally small grain ($a \ll \lambda_D$) in the continuum limit ($\ell_i \ll a$), which can be written as^{17,20,37} $J_i \approx 4\pi az\pi_0 \ell_i v_{Ti}$. From Eq. (10), we then get the following expression for the normalized electric field ($\tilde{E}_1 = eE_1\lambda_D/T_i$):

$$\tilde{E}_1 = -\beta \frac{\tau}{\tau+1} \frac{1}{x^2} [1 + \tau^{-1}(1+x)\exp(-x)] + \frac{\beta M_T}{2\xi} \frac{\tau}{(\tau+1)^2} \frac{1}{x^3} [8 - (x^3 + 4x^2 + 8x + 8)\exp(-x)]. \quad (12)$$

The first term represents isotropic part of the electric field,

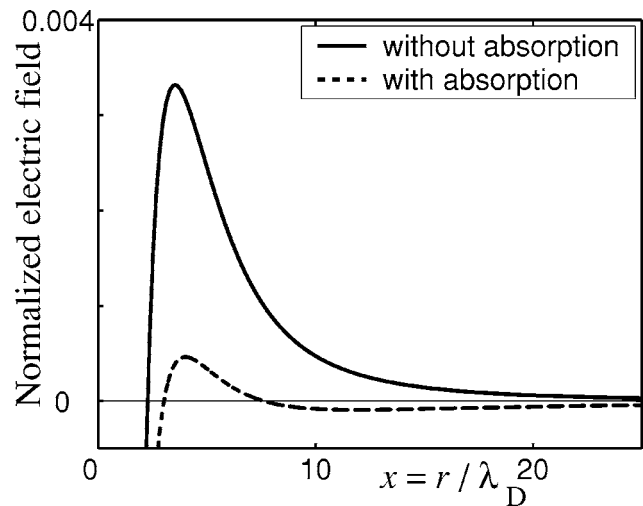


FIG. 1. Spatial variation of the normalized electric field behind a spherical grain in a highly collisional plasma with drifting ions for two cases: with and without plasma absorption on the grain. The calculation is for $z=1$, $\tau=2$, $\beta=0.06$, $M_T=0.06$, and $\xi=0.01$.

while the second term represents its anisotropic part.

It is evident from Eq. (12) that the normalized electric field is proportional to the scattering parameter β and depends on three dimensionless parameters: τ , M_T , and ξ . We have investigated these dependencies numerically, and results are shown in Figs. 1–4. First, we demonstrate that the effect of absorption leads to the considerable changes in the behavior of the electric field. Figure 1 represents an example of the electric field distribution behind the grain along the ion flow with and without effect of absorption taken into account. As discussed above, the effect of absorption changes the sign of the long-range electric field. In the considered regime, absorption allows the electric field to be positive at intermediate distances, but the magnitude of the field is considerably reduced compared to the case of nonabsorbing grain. However, in a wide range of plasma param-

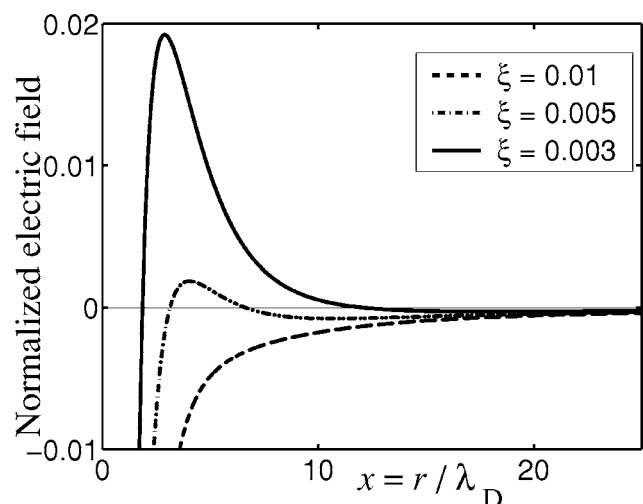


FIG. 2. Spatial variation of the normalized electric field behind a spherical absorbing grain in a highly collisional plasma with drifting ions for three different normalized ion mean-free paths, $\xi = \ell_i/\lambda_D$. Other complex plasma parameters are $z=1$, $\tau=10$, $\beta=0.3$, $M_T=0.1$ (for details see text).

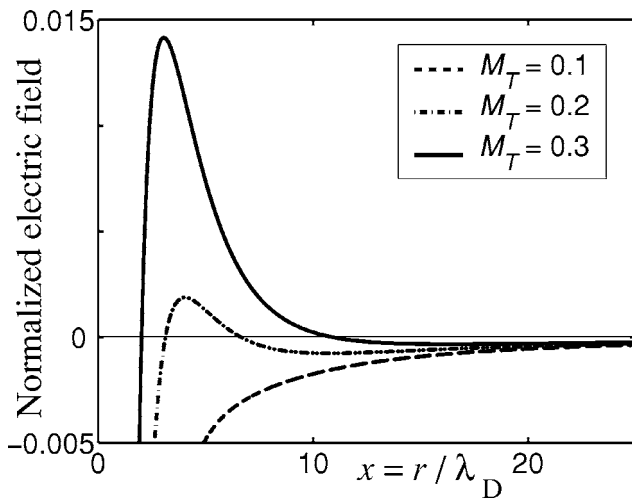


FIG. 3. Spatial variation of the normalized electric field behind a spherical absorbing grain in a highly collisional plasma with drifting ions for three different values of the thermal Mach number M_T . Other complex plasma parameters are $z=1$, $\tau=10$, $\beta=0.3$, and $\xi=0.01$ (for details see text).

eters, absorption can make the electric field to be negative at all distances, as demonstrated below. Figure 2 shows the dependence $\tilde{E}_1(x)$ for three different values of the ion collisionality. It is clear that the electric field can acquire positive value only in the highly collisional regime. The transition to negative field at all distances occurs at $\xi \approx 0.006$. Figure 3 shows the dependence $\tilde{E}_1(x)$ for three different values of the ion drift velocity. The electric field can be locally positive for relatively large drift velocities. In the case investigated, this occurs for $M_T \geq 0.2$. Figure 4 represents the behavior of the electric field for three different electron-to-ion temperature ratios τ . The electric field is locally positive for low values of τ . In the regime investigated the transition occurs at $\tau \approx 5$. Thus, the attraction between two like-charged absorbing

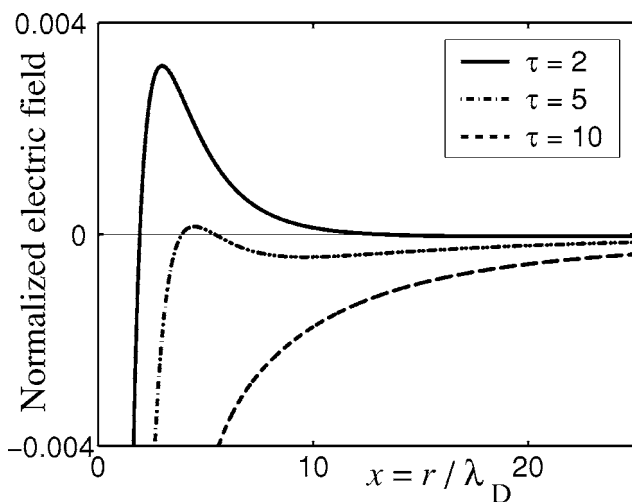


FIG. 4. Spatial variation of the normalized electric field behind a spherical absorbing grain in a highly collisional plasma with drifting ions for three different values of the electron-to-ion temperature ratio τ . Other complex plasma parameters are $z=1$, $a/\lambda_D=0.03$, $M_T=0.1$, and $\xi=0.01$ (for details see text).

grains aligned along the ion flow is still possible, but requires high ion collisionality, large drift velocities, and low electron-to-ion temperature ratios.

IV. SUMMARY

The effect of plasma absorption on the electric field (potential) behind a small spherical object immersed in a plasma with flowing ions is studied in the limiting case of high collisionality. It is demonstrated that the effect of absorption influences both isotropic and anisotropic components of the electric field. At large distances, absorption completely determines the behavior of the electric field, and it decays as $\propto r^{-2}$. At moderate distances, the field is also considerably modified as compared to a nonabsorbing object. With respect to the interaction between a pair of grains aligned along the ion flow, it is shown that both short- and long-range asymptotes are repulsive, but at moderate distances, attraction can take place in certain parameter regimes. This result can be important in understanding intergrain interactions in high pressure weakly anisotropic complex plasmas.

- ¹P. K. Shukla and A. A. Mamun, *Introduction to Dusty Plasma Physics* (IOP, London, 2002).
- ²V. E. Fortov, A. G. Khrapak, S. A. Khrapak, V. I. Molotkov, and O. F. Petrov, *Phys. Usp.* **47**, 447 (2004).
- ³S. V. Vladimirov and K. Ostrikov, *Phys. Rep.* **393**, 175 (2004).
- ⁴G. E. Morfill, A. V. Ivlev, S. A. Khrapak, B. A. Klumov, M. Rubin-Zuzic, U. Konopka, and H. M. Thomas, *Contrib. Plasma Phys.* **44**, 450 (2004).
- ⁵V. E. Fortov, A. V. Ivlev, S. A. Khrapak, A. G. Khrapak, and G. E. Morfill, *Phys. Rep.* **421**, 1 (2005).
- ⁶D. A. Mendis, *Plasma Sources Sci. Technol.* **11**, A219 (2002).
- ⁷J. Winter, *Phys. Plasmas* **7**, 3862 (2000).
- ⁸A. Yu. Pigarov, S. I. Krasheninnikov, T. K. Soboleva, and T. D. Rognlien, *Phys. Plasmas* **12**, 122508 (2005).
- ⁹U. de Angelis, *Phys. Plasmas* **13**, 012514 (2006).
- ¹⁰V. N. Tsytovich, *Phys. Usp.* **40**, 53 (1997).
- ¹¹U. Konopka, G. E. Morfill, and L. Ratke, *Phys. Rev. Lett.* **84**, 891 (2000).
- ¹²J. E. Daugherty, M. D. Kilgore, R. K. Porteous, and D. B. Graves, *J. Appl. Phys.* **72**, 3934 (1992).
- ¹³J. E. Allen, B. M. Annaratone, and U. de Angelis, *J. Plasma Phys.* **63**, 299 (2000).
- ¹⁴Y. L. Al'pert, A. V. Gurevich, and L. P. Pitaevsky, *Plasma Physics with Artificial Satellites* (Consultants Bureau, New York, 1965).
- ¹⁵S. A. Khrapak, A. V. Ivlev, and G. Morfill, *Phys. Rev. E* **64**, 046403 (2001).
- ¹⁶S. A. Khrapak, G. E. Morfill, A. V. Ivlev, H. M. Thomas, D. A. Beysens, B. Zappoli, V. E. Fortov, A. M. Lipaev, and V. I. Molotkov, *Phys. Rev. Lett.* **96**, 015001 (2006).
- ¹⁷C. H. Su and S. H. Lam, *Phys. Fluids* **6**, 1479 (1963).
- ¹⁸I. M. Cohen, *Phys. Fluids* **6**, 1492 (1963).
- ¹⁹O. Bystrenko and A. Zagorodny, *Phys. Rev. E* **67**, 066403 (2003).
- ²⁰S. A. Khrapak, G. E. Morfill, A. G. Khrapak, and L. G. D'yachkov, *Phys. Plasmas* **13**, 052114 (2006).
- ²¹S. A. Khrapak, S. K. Zhdanov, A. V. Ivlev, and G. E. Morfill, "Drag force on an absorbing body in highly collisional plasmas," *J. Appl. Phys.* (to be published).
- ²²D. Montgomery, G. Joyce, and R. Sugihara, *Plasma Phys.* **10**, 681 (1968).
- ²³G. Cooper, *Phys. Fluids* **12**, 2707 (1969).
- ²⁴E. W. Laing, A. Lamont, and P. J. Fielding, *J. Plasma Phys.* **5**, 441 (1971).
- ²⁵L. Stenflo, M. Y. Yu, and P. K. Shukla, *Phys. Fluids* **16**, 450 (1973).
- ²⁶S. V. Vladimirov and M. Nambu, *Phys. Rev. E* **52**, R2172 (1995).
- ²⁷O. Ishihara and S. V. Vladimirov, *Phys. Plasmas* **4**, 69 (1997).
- ²⁸G. Lapenta, *Phys. Rev. E* **62**, 1175 (2000).
- ²⁹M. Lampe, G. Joyce, G. Ganguli, and V. Gavrishchaka, *Phys. Plasmas* **7**, 3851 (2000).
- ³⁰M. Lampe, G. Joyce, and G. Ganguli, *Phys. Scr., T* **89**, 106 (2001).
- ³¹S. A. Maiorov, S. V. Vladimirov, and N. F. Cramer, *Phys. Rev. E* **63**, 017401 (2001).

- ³²D. Winske, IEEE Trans. Plasma Sci. **29**, 191 (2001).
- ³³F. Melandsø and J. Goree, Phys. Rev. E **52**, 5312 (1995).
- ³⁴A. V. Ivlev, S. A. Khrapak, S. K. Zhdanov, G. E. Morfill, and G. Joyce, Phys. Rev. Lett. **92**, 205007 (2004).
- ³⁵S. A. Khrapak, A. V. Ivlev, G. E. Morfill, and H. M. Thomas, Phys. Rev. E **66**, 046414 (2002); S. A. Khrapak, A. V. Ivlev, G. E. Morfill, and S. K. Zhdanov, Phys. Rev. Lett. **90**, 225002 (2003).
- ³⁶S. A. Khrapak, A. V. Ivlev, and G. E. Morfill, Phys. Rev. E **70**, 056405 (2004).
- ³⁷J.-S. Chang and J. G. Laframboise, Phys. Fluids **19**, 25 (1976).

Effective charge of a small absorbing body in highly collisional plasma subject to an external electric field

M. Chaudhuri,^{a)} S. A. Khrapak, and G. E. Morfill
Max-Planck Institut für Extraterrestrische Physik, D-85741 Garching, Germany

(Received 26 February 2007; accepted 20 March 2007; published online 11 May 2007)

The total force which is the resultant of the electric, ion, and electron drag forces has been calculated for a small absorbing spherical grain immersed in a highly collisional, weakly ionized plasma subject to a weak external electric field. Linear dielectric response formalism has been used and both ion and electron absorption on the grain have been taken into account. It is shown that the total force is always directed along the direction of the electric force. The “effective” charge of the grain which can be defined as the ratio of the total force to the strength of the electric field is calculated. It is shown that its magnitude is comparable to the magnitude of the actual grain’s charge. © 2007 American Institute of Physics. [DOI: 10.1063/1.2724806]

“Complex” or “dusty” plasmas consist of ions, electrons, highly charged micron sized dust grains and a neutral gas. In complex plasma research one of the most fundamental issues is to understand and analyze the forces that the charged grains experience in different conditions. This is important because relative magnitudes of different forces often determine the static and dynamic properties of the grain component, shape and structure of the grain clouds, induce grain flows, affect wave phenomena, etc.¹⁻⁴

Very often complex plasmas are subjected to external large-scale electric fields. The direct effect of the electric field on the charged grains is to generate electric force, $\mathbf{F}_{el} = Q\mathbf{E}$, where Q is the grain charge and \mathbf{E} is the electric field. The indirect effect is the generation of ion and electron flows and the corresponding ion and electron drag forces associated with the momentum transfer from drifting ions and electrons to the charged grains.

The ion drag force often dominates over the electron drag force because of large ion-to-electron mass ratio. This is true for instance for the ambipolar diffusion regime in the bulk isotropic plasma or when the grain is moving with respect to stationary electron-ion background. However, in the presence of external large-scale electric field and mobility limited ion and electron drifts, electrons are drifting much faster than ions, $u_e \gg u_i$, due to much higher electron mobility. Such a situation (which occurs for example in a positive column of a dc discharge) was considered in an earlier work by Khrapak and Morfill⁵ in the regime of collisionless ion and electron trajectories in the vicinity of the grain and it was shown that the electron drag force can dominate over the electric and ion drag forces, provided the electron-to-ion temperature ratio is not too large. The effect is especially pronounced for most of the noble gases where electron mobility has a maximum around $T_e \sim 1$ eV.

The focus of the present paper is on the analysis of the electric force, ion and electron drag forces and the competition between them in the highly collisional plasma subject to a weak electric field. Plasma absorption on the grain surface

whose importance has been discussed recently^{6,7} is taken into account. The total force acting on a grain which is the sum of electric, ion drag and electron drag forces is calculated and it is found that it always acts in the direction of the electric force. The total force is proportional to the electric field and the proportionality constant represents the “effective” charge, such as $\mathbf{F} = Q_{\text{eff}}\mathbf{E}$. The expression for the “effective” charge is derived and it turns out that $Q_{\text{eff}} \approx Q$, i.e., in the considered regime both ion and electron drag forces are of minor importance as compared to the electric force.

We consider the following problem: A small negatively charged spherical grain is placed in highly collisional, weakly ionized quasineutral plasma with a constant electric field \mathbf{E}_0 . The grain is stationary and absorbs plasma on its surface. Ion and electron temperatures are uniform but not necessarily equal to each other. Ion and electron drift velocities are $\mathbf{u}_\alpha = \pm e\mathbf{E}_0/m_\alpha\nu_\alpha$ where ν_α is the (constant) collision frequency with neutrals and m_α is the mass of the corresponding species ($\alpha = i, e$). The positive sign is for ions which drift in the direction of the electric field, whereas the negative sign is for electrons which drift in the opposite direction. The electric field is sufficiently weak so that both electron and ion drifts are subthermal $M_{T_\alpha} = |u_\alpha|/v_{T_\alpha} < 1$ where $v_{T_\alpha} = \sqrt{T_\alpha/m_\alpha}$ is the thermal velocity and M_{T_α} is the thermal Mach number for the corresponding species. There are no plasma sources or sinks except at the grain surface, which is fully absorbing. In the highly collisional regime $\ell_\alpha \ll \lambda_D$, where ℓ_α denotes the mean free path and λ_D is the plasma screening length, both the ion and electron components are mobility controlled and are suitably described by the hydrodynamic equations. The corresponding continuity and momentum equations are:

$$\nabla(n_\alpha\mathbf{v}_\alpha) = -J_\alpha\delta(\mathbf{r}), \quad (1)$$

$$(\mathbf{v}_\alpha \nabla)\mathbf{v}_\alpha = q_\alpha(e/m_\alpha)\mathbf{E} - (\nabla n_\alpha/n_\alpha)v_{T_\alpha}^2 - \nu_\alpha\mathbf{v}_\alpha, \quad (2)$$

where n_α , \mathbf{v}_α are the density and velocity of the corresponding species, $J_{i(e)}$ denotes the ion (electron) fluxes that the grain collects from the plasma and \mathbf{E} is the electric field. In

^{a)}Electronic mail: chaudhuri@mpe.mpg.de

Eq. (2) $q_i=+1$ and $q_e=-1$. The above set of equations is closed with the Poisson equation:

$$\Delta\phi = -4\pi e(n_i - n_e) - 4\pi Q\delta(\mathbf{r}). \quad (3)$$

The test grain in our model is described as a point-like particle with charge Q located at the position $\mathbf{r}=0$. Our next step is to calculate the electric field $\mathbf{E}=\mathbf{E}_0+\mathbf{E}_p$ at the position of the grain which will give us the total force acting on it. Here \mathbf{E}_p is the polarization electric field induced in the flowing plasma by the absorbing grain. (Note that the ratio $|\mathbf{E}_p/\mathbf{E}_0|$ can, in principle, be arbitrary.) In doing so we will use the procedure similar to that outlined in our earlier works.^{6,7}

Specifically, we apply the linear dielectric response formalism^{8,9} to calculate the self-consistent electrostatic potential around the absorbing point-like grain from Eqs. (1)–(3). Assuming the plasma perturbation to be proportional to $\propto\exp(i\mathbf{k}\mathbf{r})$ we get⁶

$$\phi_p(\mathbf{r}) = \frac{4\pi Q}{(2\pi)^3} \int \frac{\exp(i\mathbf{k}\mathbf{r})d\mathbf{k}}{\chi_1} + \frac{4\pi e}{(2\pi)^3} \sum_{\alpha=i,e} \int \frac{\exp(i\mathbf{k}\mathbf{r})d\mathbf{k}}{\chi_\alpha}, \quad (4)$$

where

$$\chi_1 = k^2 \left[1 + \sum_{\alpha=i,e} \left(\frac{\omega_{p\alpha}}{\Omega_\alpha} \right)^2 \right], \quad \chi_\alpha = iq_\alpha \left[\frac{\chi_1 \Omega_\alpha^2}{J_\alpha(\mathbf{k}\mathbf{u}_\alpha - i\nu_\alpha)} \right].$$

Here $\omega_{p\alpha}=\sqrt{4\pi n_\alpha e^2/m_\alpha}$ is the plasma frequency of the corresponding species and $\Omega_\alpha^2=k^2 v_{T\alpha}^2 - \mathbf{k}\mathbf{u}_\alpha(\mathbf{k}\mathbf{u}_\alpha - i\nu_\alpha)$. The first term in Eq. (4) represents the potential of a nonabsorbing point-like grain,⁸ while the second term represents the sum of the contribution to the potential due to ion and electron absorptions, respectively.⁶

From Eq. (4) we get the polarization part of the total force experienced by the test grain using the relation $F_p = -Q\nabla\phi_p|_{r=0}$. This yields

$$F_p = \pi^{-1} \int_0^\infty k^3 dk \int_{-1}^1 \mu d\mu \left[Q^2 \text{Im}\{\chi_1^{-1}(\mu, k)\} + Qe \sum_{\alpha=i,e} \text{Im}\{\chi_\alpha^{-1}(\mu, k)\} \right], \quad (5)$$

where $\mu=\cos\theta$ and θ is the angle between \mathbf{k} and \mathbf{E}_0 . In our model we have considered the hydrodynamic approach both for ions and electrons, the applicability of which requires the condition $k\ell_\alpha \ll 1$. We also consider the limit of small ion and electron drift velocities, $k\ell_\alpha \gg M_{T_\alpha}$. In this regime the imaginary parts of χ_1^{-1} and χ_α^{-1} can be written as

$$\text{Im}\{\chi_1^{-1}\} \simeq \frac{\mu}{k(k^2 + k_D^2)^2} \sum_{\alpha=i,e} \frac{q_\alpha k_{D\alpha}^2 M_{T_\alpha}}{\ell_\alpha}, \quad (6)$$

$$\text{Im}\{\chi_\alpha^{-1}\} \simeq \frac{\mu J_\alpha M_{T_\alpha}}{k^3(k^2 + k_D^2)^2 \ell_i \ell_e v_{T_\alpha}} \left[(k^2 + k_D^2 - k_{D\alpha}^2) \left(\frac{\ell_e}{\ell_i} \right)^{q_\alpha} + (k_D^2 - k_{D\alpha}^2) \left(\frac{M_{T_e}}{M_{T_i}} \right)^{q_\alpha} \right], \quad (7)$$

where $k_{D\alpha}=\lambda_{D\alpha}^{-1}$ is the inverse Debye radii of the corresponding species ($\lambda_{D\alpha}=\sqrt{T_\alpha/4\pi n_\alpha e^2}$) and $k_D=\sqrt{k_{De}^2 + k_{Di}^2}$ is the inverse linearized Debye radius.

After substituting Eqs. (6) and (7) in Eq. (5) and using the flux balance condition $J_i=J_e$ for a floating grain, we get after integration

$$F_p = (1/6)(Q^2/k_D) \sum_{\alpha=i,e} (q_\alpha k_{D\alpha}^2 / \ell_\alpha) M_{T_\alpha} + (1/6) \times (Qe/k_D) \sum_{\alpha=i,e} (J_\alpha M_{T_\alpha} / \ell_\alpha^2 v_{T_\alpha}) [(2 - k_{D\alpha}^2/k_D^2) + (\ell_i v_{T_i} / \ell_e v_{T_e})^{q_\alpha} (k_{D\alpha}/k_D)^2]. \quad (8)$$

Careful investigation of Eq. (8) reveals that the first part represents the sum of ion and electron drag forces for a non-absorbing grain. In the considered limit of highly collisional ions ($\ell_i \ll \lambda_D$) the expression for the ion drag force acting on a nonabsorbing grain coincides with the earlier expression derived by Ivlev *et al.*⁸ using a more generalized kinetic approach. The ion and electron drag forces experienced by a nonabsorbing grain are directed along the drift velocity of the corresponding species, i.e., they act in the opposite directions. The ratio of the absolute magnitudes of the ion-to-electron drag forces on a nonabsorbing grain is $(T_e/T_i)^2$. This implies that in one temperature plasmas ($T_e=T_i$) they exactly cancel each other. In highly nonthermal plasma ($T_e \gg T_i$), the ion drag force (directed opposite to the electric force) dominates. The ratio of the ion drag force to the electric one is $(1/6)\beta$ where $\beta=z\tau(a/\lambda_D)$ is the so-called scattering parameter.^{10–12} Here $z=|Q|e/aT_e$ is the dimensionless charge, $\tau=T_e/T_i$ is the electron-to-ion temperature ratio and a is the grain radius.

The second sum in Eq. (8) is the contribution to the drag forces due to ion and electron absorptions. Under most typical plasma conditions $\ell_e/\ell_i \sim 10-100$, $v_{T_e}/v_{T_i} \sim 10^2-10^3$ and $T_e/T_i \sim 1-100$ and thus we have $(\ell_i/\ell_e)(v_{T_i}/v_{T_e}) \times (k_{Di}/k_D)^2 \ll 1$ and $(\ell_e/\ell_i)(v_{T_e}/v_{T_i})(k_{De}/k_D)^2 \gg 1$ and we can simplify the absorption parts of the ion and electron drag forces, $(F_i)_{\text{abs}} \simeq (1/6)(Qe/k_D)(J_i M_{T_i} / \ell_i^2 v_{T_i})(1 + k_{De}^2/k_D^2)$ and $(F_e)_{\text{abs}} = (1/6)(Qe/k_D)(J_e M_{T_e} / \ell_e \ell_e v_{T_e})(k_{De}/k_D)^2$. The ratio of ion-to-electron absorption forces, $|F_i/F_e|_{\text{abs}} \simeq (T_e/T_i)^2$. The important point, however, is that for negatively charged grains the effect of ion absorption reduces the absolute magnitude of the total ion drag force whereas the effect of electron absorption increases the total electron drag force. Note that neglecting electron absorption ($J_e=0$) and electron drift ($u_e=0$) we get back the expression for the ion drag force identical to that in earlier work by Khrapak *et al.*⁶

Since the absorption terms are dependent on the ion and electron fluxes to the grain surface, for further analysis it is essential to use correct expressions for these fluxes. We use simple analytical asymptotic expressions for the charging

fluxes in the continuum regime ($\ell_a \ll a$) for infinitesimally small grain ($a \ll \lambda_D$).¹³⁻¹⁵ In the present notation the expression for the plasma fluxes to a floating grain are $J_e = J_i \approx 4\pi a z n_0 \ell_i v_{T_i}$ where n_0 is the unperturbed plasma density. In this regime the expression for the total drag force is

$$F_p = - (1/6) Q^2 k_D^2 [M_{T_i}(\ell_i k_D)^{-1} (k_{D_i}/k_D)^2 + M_{T_e}(\ell_e k_D)^{-1} (1 + k_{D_i}^2/k_D^2)] = (1/6)(QE)(\beta/\tau) \quad (9)$$

i.e., both ion and electron drag forces are directed in the same direction (opposite to the electric field). This is associated with the fact that the ion absorption changes the direction of the ion drag force in highly collisional plasmas,⁶ whilst electron absorption increases the magnitude of the electron drag force. The absolute ratio of total ion-to-electron drag force is, $|F_i/F_e| \approx (T_e/T_i)$.

In the formalism used we cannot consistently take into account the mechanical momentum transfer from the ions and electrons when they hit the grain. However, this effect seems to be of minor importance. To demonstrate this, let us make an estimate of the forces associated with the “drift momentum” transfer from ions and electrons absorbed by the grain. This force is roughly $\sim J_0 m_{i(e)} u_{i(e)}$ for ions (electrons). Comparing these contributions with the first and second term of Eq. (9) we see that they are smaller than the corresponding drag forces by a factor of $\sim (\tau/\beta)(\ell_i/\lambda_D)^2$ for ions and $\sim (\tau^2/\beta)(v_{T_i}/v_{T_e})(\ell_i/\lambda_D)(\ell_e/\lambda_D)$ for electrons. Thus, in highly collisional plasma it is reasonable to neglect the above mentioned effect.

The total force acting on the grain is $F = F_i + F_e + F_{el} = Q_{\text{eff}} E$. The grain effective charge in the considered parameter regime can be written as:

$$Q_{\text{eff}}/Q = 1 + (1/6)(\beta/\tau). \quad (10)$$

The application of the linear theory requires $\beta \lesssim 1$.⁸ Thus, we have $Q_{\text{eff}} \approx Q$. This implies that both the ion and electron drag forces acting on an absorbing grain are small compared

to the electric force in the considered regime.

To summarize, in this work the effect of weak electric field on a small absorbing grain immersed in a highly collisional plasmas has been investigated. It is shown that the total force acting on a grain which is the sum of electric, ion drag and electron drag forces always acts in the direction of the electric force. The total force can be presented as a product of effective charge and electric field. The effective charge has been calculated and has been shown to be close to the actual one. Thus, in the parameter regime investigated, the drag forces are of minor importance compared to the electric force.

S. A. K. was supported by DLR under Grant No. 50WPO203.

¹P. K. Shukla and A. A. Mamun, *Introduction to Dusty Plasma Physics* (IOP, London, 2002).

²V. E. Fortov, A. G. Khrapak, S. A. Khrapak, V. I. Molotkov, and O. F. Petrov, *Phys. Usp.* **47**, 447 (2004).

³S. V. Vladimirov and K. Ostrikov, *Phys. Rep.* **393**, 175 (2004).

⁴V. E. Fortov, A. V. Ivlev, S. A. Khrapak, A. G. Khrapak, and G. E. Morfill, *Phys. Rep.* **421**, 1 (2005).

⁵S. A. Khrapak and G. E. Morfill, *Phys. Rev. E* **69**, 066411 (2004).

⁶S. A. Khrapak, S. K. Zhdanov, A. V. Ivlev, and G. E. Morfill, *J. Appl. Phys.* **101**, 033307 (2007).

⁷M. Chaudhuri, S. A. Khrapak, and G. E. Morfill, *Phys. Plasmas* **14**, 022102 (2007).

⁸A. V. Ivlev, S. A. Khrapak, S. K. Zhdanov, G. E. Morfill, and G. Joyce, *Phys. Rev. Lett.* **92**, 205007 (2004).

⁹D. Montgomery, G. Joyce, and R. Sugihara, *Plasma Phys.* **10**, 681 (1968).

¹⁰S. A. Khrapak, A. V. Ivlev, G. E. Morfill, and H. M. Thomas, *Phys. Rev. E* **66**, 046414 (2002).

¹¹S. A. Khrapak, A. V. Ivlev, G. E. Morfill, and S. K. Zhdanov, *Phys. Rev. Lett.* **90**, 225002 (2003).

¹²S. A. Khrapak, A. V. Ivlev, and G. E. Morfill, *Phys. Rev. E* **70**, 056405 (2004).

¹³C. H. Su and S. H. Lam, *Phys. Fluids* **6**, 1479 (1963).

¹⁴J.-S. Chang and J. G. Laframboise, *Phys. Fluids* **19**, 25 (1976).

¹⁵S. A. Khrapak, G. E. Morfill, A. G. Khrapak, and L. G. D'yachkov, *Phys. Plasmas* **13**, 052114 (2006).

Ion drag force on a small grain in highly collisional weakly anisotropic plasma: Effect of plasma production and loss mechanisms

M. Chaudhuri,^{a)} S. A. Khrapak, and G. E. Morfill
Max-Planck-Institut für Extraterrestrische Physik, D-85741 Garching, Germany

(Received 13 February 2008; accepted 7 April 2008; published online 20 May 2008)

The ion drag force acting on a small absorbing grain has been calculated in highly collisional plasma with slowly drifting ions taking into account plasma production and loss processes in the vicinity of the grain. It is shown that the strength of the plasma production and loss mechanisms not only affects the magnitude of the ion drag force, but also determines the direction of the force. The parameter regimes for the “positive” and “negative” ion drag forces have been identified. In addition, the qualitative features of the electric potential distribution around the grain in isotropic conditions (in the absence of the ion drift) are investigated. © 2008 American Institute of Physics.
 [DOI: 10.1063/1.2917906]

I. INTRODUCTION

Complex (dusty) plasma is an overall charge neutral assembly of ions, electrons, highly charged microparticles (grains), and neutral gas. The microparticles are large enough to be visualized individually which allow experimental investigations with high temporal and spatial resolution (in terms of the appropriate plasma frequency and particle separation). Hence, complex plasma is used as a valuable model system to investigate various phenomena (e.g., phase transitions, self-organizations, waves, transport, etc.) at the most detailed kinetic level.^{1–7} Apart from importance in fundamental studies, dusty plasmas also play a very important role in connection to astrophysical plasmas,⁸ planetary rings,⁹ technological plasma applications,^{3,10} fusion devices,^{11–13} etc.

The interaction and momentum transfer between different plasma components and charged grains play an exceptionally important role in complex plasmas.¹⁴ In this work we focus on the ion drag force which is caused by the momentum transfer between flowing ions and a negatively charged grain. This force appears to be quite important in describing a number of interesting phenomena in complex plasma, e.g., void formation in the central region of an rf discharge under microgravity condition,^{15–19} rotation of the dust structures in the presence of the magnetic field,^{20,21} location and configuration of the dust structures in laboratory experiments,^{22–24} properties of low-frequency waves,^{25–27} etc. Not surprisingly, the ion drag force has been the subject of extensive investigation over the last years. This includes analytical theories,^{23,28–34} numerical simulations,^{35–38} and experiments.^{39–44}

It should be noted that despite its high importance in complex plasmas, a complete self-consistent model of the ion drag force, describing all cases of interest, has not yet been constructed. Rather, there exists several approaches, which can be employed under certain well defined conditions.^{2,4,31,45} Let us briefly outline these approaches.

The traditional way to derive the ion-drag force is the “binary collision (BC) formalism,” which is based on the solution of the mechanical problem of the ion motion in the electric field around the charged particle. Analyzing ion trajectories one can obtain the velocity-dependent momentum-transfer cross section $\sigma(v)$, integration of which with appropriate velocity distribution function of the ions gives the ion-drag force. In deriving $\sigma(v)$ an isotropic attractive Debye–Hückel (Yukawa) interaction potential between the ions and the grain is typically assumed. An important quantity characterizing momentum transfer in the Yukawa potential is the so-called *scattering parameter*, $\beta = R_c/\lambda$, where $R_c = |Q|e/m_i v^2$ is the Coulomb radius at which the ion-grain electrostatic interaction energy is of the order of the ion kinetic energy, λ is the effective plasma screening length, Q is the grain charge, and m_i is the ion mass. For a small (point-like) grain the normalized momentum transfer cross section, $\sigma(v)/\lambda^2$, depends only on β .³⁰ Thus, β is a unique parameter which describes scattering for the Debye–Hückel (Yukawa) central potential. The value of β characterizes the strength of the ion-grain coupling and determines how the momentum transfer occurs. For weak coupling ($\beta \ll 1$), the length scale of strong (nonlinear) interaction and scattering at large angles ($\sim R_c$) is much shorter than the screening length λ . In this regime the conventional Coulomb scattering theory (small-angle scattering approximation) is applicable. An extension of the Coulomb scattering theory to the regime of moderate coupling ($\beta \sim 1$) has been proposed in Ref. 29. In this case the interaction range can be comparable or even exceeds the screening length which requires a proper choice of the upper cutoff impact parameter and basically leads to a modification of the Coulomb logarithm. This model predicts larger values of the ion drag force than the standard Coulomb scattering theory and it has been shown to agree reasonably well with experimental results at low and moderate neutral gas pressures,⁴³ as well as with PIC simulation.³⁸ In the case of strong coupling ($\beta \gg 1$) the interaction range considerably exceeds the screening length and most of the contribution to the momentum transfer is from scattering at large angles. In this regime the traditional Coulomb scattering theory is not

^{a)}Electronic mail: chaudhuri@mpe.mpg.de.

applicable at all. An importance of ion scattering at large angles was demonstrated in Ref. 46 where three-dimensional molecular dynamics simulation method has been used to study plasma kinetics around a dust grain in an ion flow. This work was, however, focused on electric potential distribution around the grain rather than on the ion drag force. A model describing the ion drag force in this strong coupling regime has been developed in Refs. 30 and 31 assuming subthermal ion drifts. This model has been further extended to arbitrary ion drift velocities in Ref. 44. The experimental results have been shown to agree reasonably well with this analytical approach.⁴⁴ Thus, within the BC formalism one can describe the momentum transfer for any given degree of ion-grain coupling. Overall, there is a reasonable quantitative agreement between theory and experiments in collisionless and weakly collisional plasma. However, since this approach considers only ballistic ion trajectories, the effect of ion-neutral collisions, which is often important in complex plasmas cannot be consistently accounted for.

An alternative way to calculate the ion drag force is based on the so-called “linear dielectric response (LR) formalism.” Unlike the BC approach, instead of calculating single ion trajectories and then the momentum transfer cross section, one can solve the Poisson equation coupled to the kinetic (or hydrodynamic) equations for the ions and electrons and obtain the self-consistent electrostatic potential distribution around the grain. Then the product of the polarization component of the electric field induced by the ion flow at the position of the grain and grain charge gives the ion drag force on the grain.^{32,33,45,47} As long as LR formalism is concerned, the whole problem is basically reduced to the calculation of the proper plasma response function (permittivity). This approach consistently accounts for ion-neutral collisions, potential anisotropy caused by the ion flow, and allows us to calculate the ion velocity distribution function self-consistently, but it is applicable only in the regime of weak ion-grain coupling, $\beta \ll 1$, since linearization is used.

The following predictions about the behavior of the ion drag force in collisional plasmas have been made. The ion drag force acting on a *nonabsorbing* grain increases with the ion collisionality due to ion focusing behind the grain.³² This effect is related to the local increase in the ion density downstream from the grain which induces an additional electric field and increases a total (drag) force acting on a negatively charged grain. However, continuous plasma absorption on the grain surface plays a significant role in this regime. Ion absorption causes a rarefaction of the ion density downstream from the grain. This effect reduces the ion drag force. In certain parameter regimes ion rarefaction can dominate over ion focusing and the ion drag force reverses direction.⁴⁷ Sign reversal of the ion drag force acting on an absorbing grain in collisional plasmas has been also observed in numerical simulations.^{35,36} A simple model considering an absorbing sphere in highly collisional plasma under the assumption of central Coulomb-type interaction potential between the ions and the sphere also predicts negative ion drag force.⁴⁸ One of the interesting consequences of the ion drag force sign reversal—a possibility of free undamped superfluidlike motion of the grain component and superconduc-

tive grain current—has been recently discussed by Vladimirov *et al.*⁴⁹

A physical process that has been neglected in previous considerations is related to plasma production and loss mechanisms. An assumption of the absence of plasma sources and sinks in the vicinity of the grain (except at the grain surface), which physically corresponds to the situation when the characteristic ionization/recombination length is considerably larger than the length scale of plasma perturbation by the grain, has been usually used. At the same time, even when plasma losses on the grain component due to absorption are unimportant (e.g., individual grain) other loss mechanisms such as three body volume recombination and/or ambipolar diffusion towards discharge walls and electrodes are still present.⁵⁰ Hence, in a realistic plasma environment, some plasma production and loss are inevitably present. Since these processes were neglected in previous theoretical considerations, it is interesting to investigate their effect on the ion drag force acting on the grain.

In this paper we assume that electron impact ionization is responsible for the plasma production while plasma loss is either due to volume recombination or due to ambipolar diffusion to the discharge walls and electrodes. Expressions for the ion drag force acting on a small absorbing grain in a highly collisional regime are obtained for these two cases. It is shown that not only the magnitude of the ion drag force, but also its direction depend on the plasma loss mechanisms and relative strength of plasma production. In addition, we briefly discuss the peculiarities of the electrostatic potential distribution around the grain in isotropic plasma for the two considered plasma loss mechanisms.

II. MODEL

We consider a small stationary negatively charged spherical grain in a highly collisional, weakly ionized quasineutral plasma with a constant weak ambipolar electric field. The electric field \mathbf{E}_0 generates ion flow with subthermal drift velocity $\mathbf{u} = e\mathbf{E}_0/m_i\nu$, where ν is the (constant) ion-neutral collision frequency. The electrons form a quasistationary background. Plasma sources and sinks are present in the vicinity of the grain which itself also acts as a sink due to plasma absorption on its surface. In the highly collisional regime, $\ell_i \ll \lambda_D$, where ℓ_i denotes the ion mean free path and λ_D is the linearized Debye radius, the ion component can be suitably described by the continuity and momentum equations in the hydrodynamic approximation,

$$\nabla(n_i\mathbf{v}_i) = Q_I - Q_L - J_i\delta(\mathbf{r}), \quad (1)$$

$$(\mathbf{v}_i \nabla)\mathbf{v}_i = (e/m_i)\mathbf{E} - (\nabla n_i/n_i)v_{Ti}^2 - \nu\mathbf{v}_i. \quad (2)$$

The electron density closely follows the Boltzmann relation even in the presence of plasma production/loss as recent numerical simulation indicates,⁵¹

$$n_e \approx n_0 \exp(e\phi/T_e). \quad (3)$$

Here $n_{i(e)}$ is the ion (electron) density, \mathbf{v}_i is the ion velocity, J_i is the ion flux to the grain surface, $v_{Ti} = \sqrt{T_i/m_i}$ is the ion thermal velocity, n_0 is the unperturbed plasma density (far

from the grain), $T_{i(e)}$ is the ion (electron) temperature. In the continuity equation Q_I and Q_L represent plasma production and loss terms, respectively. In our model we consider electron impact ionization as the only mechanism responsible for plasma production, i.e., $Q_I = \nu_I n_e$, where ν_I is the ionization frequency; plasma loss is either due to electron-ion volume recombination, $Q_L = \nu_R n_e n_i$, or due to ambipolar diffusion towards the discharge chamber walls or electrodes, $Q_L = \gamma_L n_i$. Here ν_R is the recombination coefficient and γ_L is the characteristic frequency of (ambipolar) plasma losses. In the unperturbed plasma, the above coefficients are related as $\nu_I = \nu_R n_0$ or $\nu_I = \gamma_L$. The first loss mechanism is relevant to high pressure plasmas, while the second mechanism can operate in low and moderate-pressure gas discharges.⁵⁰ Note that the assumption of mobility-limited subthermal ion drift requires that the ion-neutral collision frequency is much higher than the ionization frequency, $\nu \gg \nu_I$.

The above set of equations is closed with the Poisson equation

$$\Delta \phi = -4 \pi e (n_i - n_e) - 4 \pi Q \delta(\mathbf{r}), \quad (4)$$

where the second term in the right-hand side represents the charge density distribution of a pointlike grain ($a \ll \lambda_D$) of charge Q located at the position \mathbf{r} . Here a is the grain radius.

The above set of Eqs. (1)–(4) is linearized assuming $\mathbf{E} = \mathbf{E}_0 + \mathbf{E}_1$, $\mathbf{v}_i = \mathbf{u} + \mathbf{v}_1$, and $n_{i(e)} = n_0 + n_{i1(e)}$, where $\mathbf{E}_1 = -\nabla \phi$ is the electric field perturbation, \mathbf{v}_1 is the ion velocity perturbation, and $n_{i1(e)}$ is the perturbation of the ion (electron) density. Assuming that the plasma perturbations are proportional to $\propto \exp(i\mathbf{k}\mathbf{r})$ and using linear response technique we get an expression for the electric potential,^{47,52,53}

$$\begin{aligned} \phi(\mathbf{r}) = & (Q/2\pi^2) \int \chi_1(\mathbf{k}\mathbf{u}, k) \exp(i\mathbf{k}\mathbf{r}) d\mathbf{k} \\ & + (e/2\pi^2) \int \chi_2(\mathbf{k}\mathbf{u}, k) \exp(i\mathbf{k}\mathbf{r}) d\mathbf{k}, \end{aligned} \quad (5)$$

where χ_1 is the component of the plasma response associated with the presence of a nonabsorbing pointlike charged grain and χ_2 is the component associated with plasma absorption on the grain. In order to calculate ion drag force experienced by the grain we use the relation $F_i = -Q \nabla \phi|_{r=0}$. Then from Eq. (5) we get

$$\begin{aligned} F_i = & \pi^{-1} \int_0^\infty k^3 dk \int_{-1}^1 \mu d\mu \{ Q^2 \text{Im}[\chi_1(\mu, k)] \\ & + Qe \text{Im}[\chi_2(\mu, k)] \}, \end{aligned} \quad (6)$$

where $\mu = \cos \theta$ and θ is the angle between \mathbf{k} and \mathbf{E}_0 . In the following section we present the results for two different plasma loss mechanisms.

III. RESULTS AND DISCUSSION

A. Plasma loss due to electron-ion volume recombination

In this case the plasma response functions χ_1 and χ_2 are

$$\chi_1(\mathbf{k}\mathbf{u}, k) = \frac{k^2 v_{Ti}^2 - (\mathbf{k}\mathbf{u} - i\nu_I)(\mathbf{k}\mathbf{u} - i\nu)}{k^2 v_{Ti}^2 (k^2 + k_D^2) - (\mathbf{k}\mathbf{u} - i\nu_I)(\mathbf{k}\mathbf{u} - i\nu)(k^2 + k_{De}^2)}, \quad (7)$$

$$\chi_2(\mathbf{k}\mathbf{u}, k) = - \frac{iJ_i(\mathbf{k}\mathbf{u} - i\nu)}{k^2 v_{Ti}^2 (k^2 + k_D^2) - (\mathbf{k}\mathbf{u} - i\nu_I)(\mathbf{k}\mathbf{u} - i\nu)(k^2 + k_{De}^2)}, \quad (8)$$

where $k_{D_{i(e)}} = \lambda_{D_{i(e)}}^{-1}$ is the inverse Debye radius of the ions (electrons), $\lambda_{D_{i(e)}} = \sqrt{T_{i(e)}/4\pi n_0 e^2}$, and $k_D = \sqrt{k_{De}^2 + k_{Di}^2}$ is the inverse linearized Debye radius.

At first we consider isotropic plasma condition. In this case we put $\mathbf{k}\mathbf{u} = 0$ in Eqs. (7) and (8) to obtain

$$\chi_1 = \frac{k^2 v_{Ti}^2 + \nu_I \nu}{k^2 v_{Ti}^2 (k^2 + k_D^2) + \nu_I \nu (k^2 + k_{De}^2)}$$

and

$$\chi_2 = - \frac{J_i \nu}{k^2 v_{Ti}^2 (k^2 + k_D^2) + \nu_I \nu (k^2 + k_{De}^2)}.$$

Inserting the above expressions into Eq. (5) we obtain the potential distribution around the grain,

$$\phi_1 = (Q_+/r) \exp(-rk_+) + (Q_-/r) \exp(-rk_-), \quad (9)$$

where

$$k_\pm^2 = \frac{1}{2} \left(k_D^2 + \frac{\nu_I}{D_i} \right) \pm \frac{1}{2} \sqrt{\left(k_D^2 + \frac{\nu_I}{D_i} \right)^2 - \frac{4\nu_I k_{De}^2}{D_i}} \quad (10)$$

and

$$Q_\pm = \mp \frac{Q[k_\pm^2 - k_D^2 - (eJ_i/QD_i)]}{k_+^2 - k_-^2}. \quad (11)$$

Here $D_i \approx \ell_i \nu_{Ti} = \ell_i^2 \nu$ is the ion diffusion coefficient.

In this case the potential is screened exponentially but unlike the Debye–Hückel theory, it is described by the superposition of the two exponentials with different inverse screening lengths k_+ and k_- . Both these screening lengths depend on the strength of plasma production. The effective charges Q_+ and Q_- also depend on plasma production strength as well as on the ion flux collected by the grain. The long-range asymptote of the potential is determined by the smaller screening constant k_- with effective charge Q_- . The obtained expressions are similar to those derived recently by Filippov *et al.*⁵⁴ The only difference is associated with the fact that electron absorption on the grain was retained in Ref. 54 while we have neglected this effect for simplicity. The difference is however small: if in the expressions for screening lengths and effective charges of Ref. 54 we substitute $(D_e - D_i)/D_e D_i$ by $1/D_i$ and neglect $k_{Di}^2 (\nu_I/D_e)$ in comparison to $k_{De}^2 (\nu_I/D_i)$, then they reduce to our Eqs. (10) and (11).

Both simplifications are quite reasonable since $D_e \gg D_i$ and $\mu_e \gg \mu_i$, where $\mu_{i(e)}$ is the ion (electron) mobility.

Now let us analyze Eqs. (9)–(11) considering some limiting cases. At first we neglect plasma production and loss in the vicinity of the grain. We put $\nu_l=0$ in the above equations and obtain $k_+=k_D$, $k_-=0$, $Q_+=Q+(eJ_i/D_i k_D^2)$ and $Q_-=-eJ_i/D_i k_D^2$. The resulting expression for the potential is $\phi_l=(Q/r)\exp(-rk_D)-(e/r)(J_i \nu_l/v_T^2 k_D^2)[1-\exp(-rk_D)]$ which coincides with that obtained in Ref. 47. The first term is the usual Debye–Hückel potential while the second term is due to the effect of ion absorption on the grain surface. The far asymptote of the potential is completely determined by absorption and is of the Coulomb-type with effective charge $(eJ_i \nu_l/v_T^2 k_D^2)$. This result is known from probe theory^{55,56} and was recently reproduced in the context of highly collisional complex plasma in Refs. 57 and 58.

Next, we account for plasma production and losses in the vicinity of the grain. Then, depending on the strength of plasma production two limiting cases can be considered: low and high ionization rate. In the limit of low ionization rate, $\nu_l/D_i \ll k_D^2$, we obtain $k_+ \approx k_D$, $k_- \approx k_{De}(\ell_i k_D)^{-1} \sqrt{\nu_l/\nu}$, $Q_+ \approx Q+(eJ_i/D_i k_D^2)$, and $Q_- \approx -(eJ_i/D_i k_D^2)$. The potential is screened completely. The screening is dominated by ionization/recombination effects and the screening length $\lambda_{De}(\ell_i k_D) \sqrt{\nu_l/\nu}$ is considerably larger than the electron Debye radius since $(\ell_i k_D) \gg \sqrt{\nu_l/\nu}$ in the considered regime. For distances $\lambda_D \ll r \ll \lambda_{De}(\ell_i k_D) \sqrt{\nu_l/\nu}$ the potential behaves as Coulomb-type with the effective charge $Q_- \approx -(eJ_i/D_i k_D^2)$, i.e., we recover the result of the previous (no ionization/recombination) limit. Thus the distance $\lambda_{De}(\ell_i k_D) \sqrt{\nu_l/\nu}$ determines the length scale below which plasma production is not important and sets up the upper limit of applicability of the results obtained within the assumption of no ionization/recombination processes in the vicinity of the grain (see, e.g., Refs. 47 and 59).

In the opposite case of high ionization rate, $\nu_l/D_i \gg k_D^2$, we obtain $k_+ \approx \sqrt{\nu_l/D_i}$, $k_- \approx k_{De}$, $Q_+ \approx Q(k_D^2 D_i/\nu_l) + (eJ_i/\nu_l)$, and $Q_- \approx Q - (eJ_i/\nu_l)$. The potential is again screened completely. The screening length is given by the electron Debye radius λ_{De} and is independent of the ionization rate ν_l . The effective charge $Q_- \approx Q - eJ_i/\nu_l$ is somewhat larger in the absolute magnitude than the actual charge. To estimate quantitatively the contribution of absorption to effective charge an expression for the ion flux J_i is required. We use the asymptotic expression for the ion flux on the infinitesimally small particle ($a/\lambda_D \rightarrow 0$) in the continuum limit ($\ell_i/a \rightarrow 0$),^{55,56,58}

$$J_i \approx 4\pi(|Q|e/T_i)n_0\ell_i\nu_{Ti}. \quad (12)$$

Although this expression has been derived neglecting plasma production and losses in the vicinity of a pointlike grain, numerical simulations of Ref. 57 indicate that these effects do not contribute substantially to the collected ion flux, provided the ionization rate is not too high and the grain size is not too large ($a \leq \lambda_D$). Then Eq. (12) yields $Q_- \approx Q[1+k_D^2 D_i/\nu_l] \approx Q$ since $k_D^2 D_i/\nu_l \ll 1$ in the limit of high ionization rate. Note that for low ionization rate we get $Q_- \approx Q(k_{Di}/k_D)^2 = Q(1+T_i/T_e)^{-1}$, i.e., $Q_- = Q/2$ for one-

temperature plasma ($T_e=T_i$) and $Q_- \approx Q$ for two-temperature plasma with $T_e \gg T_i$.

Next we calculate the ion drag force assuming vanishingly slow ion drift and taking into account that applicability of the hydrodynamic approximation requires $k\ell_i \ll 1$. In this regime the expressions for $\text{Im}\{\chi_1\}$ and $\text{Im}\{\chi_2\}$ can be simplified,

$$\text{Im}\{\chi_1\} \approx \frac{k^2 k_{Di}^2 \nu_{Ti}^2 (\nu + \nu_l) \mathbf{k} \mathbf{u}}{[k^4 \nu_{Ti}^2 + k^2 (k_D^2 \nu_{Ti}^2 + \nu \nu_l) + \nu \nu_l k_{De}^2]^2}, \quad (13)$$

$$\text{Im}\{\chi_2\} \approx \frac{J_i \nu^2 (k^2 + k_{De}^2) \mathbf{k} \mathbf{u}}{[k^4 \nu_{Ti}^2 + k^2 (k_D^2 \nu_{Ti}^2 + \nu \nu_l) + \nu \nu_l k_{De}^2]^2}. \quad (14)$$

Substituting Eqs. (13) and (14) in Eq. (6) and then performing integrations we get an expression for the ion drag force,

$$F_i \approx \frac{1}{6} Q^2 k_{Di}^2 M_{Ti}(\ell_i k_D)^{-1} \left(\frac{k_D \kappa_1^2}{\kappa_2^3} \right) \times \left[1 + \left(\frac{\nu_l}{\nu} \right) + \left(\frac{e}{Q} \right) \left(\frac{J_i}{D_i k_{Di}^2} \right) \left(1 + \frac{k_{De}^2}{\kappa_1^2} \right) \right], \quad (15)$$

where $\kappa_1^2 = k_D^2 + 3k_{De} \sqrt{\nu_l/D_i} + (\nu_l/D_i)$, $\kappa_2^2 = k_D^2 + 2k_{De} \sqrt{\nu_l/D_i} + (\nu_l/D_i)$ and $M_{Ti} = u/v_{Ti}$ is the ion-thermal Mach number.

The first two terms in the above expression correspond to the force acting on a nonabsorbing grain in the presence of ionization and recombination around the grain. The third term represents contribution to the drag force due to ion absorption on the grain. For the negatively charged grain, ion absorption reduces the magnitude of the ion drag force, since $Q < 0$. It is clear that the effect of ionization and recombination in the vicinity of the grain modifies the amplitude of both terms. In the absence of ionization ($\nu_l=0$) we get $\kappa_1 = \kappa_2 = k_D$ and $F_i = (1/6) Q^2 k_{Di}^2 M_{Ti}(\ell_i k_D)^{-1} [1 + (e/Q)(J_i/D_i k_{Di}^2) \times (1 + k_{De}^2/k_D^2)]$ which is identical to that obtained by Khrapak *et al.*⁴⁷ In the case of nonabsorbing grain we substitute $J_i=0$ in Eq. (15) and obtain

$$F_i \approx (1/6) Q^2 k_{Di}^2 M_{Ti} (1 + \nu_l/\nu) (k_D/\kappa_2) (\kappa_1^2/\kappa_2^2) (\ell_i k_D)^{-1}. \quad (16)$$

Thus, the ion drag force acting on a nonabsorbing grain is always positive, i.e., it is directed along the direction of the ion drift. For $\nu_l=0$, we have $F_i \approx (1/6) Q^2 k_{Di}^2 M_{Ti}(\ell_i k_D)^{-1}$, which in the highly collisional limit coincides with the earlier expression obtained using a more general kinetic approach and neglecting absorption.³² The presence of ionization and recombination in the vicinity of a nonabsorbing grain modifies the magnitude of the ion drag force by a factor $\sim (1 + \nu_l/\nu)(k_D \kappa_1^2/\kappa_2^3)$. In the limit of low ionization rate this factor is $\sim [1 - (\nu_l/2D_i k_D^2)] \approx 1$ and in the opposite limit of high ionization rate it is $\sim \sqrt{D_i k_D^2/\nu_l} (1 + \nu_l/\nu)$. Thus, for low ionization rate, ionization/recombination processes only slightly reduce the magnitude of the ion drag force, but in the opposite limit of high ionization rate the force is considerably reduced since $D_i k_D^2/\nu_l \ll 1$ in this case.

For further analysis we rewrite Eq. (15) introducing three dimensionless parameters: $\vartheta = \nu_l/\nu$, the ratio of ionization and ion-neutral collision frequencies, $\tau = T_e/T_i$, the electron-to-ion temperature ratio and $\xi_i = \lambda_{Di}/\ell_i$, the inverse

normalized ion mean free path, and use Eq. (12) for the ion flux collected by the grain. Then the expression for the ion drag force is

$$F_i = \frac{1}{6} Q^2 k_D^2 M_{T_i} (\ell_i k_D)^{-1} \mathcal{F}_1(\vartheta, \tau, \xi_i), \quad (17)$$

where the dimensionless function \mathcal{F}_1 is

$$\mathcal{F}_1(\vartheta, \tau, \xi_i) = \frac{(\tau + 1)^{1/2} [\tau \vartheta^2 \xi_i^2 + 3 \xi_i \vartheta \sqrt{\vartheta \tau + \vartheta(\tau + 1)} - 1]}{(\tau \vartheta \xi_i^2 + 2 \xi_i \sqrt{\vartheta \tau + \tau + 1})^{3/2}}. \quad (18)$$

The most interesting point is that the numerator of \mathcal{F}_1 can change sign which indicates reversal of the direction of the

ion drag force. In the absence of ionization and recombination $\mathcal{F}_1 = -(\tau + 1)^{-1}$ and the ion drag force is negative, i.e., it is directed oppositely to the ion drift. The same is true for low ionization rate. When ionization rate increases the numerator in Eq. (18) changes sign and the ion drag force reverses its direction. The value of ϑ for which this reversal occurs is plotted as a function of ξ_i in Fig. 1 for three different values of τ . Note that for large ξ_i the transition from negative to positive values of the ion drag force can be well described by $\vartheta \approx 1/\xi_i \sqrt{\tau}$. Thus, in a plasma with sufficiently developed ionization the ion drag force is always directed along the ion motion.

B. Case 2: Plasma loss due to ambipolar diffusion

In this case the plasma response functions are

$$\chi_1(\mathbf{k}, k) = \frac{k^2 v_{T_i}^2 - (\mathbf{k}\mathbf{u} - i\nu_l)(\mathbf{k}\mathbf{u} - i\nu)}{k^2 v_{T_i}^2 (k^2 + k_D^2) - k^2 (\mathbf{k}\mathbf{u} - i\nu_l)(\mathbf{k}\mathbf{u} - i\nu) - k_{De}^2 \mathbf{k}\mathbf{u}(\mathbf{k}\mathbf{u} - i\nu)}, \quad (19)$$

$$\chi_2(\mathbf{k}, k) = \frac{iJ_i(\mathbf{k}\mathbf{u} - i\nu)}{k^2 v_{T_i}^2 (k^2 + k_D^2) - k^2 (\mathbf{k}\mathbf{u} - i\nu_l)(\mathbf{k}\mathbf{u} - i\nu) - k_{De}^2 \mathbf{k}\mathbf{u}(\mathbf{k}\mathbf{u} - i\nu)}. \quad (20)$$

For isotropic plasma we substitute $\mathbf{k}\mathbf{u} = 0$ in the above expressions to obtain

$$\chi_1 = \frac{k^2 v_{T_i}^2 + \nu_l \nu}{k^2 v_{T_i}^2 (k^2 + k_D^2) + k^2 \nu_l \nu}$$

and

$$\chi_2 = -\frac{J_i \nu}{k^2 v_{T_i}^2 (k^2 + k_D^2) + k^2 \nu_l \nu}.$$

The potential around the grain is

$$\phi_1 = (Q_1/r) \exp(-k_{\text{eff}} r) + Q_2/r, \quad (21)$$

where Q_1 and Q_2 are the effective charges, $Q_1 = Q \{1 - [\nu_l - (e/Q) J_i / D_i k_{\text{eff}}^2]\}$ and $Q_2 = Q - Q_1 = (Q \nu_l - e J_i) / D_i k_{\text{eff}}^2$. The inverse effective screening length is $k_{\text{eff}}^2 = k_D^2 + \nu_l / D_i$. Thus, in the case of plasma loss due to ambipolar diffusion the potential is not completely screened, but has a Coulomb-type long-range asymptote. The effective charge Q_2 depends both on the strength of ionization ν_l and the ion flux J_i collected by the grain. In the absence of ionization and ambipolar loss processes in the vicinity of the grain we obtain $k_{\text{eff}} = k_D$, $Q_1 = Q + (e J_i / D_i k_D^2)$, and $Q_2 = -(e J_i / D_i k_D^2)$, which is identical to that obtained recently in Ref. 47 as well as in the previous subsection.

In the presence of ionization and ambipolar loss processes we consider two limiting cases as before: low and high ionization rate. In the limit of low ionization rate, $\nu_l / D_i \ll k_D^2$, we obtain $k_{\text{eff}} \approx k_D$, $Q_1 \approx Q + (e J_i / D_i k_D^2)$, and

$Q_2 \approx (Q \nu_l - e J_i) / D_i k_D^2$. Using Eq. (12) for the ion flux collected by the grain we get $Q_2 \approx -e J_i / D_i k_D^2 = Q (k_{D_i}^2 / k_D^2) = Q (1 + T_i / T_e)^{-1}$, i.e., plasma production and ambipolar loss are not important in this regime.

In the opposite limit of high ionization rate $\nu_l / D_i \gg k_D^2$ we obtain $k_{\text{eff}}^2 \approx \nu_l / D_i$, $Q_1 \approx (e J_i / \nu_l)$, and $Q_2 \approx Q - (e J_i / \nu_l)$. In this case the screening length is completely determined by

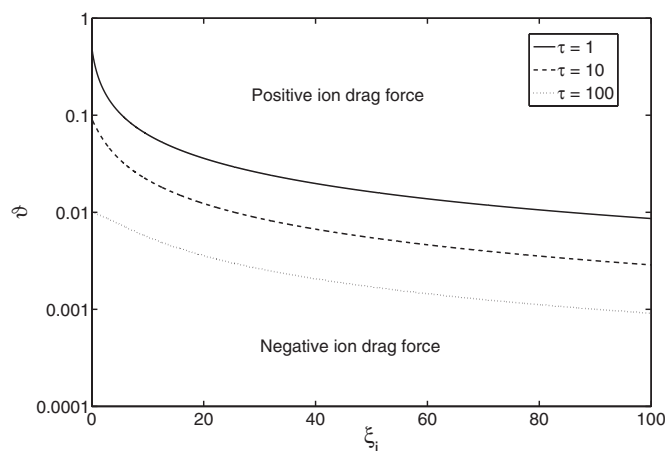


FIG. 1. Variation of transitional normalized ionization frequency, $\vartheta = \nu_l / \nu$ with normalized inverse ion mean free path, $\xi_i = \lambda_{D_i} / \ell_i$ for three different electron-to-ion temperature ratios, $\tau = 1, 10$, and 100 . In this case the plasma production is due to electron impact ionization and plasma loss is due to electron-ion volume recombination. Curves correspond to transition between positive and negative values of the ion drag force. With a reasonable accuracy $\vartheta \approx 1 / \xi_i \sqrt{\tau}$.

ionization and loss processes through the ionization rate ν_I . Using the asymptotic expression for the ion flux Eq. (12), the effective charge that governs the long-range asymptote of the potential is $Q_2 \approx Q[1 + (k_D^2 D_i / \nu_I)] \approx Q$. The charge is therefore almost unscreened in this case.

Next, we calculate the ion drag force acting on the dust grain. Again considering very slow ion drift we can approximate the imaginary parts of the expressions for χ_1 and χ_2 as

$$\text{Im}(\chi_1) \approx \frac{[k^2 k_{Di}^2 \nu_{Ti}^2 (\nu + \nu_I) - \nu_I \nu^2 k_{De}^2] \mathbf{k} \mathbf{u}}{k^4 \nu_{Ti}^4 (k^2 + k_{\text{eff}}^2)^2}, \quad (22)$$

$$\text{Im}(\chi_2) \approx \frac{J_i \nu_i^2 (k^2 + k_{De}^2) \mathbf{k} \mathbf{u}}{k^4 \nu_{Ti}^4 (k^2 + k_{\text{eff}}^2)^2}. \quad (23)$$

After substituting Eqs. (22) and (23) in Eq. (6) we obtain ion drag force,

$$F_i \approx \frac{1}{6} Q^2 k_{Di}^2 M_{Ti} (\ell_i k_D)^{-1} \left(\frac{k_D}{k_{\text{eff}}} \right)^3 \left[\left(1 + \frac{\nu_I}{\nu} \right) \left(\frac{k_{\text{eff}}}{k_D} \right)^2 - \left(\frac{\nu_I}{D_i k_D^2} \right) \left(\frac{k_{De}}{k_{Di}} \right)^2 + \left(\frac{e}{Q} \right) \left(\frac{J_i}{D_i k_D^2} \right) \left(\frac{k_{\text{eff}}^2 + k_{De}^2}{k_{Di}^2} \right) \right]. \quad (24)$$

At first we consider the situation without ionization, $\nu_I=0$. In this limit we get the same expression as obtained in Ref. 47 as expected. For a nonabsorbing grain ($J_i=0$) the ion drag force is

$$F_i = (1/6) Q^2 k_{Di}^2 M_{Ti} (k_D / k_{\text{eff}}) (\ell_i k_D)^{-1} \times [1 + \nu_I / \nu - (T_i / T_e) (1 + k_D^2 D_i / \nu_I)^{-1}].$$

The force is always positive since $T_e \geq T_i$. Further if we neglect ionization ($\nu_I=0$), then we recover the expression from Ref. 32. The presence of ionization and ambipolar plasma loss processes modify the ion drag force experienced by a nonabsorbing grain by a factor $\sim (k_D / k_{\text{eff}}) [1 + \nu_I / \nu - (T_i / T_e) \times (1 + k_D^2 D_i / \nu_I)^{-1}]$. In the limit of low ionization rate $\nu_I / D_i \ll k_D^2$ this factor becomes $\sim [1 - (\nu_I / 2 D_i k_D^2)] \approx 1$, i.e., the force is only slightly reduced. In the opposite limit of high ionization rate the factor is $\sim k_D \sqrt{D_i / \nu_I} (1 - \nu_I / \nu - T_i / T_e)$, i.e., the force is considerably reduced.

We can further simplify Eq. (24) by using the asymptotic expression for the ion flux in the continuum limit [Eq. (12)] as well as three dimensionless parameters (τ, ξ_i, ϑ) introduced above. The result is

$$F_i = \frac{1}{6} Q^2 k_{Di}^2 M_{Ti} (\ell_i k_D)^{-1} \mathcal{F}_2(\vartheta, \tau, \xi_i), \quad (25)$$

where

$$\mathcal{F}_2(\vartheta, \tau, \xi_i) = \frac{[(\vartheta \xi_i^2 + 1)(\vartheta \tau - 1) + \vartheta](\tau + 1)^{1/2}}{(\vartheta \tau \xi_i^2 + \tau + 1)^{3/2}}. \quad (26)$$

In the absence of ionization and ambipolar loss ($\vartheta=0$) we obtain $\mathcal{F}_1 = -(\tau + 1)^{-1}$ and the ion drag force is negative.⁴⁷ For sufficiently low ionization strength the ion drag force remains negative as well. The transition from negative-to-positive ion drag forces occur when $\vartheta \approx 1/\tau$, as can be seen in Fig. 2. Unlike the previous case where the transitional value of θ depends on both ξ_i and τ , now it depends only on

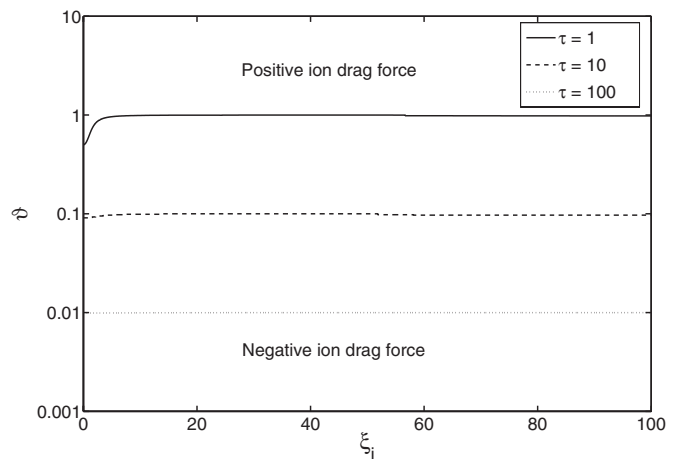


FIG. 2. Variation of transitional normalized ionization frequency, $\vartheta = \nu_I / \nu$ with normalized inverse ion mean free path, $\xi_i = \lambda_{Di} / \ell_i$ for three different electron-to-ion temperature ratios, $\tau = 1, 10$, and 100 . In this case the plasma production is due to electron impact ionization and plasma loss is due to ambipolar diffusion to the discharge walls and electrodes. Curves correspond to transition between positive and negative values of the ion drag force. With a good accuracy $\vartheta \approx 1/\tau$.

τ . Thus, for both considered mechanisms of plasma loss the ion drag force becomes positive, i.e., directed along the ion drift provided the ionization strength is high enough.

IV. SUMMARY

To summarize, we have analytically investigated the effect of plasma production and losses on the ion drag force acting on a small grain in highly collisional plasma with slowly drifting ions. In our model the plasma production is due to electron impact ionization, whereas the loss processes can be either due to electron-ion volume recombination or due to ambipolar diffusion towards discharge walls and electrodes. We have demonstrated that the ion drag force is strongly influenced by the plasma production and loss processes in the vicinity of the grain. For a nonabsorbing grain the ion drag force is positive, i.e., it acts along the direction of the ion drift independently of the loss mechanisms that have been investigated. The magnitude of the ion drag force is practically unaffected by plasma production when ionization rate is weak $\nu_I / k_D^2 D_i \lesssim 1$. When ionization rate is strong, $\nu_I / k_D^2 D_i \gg 1$ the force is strongly reduced. The ion drag force acting on the absorbing grain is negative when ionization rate is low. However, when ionization rate increases, the force reverses its direction. For sufficiently high ionization rate the ion drag force is positive independently of the plasma loss mechanism. The parameter regimes for the positive and negative ion drag forces have been identified for both plasma loss mechanisms considered.

We have also briefly discussed peculiarities of the electric potential distribution in isotropic plasma with ionization and loss processes. It is shown that the conventional Debye-Hückel (Yukawa) potential distribution around the grain operates only in the absence of ionization and absorption processes. For volume recombination mechanism the potential consists of two exponential terms and the long-range potential is of the Debye-Hückel-type. On the other hand, for

ambipolar diffusion loss mechanism the long-range potential is of the Coulomb-type. The effective charge turns out to be of the order of the actual one.

ACKNOWLEDGMENTS

This work was partially supported by DLR under Grant No. 50WP0203.

- ¹P. K. Shukla and A. A. Mamun, *Introduction to Dusty Plasma Physics* (IOP, London, 2002).
- ²V. E. Fortov, A. G. Khrapak, S. A. Khrapak, V. I. Molotkov, and O. F. Petrov, *Phys. Usp.* **47**, 447 (2004).
- ³S. V. Vladimirov and K. Ostrikov, *Phys. Rep.* **393**, 175 (2004).
- ⁴V. E. Fortov, A. V. Ivlev, S. A. Khrapak, A. G. Khrapak, and G. E. Morfill, *Phys. Rep.* **421**, 1 (2005).
- ⁵H. M. Thomas, G. E. Morfill, V. Demmel, J. Goree, B. Feuerbacher, and D. Möhlmann, *Phys. Rev. Lett.* **73**, 652 (1994).
- ⁶J. H. Chu and L. I., *Phys. Rev. Lett.* **72**, 4009 (1994).
- ⁷H. M. Thomas and G. E. Morfill, *Nature (London)* **379**, 806 (1996).
- ⁸D. A. Mendis, *Plasma Sources Sci. Technol.* **11**, A219 (2002).
- ⁹G. E. Morfill and H. M. Thomas, *Icarus* **179**, 539 (2005).
- ¹⁰A. Bouchule, in *Dusty Plasmas: Physics, Chemistry and Technological Impacts in Plasma Processing*, edited by A. Bouchule (Wiley, Chichester, 1999).
- ¹¹J. Winter, *Phys. Plasmas* **7**, 3862 (2000).
- ¹²A. Yu. Pigarov, S. I. Krasheninnikov, T. K. Soboleva, and T. D. Rognlien, *Phys. Plasmas* **12**, 122508 (2005).
- ¹³U. de Angelis, *Phys. Plasmas* **13**, 012514 (2006).
- ¹⁴S. A. Khrapak, A. V. Ivlev, and G. E. Morfill, *Phys. Rev. E* **70**, 056405 (2004).
- ¹⁵G. E. Morfill, H. M. Thomas, U. Konopka, H. Rothermel, M. Zuzic, A. V. Ivlev, and J. Goree, *Phys. Rev. Lett.* **83**, 1598 (1999).
- ¹⁶J. Goree, G. E. Morfill, V. N. Tsytovich, and S. V. Vladimirov, *Phys. Rev. E* **59**, 7055 (1999).
- ¹⁷M. Kretschmer, S. A. Khrapak, S. K. Zhdanov, H. M. Thomas, G. E. Morfill, V. E. Fortov, A. M. Lipaev, V. I. Molotkov, A. I. Ivanov, and M. V. Turin, *Phys. Rev. E* **71**, 056401 (2005).
- ¹⁸A. M. Lipaev, S. A. Khrapak, V. I. Molotkov, G. E. Morfill, V. E. Fortov, A. V. Ivlev, H. M. Thomas, A. G. Khrapak, V. N. Naumkin, A. I. Ivanov, S. E. Tretschkev, and G. I. Padalka, *Phys. Rev. Lett.* **98**, 265006 (2007).
- ¹⁹M. Wolter, A. Melzer, O. Arp, M. Klindworth, and A. Piel, *Phys. Plasmas* **14**, 123707 (2007).
- ²⁰U. Konopka, D. Samsonov, A. V. Ivlev, J. Goree, V. Steinberg, and G. E. Morfill, *Phys. Rev. E* **61**, 1890 (2000).
- ²¹P. K. Kaw, K. Nishikawa, and N. Sato, *Phys. Plasmas* **9**, 387 (2002).
- ²²D. Samsonov and J. Goree, *Phys. Rev. E* **59**, 1047 (1999).
- ²³M. S. Barnes, J. H. Keller, J. C. Forster, J. A. O'Neill, and D. K. Coultas, *Phys. Rev. Lett.* **68**, 313 (1992).
- ²⁴S. V. Vladimirov and N. F. Cramer, *Phys. Rev. E* **62**, 2754 (2000).
- ²⁵N. D'Angelo, *Phys. Plasmas* **5**, 3155 (1998).
- ²⁶A. V. Ivlev, D. Samsonov, J. Goree, G. Morfill, and V. E. Fortov, *Phys. Plasmas* **6**, 741 (1999).
- ²⁷S. A. Khrapak and V. V. Yaroshenko, *Phys. Plasmas* **10**, 4616 (2003).
- ²⁸A. A. Uglov and A. G. Gnedovets, *Plasma Chem. Plasma Process.* **11**, 251 (1991).
- ²⁹S. A. Khrapak, A. V. Ivlev, G. E. Morfill, and H. M. Thomas, *Phys. Rev. E* **66**, 046414 (2002).
- ³⁰S. A. Khrapak, A. V. Ivlev, G. E. Morfill, and S. K. Zhdanov, *Phys. Rev. Lett.* **90**, 225002 (2003).
- ³¹S. A. Khrapak, A. V. Ivlev, G. E. Morfill, S. K. Zhdanov, and H. M. Thomas, *IEEE Trans. Plasma Sci.* **32**, 555 (2004).
- ³²A. V. Ivlev, S. A. Khrapak, S. K. Zhdanov, G. E. Morfill, and G. Joyce, *Phys. Rev. Lett.* **92**, 205007 (2004).
- ³³A. V. Ivlev, S. K. Zhdanov, S. A. Khrapak, and G. E. Morfill, *Phys. Rev. E* **71**, 016405 (2005).
- ³⁴S. A. Khrapak, A. V. Ivlev, S. K. Zhdanov, and G. E. Morfill, *Phys. Plasmas* **12**, 042308 (2005).
- ³⁵I. V. Schweigert, A. L. Alexandrov, and F. M. Peeters, *IEEE Trans. Plasma Sci.* **32**, 623 (2004).
- ³⁶S. A. Maiorov, *Plasma Phys. Rep.* **31**, 690 (2005).
- ³⁷I. H. Hutchinson, *Plasma Phys. Controlled Fusion* **47**, 71 (2005).
- ³⁸I. H. Hutchinson, *Plasma Phys. Controlled Fusion* **48**, 185 (2006).
- ³⁹C. Zafiu, A. Melzer, and A. Piel, *Phys. Plasmas* **9**, 4794 (2002).
- ⁴⁰C. Zafiu, A. Melzer, and A. Piel, *Phys. Plasmas* **10**, 1278 (2003); S. A. Khrapak, A. V. Ivlev, G. E. Morfill, H. M. Thomas, S. K. Zhdanov, U. Konopka, M. H. Thoma, and R. A. Quinn, *ibid.* **10**, 4579 (2003); C. Zafiu, A. Melzer, and A. Piel, *ibid.* **10**, 4582 (2003).
- ⁴¹M. Hirt, D. Block, and A. Piel, *IEEE Trans. Plasma Sci.* **32**, 582 (2004).
- ⁴²K. Matyash, M. Fröhlich, H. Kersten, G. Thieme, R. Schneider, M. Hannemann, and R. Hippler, *J. Phys. D* **37**, 2703 (2004).
- ⁴³V. Yaroshenko, S. Ratynskaia, S. A. Khrapak, M. H. Thoma, M. Kretschmer, H. Höfner, G. E. Morfill, A. Zobnin, A. Usachev, O. F. Petrov, and V. E. Fortov, *Phys. Plasmas* **12**, 093503 (2005).
- ⁴⁴V. Nosenko, R. Fisher, R. Merlino, S. A. Khrapak, G. E. Morfill, and K. Avinash, *Phys. Plasmas* **14**, 103702 (2007).
- ⁴⁵A. V. Ivlev, S. K. Zhdanov, S. A. Khrapak, and G. E. Morfill, *Plasma Phys. Controlled Fusion* **46**, B267 (2004).
- ⁴⁶S. A. Maiorov, S. V. Vladimirov, and N. F. Cramer, *Phys. Rev. E* **63**, 017401 (2000).
- ⁴⁷S. A. Khrapak, S. K. Zhdanov, A. V. Ivlev, and G. E. Morfill, *J. Appl. Phys.* **101**, 033307 (2007).
- ⁴⁸S. A. Khrapak, B. A. Klumov, and G. E. Morfill, *Phys. Plasmas* **14**, 074702 (2007).
- ⁴⁹S. V. Vladimirov, S. A. Khrapak, M. Chaudhuri, and G. E. Morfill, *Phys. Rev. Lett.* **100**, 055002 (2008).
- ⁵⁰Y. P. Raizer, *Gas Discharge Physics* (Springer, Berlin, 1991).
- ⁵¹A. V. Filippov, N. A. Dyatko, A. F. Pal, and A. N. Starostin, *Plasma Phys. Rep.* **29**, 190 (2003).
- ⁵²M. Chaudhuri, S. A. Khrapak, and G. E. Morfill, *Phys. Plasmas* **14**, 022102 (2007).
- ⁵³M. Chaudhuri, S. A. Khrapak, and G. E. Morfill, *Phys. Plasmas* **14**, 054503 (2007).
- ⁵⁴A. V. Filippov, A. G. Zagorodny, A. I. Momot, A. F. Pal, and A. N. Starostin, *JETP* **104**, 147 (2007).
- ⁵⁵C. H. Su and S. H. Lam, *Phys. Fluids* **6**, 1479 (1963).
- ⁵⁶J.-S. Chang and J. G. Laframboise, *Phys. Fluids* **19**, 25 (1976).
- ⁵⁷O. Bystrenko and A. Zagorodny, *Phys. Rev. E* **67**, 066403 (2003).
- ⁵⁸S. A. Khrapak, G. E. Morfill, A. G. Khrapak, and L. G. D'yachkov, *Phys. Plasmas* **13**, 052114 (2006).
- ⁵⁹S. A. Khrapak, G. E. Morfill, V. E. Fortov, L. G. D'yachkov, A. G. Khrapak, and O. F. Petrov, *Phys. Rev. Lett.* **99**, 055003 (2007).

Superfluidlike Motion of an Absorbing Body in a Collisional Plasma

S. V. Vladimirov

School of Physics, The University of Sydney, New South Wales 2006, Australia

S. A. Khrapak, M. Chaudhuri, and G. E. Morfill

Max-Planck-Institut für extraterrestrische Physik, D-85741 Garching, Germany

(Received 14 October 2007; published 4 February 2008)

Motion of a small charged absorbing body (micrograin) immersed in a stationary weakly ionized high pressure plasma environment is considered. It is shown that the total frictional (drag) force acting on the grain can be directed along its motion, causing the grain acceleration. At some velocity, the forces associated with different plasma components can balance each other, allowing free undamped superfluid motion of the grain. The conditions when such behavior can be realized and the possibility of a superconductive grain current are discussed in the context of complex (dusty) plasmas.

DOI: [10.1103/PhysRevLett.100.055002](https://doi.org/10.1103/PhysRevLett.100.055002)

PACS numbers: 52.27.Lw

In quantum fluids, the phenomenon of superfluidity is related to the condition of excitation of collective perturbations in the flow [1]. At zero temperatures, essentially any phononlike spectrum satisfies the condition of no excitation if the velocity of the flow does not exceed a certain threshold. At small but finite temperatures, the existing excitations can cause friction while the condition of no new excitations still supports the superfluid component. The corresponding theory is an essentially quantum one, dealing with quantum elementary excitations [1]. A fully analogous phenomenon can hardly exist in classical fluids.

Can, however, a superfluidlike behavior appear in a classical open plasma system when studying the motion of macroscopic-size (as compared to the sizes of electrons and atoms) grains absorbing plasma? Note that the interaction between a body (e.g., a dust particle) and a surrounding plasma is itself a fundamental physical problem with many applications ranging from astrophysical topics [2,3] and technological plasma applications [4,5] to dusty (complex) plasmas [6–10] and fusion related problems [11–13]. An absorbing grain immersed in a plasma becomes charged by collecting ion and electron fluxes on its surface. In the stationary state these fluxes balance each other, resulting in a negative (floating) surface potential (and correspondingly, negative charge) because of the higher mobility of plasma electrons as compared to that of ions. Thus, the grain-plasma system appears as an essentially open system, in which the plasma loss to the grain should be balanced by an ionization source.

When a grain moves in a plasma, it experiences the frictional (drag) force associated with all plasma components—positive ions, negative electrons, and neutral gas (we consider a three-component plasma; negative ions are absent). The neutral drag force is likely to be dominant in most cases as long as the plasma is weakly ionized. In this Letter, however, we discuss a different situation: when the plasma-related drag can overcome the neutral drag, and,

even more important, when the total drag force can be directed along the grain motion, causing the grain to accelerate until it reaches a free undamped motion with no friction, thus experiencing a superfluidlike motion. It is important that this effect takes place in a highly collisional (i.e., highly viscous) weakly ionized plasma. The main reason for such an unusual behavior is the openness of the grain-plasma system.

Let us consider a plasma in the parameter regime recently studied by Khrapak *et al.* [14]: the stationary bulk quasineutral high pressure plasma, with motions of both electrons and ions dominated by collisions with neutrals. A small individual absorbing grain of (negative) charge Q is slowly moving with respect to plasma background. There are no plasma sources and sinks in the vicinity of the grain (except for the grain surface, which is fully absorbing), which corresponds physically to the situation when the characteristic ionization or recombination length is considerably larger than the characteristic size of the plasma perturbation by the grain. For simplicity let us also assume that the temperatures of electron, ion, and neutral components are equal to each other; generalization to a nonequilibrium case is straightforward.

The total friction force consists of three contributions associated with interactions with different plasma components—the electron, ion, and neutral drags. When relative velocities between the grain and other plasma components are the same, the ratio of the electron drag force to the ion (neutral) drag forces is $\propto (m_e/m_{i(n)})^{1/2}$ [15], where m_e , m_i , and m_n are the electron, ion, and neutral mass, respectively. Hence, the electron contribution to the friction can be neglected. The expression for the ion drag force relevant to the considered regime was derived in Ref. [14]. For one-temperature plasma this expression is

$$F_i \approx -(1/24)(Q^2/\lambda_D^2)(\lambda_D/\ell_i)(u/v_{Ti}), \quad (1)$$

where $\lambda_D = \sqrt{T/8\pi e^2 n_0}$ is the linearized Debye length, n_0

is the electron and ion number densities, T is the temperature, u is the grain velocity, ℓ_i is the ion mean free path, and $v_{T_i} = \sqrt{T/m_i}$ is the ion thermal velocity. The negative sign in the above expression reveals the fact that the ion drag force on a small absorbing body in highly collisional plasma acts in the direction of its motion. Before discussing the associated physics, we note that sign reversal of the ion drag force was reported recently for a simple model considering an absorbing sphere in a highly collisional flowing plasma under the assumption of central Coulomb-like interaction potential between the ions and the sphere [16]. Negative values of the ion drag force acting on an absorbing grain were also detected previously in numerical simulations [17,18]. Although a direct comparison between results of these simulations performed in the regime of moderate ion collisionality and analytical results of Ref. [14] derived in the highly collisional limit is not possible, the physical processes responsible for the effect can be identified. These are the ion-neutral collisions (in the collisionless regime the force can never be negative due to momentum conservation in ion-grain collisions) and the ion absorption on the grain (the ion drag force acting on a nonabsorbing grain in collisional plasma has been shown to be a monotonically increasing positive function of the ion collisionality [19]).

Indeed, the ion-neutral collisions enhance the ion drag force (as compared to the collisionless case) when no absorption occurs. This is because of collision-induced ion focusing [19], an effect implying a local increase in the ion density behind the grain [20,21] which induces an electric field and a (drag) force acting in the direction opposite to the grain motion. With increasing collisional-

ity, the focusing center moves closer to the grain and the drag force increases. In contrast, the ion absorption causes a rarefaction of the ion density behind the grain. These two effects compete with each other and under certain conditions the rarefaction dominates. The ion rarefaction implies a negative space charge behind the grain and induces an electric field and a (drag) force acting in the direction of the grain motion.

To illustrate this effect, we plot a distribution of the electric potential behind nonabsorbing and absorbing grains moving slowly through a collisional plasma; see Fig. 1. For a nonabsorbing grain there is a positive peak in the potential corresponding to the ion focusing. Note that the peak amplitude increases and its position moves closer to the grain when the ion collisionality increases. This would correspond to the increase of the ion drag force. When absorption is taken into account, the peak disappears and a negative space charge region is formed behind the grain. This negative space charge repels the negatively charged grain leading to the (drag) force directed along its motion.

The analytical expression (1) is derived by using the linear plasma response formalism as well as a number of additional assumptions. Let us therefore briefly discuss its range of applicability. The expression is applicable for a small grain ($a/\lambda_D \ll 1$), in a highly collisional plasma ($\ell_i/\lambda_D \ll 1$), in the limit of vanishing velocity between the grain and the ions $u \ll v_{T_i}(\ell_i/\lambda_D)$. The applicability of the linear formalism requires $R_C = Qe/T \ll \lambda_D$, where R_C is the Coulomb radius and a is the grain radius. Additional assumptions include a negligible role of the kinetic effects that requires $\ell_i \lesssim R_C$ and ion collection

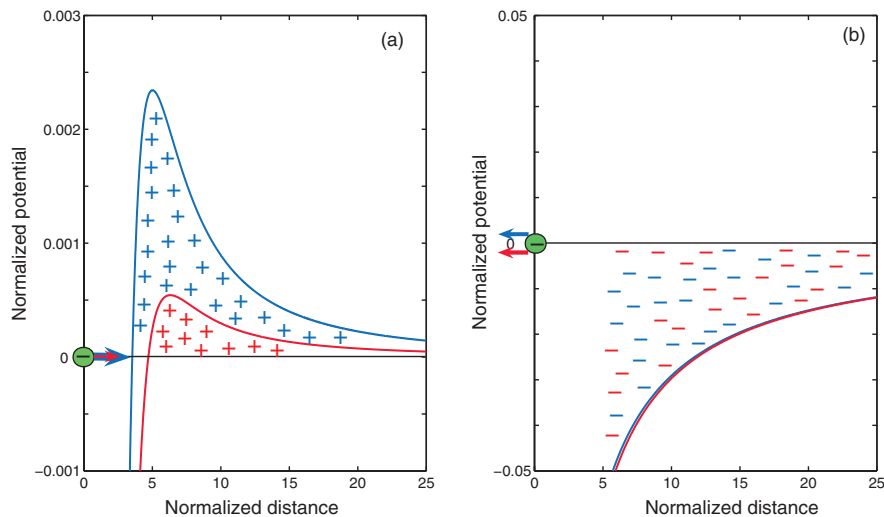


FIG. 1 (color). Electric potential behind a small negatively charged moving grain in highly collisional plasma. (a) corresponds to a nonabsorbing grain, while (b) corresponds to an absorbing grain. The grain is moving to the left. The direction of the force associated with ion focusing (a) and ion depletion (b) behind the grain is shown by arrows. The calculations are performed using the linear plasma response technique (for details see Ref. [25]) for the following set of plasma parameters: $T_e = T_i$, $Qe/aT = 3$, $a/\lambda_D = 0.2$, $u/v_T = 0.003$, and $\ell_i/\lambda_D = 0.03(0.01)$ for the red (blue) curves. Positive and negative signs correspond to the positive and negative space charge regions, respectively.

by the grain in the continuum limit $\ell_i/a \lesssim 1$. Altogether, the set of inequalities determining the applicability of Eq. (1) can be written as

$$u/v_{T_i} \ll \ell_i/\lambda_D \lesssim a/\lambda_D \lesssim R_C/\lambda_D \ll 1. \quad (2)$$

The effect of the momentum transfer from the ions hitting the grain has not been accounted in deriving Eq. (1), but it can be shown to be small in the considered regime [14].

The last contribution to the friction is the neutral drag force. At high pressures considered here, it is reasonable to assume that the grain radius is larger than the mean free path of neutrals, $\ell_n \lesssim a$. In the limit of low Reynolds number corresponding to a slow grain motion, the neutral drag force is given by the Stokes's expression

$$F_n \simeq 6\pi\eta a u, \quad (3)$$

where $\eta \simeq n_n m_n \ell_n v_{T_n}$ is the neutral gas viscosity. This component is obviously directed opposite to the grain motion.

Thus, the direction of the total friction force is determined by the competition of the ion and neutral drag forces. Let us compare their absolute magnitudes. The force ratio is

$$|F_i/F_n| \simeq (1/18)(n_0/n_n)(v_{T_n}/v_{T_i})(Qe/aT)(R_C/\ell_i) \times (\lambda_D/\ell_n). \quad (4)$$

In a weakly ionized plasma we have $n_0 \ll n_n$; it is reasonable to assume that $v_{T_n} \sim v_{T_i} = v_T$; the dimensionless grain charge $Qe/aT = R_C/a$ is usually in the range from 1 to 10; the applicability of Eq. (1) requires $R_C \gtrsim \ell_i$ and $\lambda_D \gg \ell_n$. The product of the three latter large factors can compensate for the smallness in n_0/n_n reducing the total friction force compared to the pure neutral drag force or even making the total friction negative, i.e., directed along the grain motion.

In the latter case, the grain is accelerated until $u = u_{cr}$, when the balance between the ion drag and neutral drag is reached. Note that this can happen when the condition (2) is violated, i.e., when $u_{cr} \sim v_{T_i}(\ell_i/\lambda_D)$. The existence of such a balance follows also from the simple fact that at a higher grain velocity only geometrical factors play a role and $F_{i(n)} \simeq \pi a^2 n_{0(n)} m_{i(n)} u^2$, and thus $F_i \ll F_n$ since $n_0 \ll n_n$. The final grain velocity corresponding to this balance (which is expected to be much smaller than v_T) is a stable equilibrium velocity when the grain exhibits free undamped motion as long as the plasma parameters are unchanged.

The described effect can lead to a superfluidlike behavior of the grain component in plasmas: a collection of absorbing grains can move freely in a highly collisional weakly ionized plasma. The consequences of the phenomenon can be important for astrophysics as well as laboratory-based experiments. Here we should also mention the phenomenon of “crazy” relatively fast moving

(although the velocity is much lower than the ion thermal velocity) dust particles observed in a number of laboratory and microgravity experiments and in some nuclear fusion devices. It would also be interesting to consider this effect in the context of steady-state propagation of a spherical electrode in a leaky dielectric [22,23] as well as in operation of bacterial flagellar motors [23]. This is, however, left for future work.

Note that in the considered classical problem, no collective phononlike excitations are present. This is the main difference between the quantum theory of superfluidity and the considered effect. However, some analogies with quantum fluids at near-zero temperatures still exist. Indeed, the presence of an absorption of the plasma ions is crucial for the considered effect. In some approximation, this can be considered as an analogue to the condition of no excitation of collective perturbations in a quantum fluid. The free energy supporting the absorbing grain motion comes from the distant ionization source creating plasma ions.

Finally, we point out that in the presence of other forces, such as electrostatic, an effect resembling superconductivity phenomenon can appear. Imagine a grain immersed in a highly collisional, partially ionized plasma subject to a very weak external electric field. The electric force should be taken into account in the equation of motion for the grain. As shown in [24], the components of the ion and electron drag forces associated with the ion and electron drifts in the electric field are of minor importance compared to the electric force and hence can be neglected. The main remaining terms in the equation of motion are the ion and neutral drag forces associated with the grain motion. When conditions for the “negative total friction” effect are satisfied, the grain is accelerated in the direction of electric force until the balance between electric force and a (small) total positive friction is reached. This should happen at a grain velocity somewhat higher than u_{cr} ; for a rough estimate we can take $u \sim u_{cr} \sim v_{T_i}(\ell_i/\lambda_D)$. The requirement for the ion drift velocity to be smaller than u_{cr} yields $eE\lambda_D/T \lesssim 1$, where E is the electric field strength. For the “superconductive” grain component current $j_d = Qn_d u$ to be comparable with the electron current, $j_e = en_0 u_e$, we should have $(Q/e) \times (n_d/n_0)(v_{T_i}/v_{T_e})(\ell_i/\ell_e) > eE\lambda_D/T$, where n_d is the grain density and $u_e \approx (eE\ell_e/m_e v_{T_e})$ is the electron drift velocity. Thus, for very weak electric fields we can expect the main component of the electrical current to be mostly associated with the highly negatively charged superconductive grain component, provided grain charge and density are large enough. We note, however, that while one type of the friction force (the friction with neutrals) is almost balanced by the ion drag, the energy is still dissipated even with this superconductive grain component—and this is the main difference from the quantum superconductivity effect. In the considered case, the continuous energy loss due to remaining friction with neutrals as well

as due to electron and ion absorption on the grains is balanced by the plasma production due to some ionization source. This manifests the fundamental openness of the complex plasma systems.

To conclude, we studied here motion of a small negatively charged absorbing grain immersed in a stationary weakly ionized high pressure plasma. We demonstrated that the total frictional (drag) force acting on the grain can be directed along its motion due to the rarefaction in the positive ion density behind the grain and the corresponding “negative” ion drag force dominating the neutral drag force, which always acts against grain motion. Thus, a slowly moving grain can accelerate up to a critical velocity at which these forces balance each other, thus implying free undamped “superfluid” motion. We also discussed the conditions when such an effect can be realized and the possibility of a superconductive grain current in plasmas.

This work was partially supported by the Australian Research Council and DLR under Grant No. 50WP0203.

-
- [1] E.M. Lifshitz and L.P. Pitaevsky, *Statistical Physics* (Pergamon, Oxford, 1981), p. 88.
 - [2] C. K. Goertz, *Rev. Geophys.* **27**, 271 (1989).
 - [3] D. A. Mendis, *Plasma Sources Sci. Technol.* **11**, A219 (2002).
 - [4] A. Bouchoule, in *Dusty Plasmas: Physics, Chemistry and Technological Impacts in Plasma Processing*, edited by A. Bouchoule (Wiley, Chichester, 1999).
 - [5] S. V. Vladimirov, K. Ostrikov, and A. A. Samarian, *Physics and Applications of Complex Plasmas* (Imperial College, London, 2005).
 - [6] P. K. Shukla and A. A. Mamun, *Introduction to Dusty Plasma Physics* (IoP Publishing Ltd., London, 2002).
 - [7] R. L. Merlino and J. A. Goree, *Phys. Today* **57**, No. 7, 32 (2004).
 - [8] S. V. Vladimirov and K. Ostrikov, *Phys. Rep.* **393C**, 175 (2004).
 - [9] V. E. Fortov, A. G. Khrapak, S. A. Khrapak, V. I. Molotkov, and O. F. Petrov, *Phys. Usp.* **47**, 447 (2004).
 - [10] V. E. Fortov, A. V. Ivlev, S. A. Khrapak, A. G. Khrapak, and G. E. Morfill, *Phys. Rep.* **421C**, 1 (2005).
 - [11] J. Winter, *Phys. Plasmas* **7**, 3862 (2000).
 - [12] S. I. Krasheninnikov, Y. Tomita, R. D. Smirnov, and R. K. Janev, *Phys. Plasmas* **11**, 3141 (2004).
 - [13] U. de Angelis, *Phys. Plasmas* **13**, 012514 (2006).
 - [14] S. A. Khrapak *et al.*, *J. Appl. Phys.* **101**, 033307 (2007).
 - [15] S. A. Khrapak and G. E. Morfill, *Phys. Rev. E* **69**, 066411 (2004).
 - [16] S. A. Khrapak, B. A. Klumov, and G. E. Morfill, *Phys. Plasmas* **14**, 074702 (2007).
 - [17] I. V. Schweigert, A. L. Alexandrov, and F. M. Peeters, *IEEE Trans. Plasma Sci.* **32**, 623 (2004).
 - [18] S. A. Maiorov, *Plasma Phys. Rep.* **31**, 690 (2005).
 - [19] A. V. Ivlev *et al.*, *Phys. Rev. Lett.* **92**, 205007 (2004).
 - [20] S. V. Vladimirov and M. Nambu, *Phys. Rev. E* **52**, R2172 (1995); S. V. Vladimirov and O. Ishihara, *Phys. Plasmas* **3**, 444 (1996).
 - [21] O. Ishihara and S. V. Vladimirov, *Phys. Plasmas* **4**, 69 (1997).
 - [22] G. A. Ostroumov, *Interaction of the Electric and Hydrodynamic Fields* (Nauka, Moscow, 1979).
 - [23] A. L. Yarin, *Appl. Phys. Lett.* **90**, 024103 (2007).
 - [24] M. Chaudhuri, S. A. Khrapak, and G. E. Morfill, *Phys. Plasmas* **14**, 054503 (2007).
 - [25] M. Chaudhuri, S. A. Khrapak, and G. E. Morfill, *Phys. Plasmas* **14**, 022102 (2007).